Semi Annual Report

(July 1 — December 31, 2001)

Contract Number NAS5—31363

OCEAN OBSERVATIONS WITH EOS/MODIS:

Algorithm Development and Post Launch Studies

Howard R. Gordon, PI
University of Miami
Department of Physics
Coral Gables, FL 33124

(Submitted January 15, 2002)

Preamble

This document describes our progress thus far toward completion of our research plans regarding two MODIS Ocean-related algorithms.

A. Retrieval of the Normalized Water-Leaving Radiance (Atmospheric Correction).
B. Retrieval of the Detached Coccolith/Calcite Concentration

Our plans for Fiscal Year 2001 are included in this report as **Appendix I**. [In this report, we have combined items 2 (*Implement the Initial Algorithm Enhancements*) and 3 (*Study Future Enhancements*) from Appendix I into item "2 and 3" (*Algorithm Enhancements*).]

Fiscal Year 2001 was to be heavily focused on validation of MODIS-derived products. Unfortunately, the unexpected difficulty in calibrating MODIS required modification of our initial plan. In addition, as we already know that there are certain situations in which the algorithms are unable to perform properly, or that there are items that have not been included in the initial implementation, a portion of our effort was directed toward algorithm improvement. Thus, we break our effort into two broad components for each algorithm:

- Algorithm Improvement/Enhancement;
- Validation of MODIS Algorithms and Products.

Of course, these components will overlap in some instances.

RETREIVAL OF NORMALIZED WATER-LEAVING RADIANCE (ATMOSPHERIC CORRECTION)

Algorithm Improvement/Enhancement

1. Evaluation/Tuning of Algorithm Performance

Task Progress:

As indicated in our last Semiannual Report, considerable effort has been expended by R. Evans and co-workers toward removing the instrumental artifacts from MODIS ocean imagery. Examples of such artifacts are severe striping, mirror side differences, effects of the variation of the instruments response as a function of scan angle, and the influence of instrumental polarization sensitivity. Much progress has been made along these lines, and we are nearing completion of a corrected software/calibration adjustment that can bridge the shifts from the "A-side" to the "B-side" back to the "A-side" electronics. This has been accomplished by first reworking the polarization correction, then using MOCE measurements to set the overall calibration in the various MODIS "epochs," and finally using the MOBY data to correct for the MODIS response as a function of scan angle. The results of these modifications are summarized in **Appendix II** containing the PI's presentation at the December 2001 MODIS Science Team Meeting. The water-leaving radiances are now close to being in acceptable agreement with SeaWiFS. Based on the present performance of the algorithm and the anticipated modifications to be made in January-February 2002, we anticipate being able to "validate" the normalized water-leaving radiances by June 2002.

Anticipated Future Actions:

We will continue the evaluation of MODIS imagery, and work closely with R. Evans on removing the artifacts. The studies reported in Appendix II suggest that the relative calibration of Bands 15 and 16 is very close to being correct. However, the absolute values of $\varepsilon^{SS}(765,865)$ are a little higher than the range of the MODIS candidate aerosol models, suggesting that the calibration factor (counts to radiance) of the 765 nm band may be a little too large relative to the 865 nm band. In addition, the fact that $\varepsilon^{SS}(765,865)$ shows water structure in 2000129 indicates that there is residual water-leaving radiance in the NIR. Thus, we must perform an additional calibration adjustment of the visible-NIR bands, and add a correction to the $\rho_w(765) \approx \rho_w(865) \approx 0$ assumption. This latter modification was not included in the initial processing software to avoid the concomitant increase the processing time. In addition, we shall try to calibrate the 667 and 678 nm "fluorescence" bands using an atmospheric-correction/water-leaving radiance model that is the basis for our 3-band coccolith algorithm [Gordon et al., Retrieval of Coccolithophore Calcite Concentration from SeaWiFS Imagery, *Geophys.*

Res. Lett. **28**: 1587—1590, 2001]. Our intention is to work closely with R. Evans to have these completed by March 1, 2002. Thus, our near term goals are

- refine calibration in NIR and then visible,
- add routine to include estimate of ρ_w in the NIR, and
- adjust calibration of the fluorescence bands using an ocean-atmosphere model in the red and NIR.

2. and 3. Algorithm Enhancements

There are two important issues we are examining for inclusion into the MODIS algorithm: effecting atmospheric correction in the presence of strongly absorbing aerosols and/or Case 2 waters; and including the influence of the subsurface upwelling BRDF on water-leaving radiance.

Strongly Absorbing Aerosols

The first of the two enhancements we have been considering concerns absorbing aerosols. Although success with SeaWiFS has shown that the MODIS algorithm performs well in ~ 90% of Case 1 water situations, it does not perform adequately everywhere; most notably in atmospheres containing strongly absorbing aerosols. Strongly absorbing aerosols constitute a previously unsolved atmospheric correction issue for Case 1 waters, and have a significant impact in many geographical areas. Two important situations in which absorbing aerosols make an impact are desert dust and urban pollution carried over the oceans by the winds. In the case of urban pollution the aerosol contains black carbon and usually exhibits absorption that is nonselective, i.e., the imaginary part of the refractive index (the absorption index) is independent of wavelength. In contrast, desert dust absorbs more in the blue than the red, i.e., the absorption index decreases with wavelength.

Task Progress:

We have applied the spectral optimization algorithm [R.M. Chomko and H.R. Gordon, Atmospheric correction of ocean color imagery: Test of the spectral optimization algorithm with SeaWiFS, *Applied Optics*, **40**, 2973—2984, 2001] with the Garver and Siegel reflectance model ["Inherent optical property inversion of ocean color spectra and its biogeochemical interpretation: 1 time series from the Sargasso Sea," *Geophys. Res.*, **102C**, 18607—18625, 1997] to Case 2 waters. Unlike Case 1 waters, in which phytoplankton and their immediate detritus control the optical properties, in Case 2 waters phytoplankton play a lesser role. For example, in coastal regions resuspended sediments from the bottom and/or sediments and dissolved organic material can be carried to the coasts by rivers, etc., may control the water's optical properties. These Case 2 waters are difficult to atmospherically correct because the water-leaving

reflectance in the NIR is often not negligible. We have modified the spectral optimization algorithm so that we no longer employ the simplifying assumption of negligible marine reflectance in the NIR. Such a modification enables use of the spectral optimization algorithm in waters with moderate sediment concentrations. This modification has been applied to imagery of the Chesapeake Bay; although, the Garver-Siegel reflectance model is not correct for such waters. With the Case 2 modification, the algorithm appeared to function properly. Details of our processing with the spectral optimization algorithm are provided in **Appendix III**, which consists of slides from a presentation at the Fall AGU Meeting, December 2001.

We have also replaced the Gordon et al. [A Semi-Analytic Radiance Model of Ocean Color, *Jour. Geophys. Res*., **93D**, 10909-10924 (1988)] reflectance model with the Garver and Siegel (1997) model in our spectral matching algorithm for operation in wind-blown dust [C. Moulin, H.R. Gordon, R.M. Chomko, V.F. Banzon, and R.H. Evans, Atmospheric correction of ocean color imagery through thick layers of Saharan dust, *Geophys. Res. Lett.*, **28**, 5-8, 2001]. We tested it on a dusty image off West Africa with encouraging results (**Appendix IV**), however, we continue to have problems if the candidate aerosol models include both dust and non-dust models. The problem of incorporating the spectral matching algorithm into the MODIS code is formidable because of the processing time required; however, processing small sub-scenes is feasible.

Anticipated Future Actions:

We will continue to evaluate the performance of the absorbing aerosol algorithms, as we believe they are the most versatile. However, we need to (1) be sure they perform as well as experiments thus far indicate, and (2) optimize their performance to decrease processing time. In the case of the spectral optimization algorithm for use in Case 2 waters, we will provide R. Evans with a MODIS-specific version. When this has been incorporated into the processing code and tested, it will be provided to MODAPS for routinely processing a subsetted coastal region in a research mode. Although the code is very slow, application to a small region is feasible. Our goal is to provide a demonstration of the value of MODIS imagery in Case 2 waters, as well as to provide users with the methodology and software tools for processing MODIS imagery in such waters. We are looking for coastal regions where algorithms of the Garver-Seigel type have been tuned to specific Case 2 waters. Likely candidates are the Chesapeake Bay and/or the Gulf of Maine. Thus, our longer-term goals are

- to provide code for Case 2 coastal waters, and
- to continue to evaluate retrieval in dust.

Both of these require coupled ocean and atmosphere retrievals.

The subsurface upwelling BRDF

The subsurface BRDF issue is revolves around the fact that nearly all measurements of the upwelled spectral radiance (used for bio-optical algorithm development, sensor calibration and product validation of all ocean color sensors) are made in the nadir-viewing direction, while the water-leaving radiance estimate from the signal at the remote sensor is for a particular viewing geometry that is rarely nadir. Thus, we need to understand the BRDF of the subsurface radiance distribution to reconcile these measurements. Our approach is to directly measure the BRDF as a function of the chlorophyll concentration and to develop a model that can be used for MODIS.

Task progress:

While we have spent time looking at older data sets and reducing other data, much of our effort in this task during this reporting period has been spent building the new radiance distribution camera system (NuRADS), which we brought to sea for the first time in December. The system we have been using, RADS-II, was designed to measure the entire (up and downwelling) radiance distribution for a different application. As such this instrument is much larger and heavier than we require for the MODIS application. The size is an important consideration because we have found instrument self-shadow to be a significant problem in our measurements, particularly in the green and red portion of the spectrum. The new system is smaller and lighter, thus easier to deploy and float at the surface. The combination of lighter and smaller also makes the instrument's and its support structure's shadow much smaller and allows us to improve the data quality. In addition, as there have been significant improvements in the CCD sensor technology, the data will also be less noisy and therefore more accurate. The instrument is pictured in Figure 1a on the following page.

During the first field test the instrument worked well. An example of an upwelling radiance image from this system (raw/uncalibrated image) is shown in Figure 1b on the following page. Obvious in the image is the effect of wave focusing, which causes the radial bright areas in the image, and the anti-solar point, from where all these radial lines appear to emanate. While the instrument worked well, there are many things we need to do both to improve the performance and to characterize the instrument. For example, we found that the best integration times for the individual data frames was 0.01 sec. This is a very short integration time, shorter than we want and it tends to pick up very transient features (such as the wave focusing). Since we are concerned with the average BRDF, we will slow the system down optically so that we can do more averaging during the data collection. We also need to do many steps to characterize the system, such as a spectral calibration, linearity, camera lens rolloff, and an absolute calibration. However for a first field test the instrument performed above expectations.

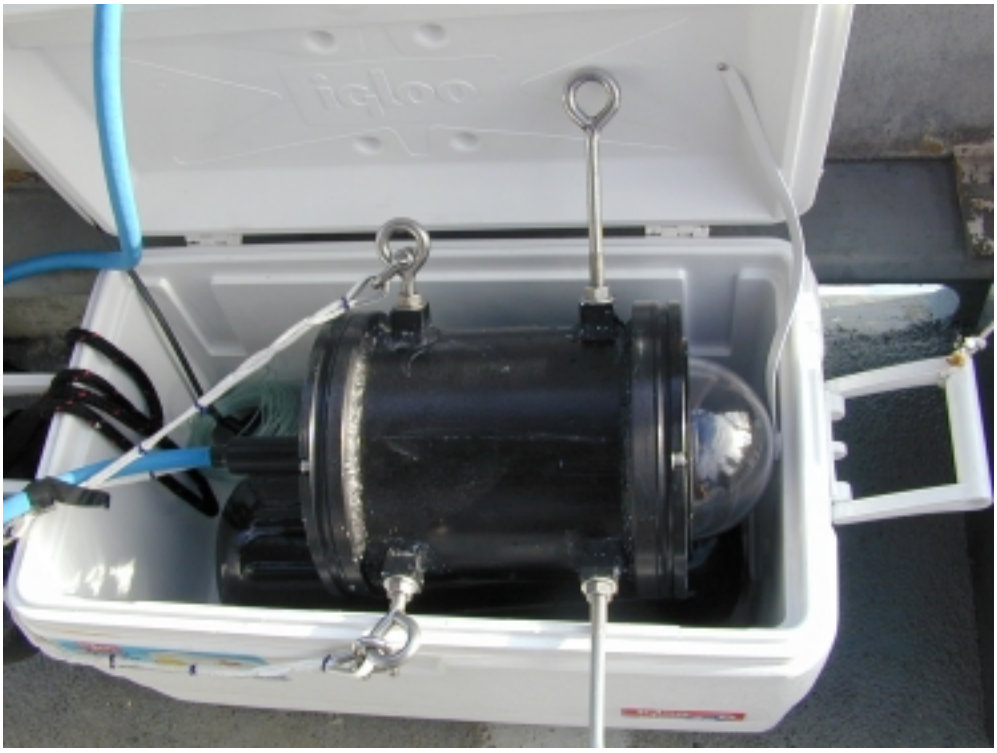

Figure 1a. The NuRADS instrument.

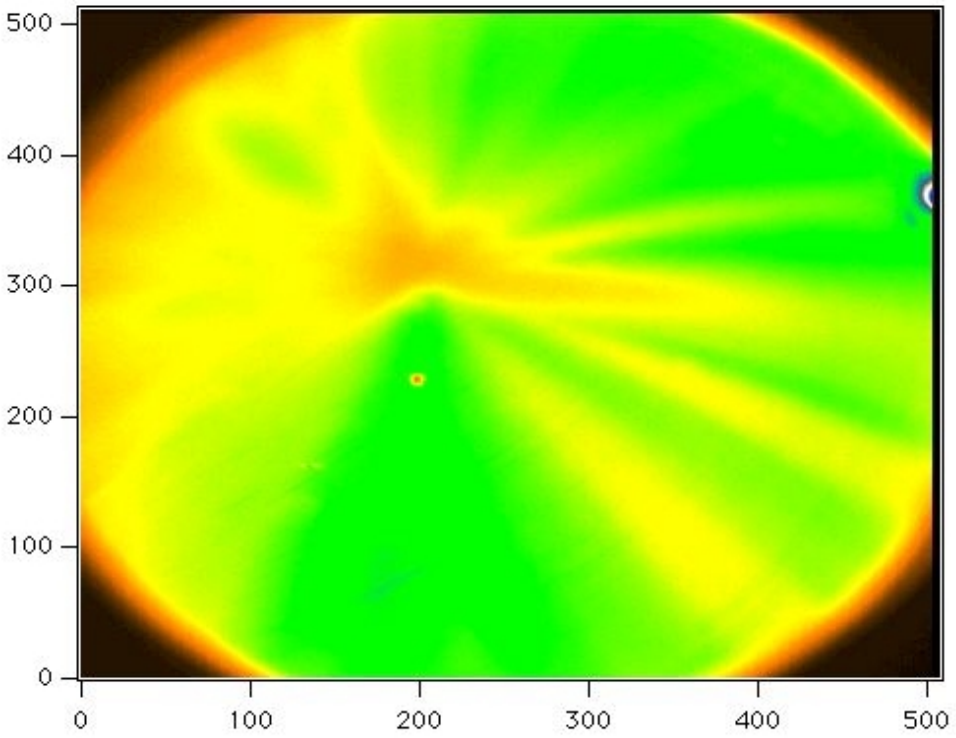

Figure 1b. Sample upwelling radiance distribution from NuRADS.

Anticipated Future Actions:

We will be preparing manuscripts based on our recent BRDF measurements in the next reporting period. In addition, we will be performing the characterization steps required for the NuRADS system, and reducing the data from the recent (MOCE-9) cruise. Finally, as discussed in the validation section below, we will be participating in a cruise in April and/or July out of Hawaii with Dennis Clark. This cruise will occur when the site experiences the maximum (90 deg) solar elevation. We will make radiance distribution measurements during this period from sunrise to sunset. This will give us a complete clear water radiance distribution, at all solar zenith angles, to enable us to make a complete model for correction of MOBY data and for MODIS data in clear water. With the new instrument, this will also give us spectral data on the radiance distribution, which we have not been able to obtain previously (due to shadowing).

Validation of MODIS Algorithms and Products

4. Participate in MODIS Initialization/Validation Campaigns

This task refers to our participation in actual Terra/MODIS validation/initialization exercises.

Task Progress:

While most of our effort the last six months has been directed towards the new radiance distribution camera system (NuRADS), we also participated in a short MODIS characterization cruise (MOCE-9) during December. In addition, we worked on reducing data from a cruise during June. On this cruise, we obtained data on the radiance distribution at a large range of solar zenith angles, but at only one wavelength.

We continued to maintain our CIMEL station in the Dry Tortugas during this period. This station will be used to help validate the MODIS derived aerosol optical depth (AOD), and aid in investigating the calibration of the near infrared (NIR) spectral bands of MODIS.

We also participated in the ACE-Asia data workshop during this period. Last spring one of our graduate students operated a micro-pulse lidar (with his travel support coming from another project) during the ACE-Asia cruise fieldwork. One of the critical aspects of atmospheric correction is how to deal with vertical structure with absorbing aerosols. Previous fieldwork, during INDOEX and Aerosols99, gave us a general picture of the vertical structure of aerosols over the Atlantic and Indian Ocean, including regions of Saharan Dust and pollution events from the Indian sub-continent. ACE-Asia gave us vertical profiles of Asian Dust over the Pacific. Participating in the ACE-Asia data workshop allowed us access to data collected during this cruise by other groups. We

have been working with our lidar data, investigating different inversion methods to improve the accuracy of our vertical structure retrievals.

Anticipated future efforts:

We will continue our analysis of the MOCE-6, 7, and 8 data. We will participate in the next MODIS ship campaign when it occurs. If this is the post-launch cruise for Aqua, we will make measurements of the sky radiance distribution (large-angle and aureole), the in-water radiance distribution, AOD, and whitecap radiance during this cruise. We also plan to participate in an experiment with Dennis Clark in either April or July. This cruise will be timed to coincide with the smallest solar zenith angle in Hawaii (solar zenith angle of 0 at solar noon). We will concentrate on the radiance distribution measurements during this cruise to get a complete suite of radiance distribution data for widely varying solar zenith angles that can be used for correction of the MOBY data set.

5. Complete Analysis of SeaWiFS Validation Campaign Data

Task Progress:

We have completed analysis of our measurements during the Aerosols99 and INDOEX campaigns, and submitted several papers for publication (See CY-2001 Publications). In addition, we have completed the reduction of the MOCE-5 BRDF data.

Anticipated future efforts:

We will continue our effort to model the MOCE-5 BRDF data as a function of the chlorophyll concentration. During the next reporting period, we will submit a paper on these results. In addition, we will be evaluating Andre Morel's model for the ocean BRDF, proposed for use in other ocean color sensors. MOCE-5 provides a good data set to test this model. If Morel's model performs well, it will be incorporated into the MODIS processing software.

RETRIEVAL OF DETACHED COCCOLITH/CALCITE CONCENTRATION

William M. Balch
Bigelow Laboratory for Ocean Sciences
POB 475
McKown Point
W. Boothbay Harbor, ME 04575

This last half year of work has focussed on several areas: 1) preparation and implementation for a large-scale manipulative experiment for testing the MODIS suspended calcite algorithm, 2) more sampling for a pixel by pixel comparison of MODIS-derived particulate inorganic carbon and ship derived values, 3) continued coccolith enumeration for Gulf of Maine samples and 4) presentation of MODIS validation results at the BWI MODIS team meeting.

Algorithm Evaluation/Improvement

Task Progress:

Our second manuscript on Arabian Sea results was published in Deep Sea Research I this last six months (Balch et al., 2001). The abstract can be found in a previous Semi-Annual report. The observation that calcium carbonate accounted for 10-40% of the total optical backscattering, is particularly significant in oceanic optics, as the particles responsible for the observed backscattering in the sea are still not well defined. The manuscript included an error analysis for our underway measurements of suspended particulate inorganic carbon (used in the MODIS validation work).

Validation of MODIS Algorithms and Products

As coccoliths and suspended PIC (particulate inorganic carbon or calcium carbonate) are new products, and as Terra was only launched in December 1999, there are relatively few data sets available for validation, particularly for the coccolith and suspended calcite products. This is because coccolith concentration (PIC) is not frequently measured at sea, while chlorophyll concentration is. In conjunction with NASA SIMBIOS activities, much of our validation estimates come from the Gulf of Maine, the site of frequent blooms of coccolithophores, and a region readily accessible from our laboratory.

Validation of regional PIC

Throughout the summer of 2001, we acquired more PIC samples from the Gulf of Maine for MODIS validation. The samples were acquired from our ship of opportunity program aboard the M/S Scotia Prince ferry. Over 90% of this year's ferry work was

done under clear skies thanks to new Navy weather forecasts which are highly accurate (beating our "clear-sky" records from previous years). While no coccolithophore bloom occurred in the Gulf of Maine during 2001 (unlike 2000), there still was a wide range of "nonbloom" PIC concentrations for validation of the algorithm. We collected a total of 109 discrete samples for validation, and 2012 four-minute underway samples. In many respects, validation in "nonbloom" waters is as useful as in blooms, since nonbloom PIC concentrations are more representative of the global ocean. The validation work that we have done to date has demonstrated an RMS error of ~ ± 2 μg PIC l^{-1} for all data ranging from 0.1 to 100 μg PIC l^{-1}. Within a given image, the two-band PIC algorithm is capable of discriminating PIC concentrations of ~ ± 0.2 μg PIC l^{-1} (Figure 2). The caveat to these observations is that these statistics applied only to validation data points from the west side of the MODIS swath. Data from the eastern side of the swath, processed with Miami code (Versions 3.3 or lower) showed large errors due to polarization and response versus scan angle problems. The complete MODIS validation data set will be re-processed with new code (Version 3.4) which should largely eliminate the differences in accuracy across the swath.

This October, we began collaboration with the Australians for getting PIC samples from a supply ship that regularly goes between Hobart and Antarctica. This area has been shown in MODIS imagery to be a regular "hotspot" for PIC, extending along the Antarctic Polar Frontal Zone. With seawater samples from this region, we expect to be able to provide some important validation to the observations. If we demonstrate that the MODIS observations are indeed correct, this will have enormous ramifications to the global PIC budget, due to its large area.

Chalk-Ex

In order to validate high PIC concentrations found in a coccolithophore bloom with MODIS, we made two small calcite patches in November of 2001 using 13 tons each of Cretaceous coccolith chalk. Note this also allows us to check the coccolithophore pigment product. The chalk that we used was ground so that it all passed a 10 μm sieve, with 50% of the particles with diameter < 1.9 μm, the diameter of E. huxleyi coccoliths. The chalk was ~ 98% pure. The reader should note that we did this in consultation with U.S. EPA, and the U.S. Coast Guard.

Our first large-scale "Chalk-Ex" experiment in August '00 (single patch with 25 tons of chalk) was also designed to sea-truth the MODIS coccolith algorithm at slightly lower concentrations than found in a bloom, but still high enough to be easily visible to MODIS. Unfortunately, the MODIS satellite sensor began having unexpected data formatting problems some11 h before we began diluting the chalk, and the instrument was turned off a few hours before our overpass! This was a most unfortunate stroke of bad luck, especially given that every other part of the experiment, including the weather, had gone perfectly. All was not lost, however, as SeaWiFS did see the patch, and we were able to do a vicarious check of the $CaCO_3$ algorithm performance (but regrettably, SeaWiFS does not have the sensitivity of MODIS). See previous progress reports for further details.

There were no satellite problems in our November '01 Chalk-Ex experiment. Instead, the challenge was to work in very high wind conditions at both stations. The southern site (39°48'N x 67°48'W) was in force 8 conditions for several days prior to our leaving Portland (with 12-15 foot seas, 45 kt winds). Jordan Basin (44^{o}N x 67^{o}40'W) had 35kt winds, but only 6 foot seas, so we chose the latter for our first site, occupied on 10 November. Thirteen T of chalk were deployed from our mixing tubs beginning 0645 on 11 November. Given the previous wind conditions, the mixed layer was 70 m deep and very active so, the chalk was mixed downwards rapidly. A cold front brought clearing skies to the Jordan Basin site, but that was 3 h after the overpass. We occupied this site until 13 November and saw a small increase in backscattering, which agreed with our predictions based on the dilution effect, size of the patch put down, etc. Radial surveys with the Scanfish (with Wet Labs EcoVSF attached) allowed undulating b_b measurements to 100 m, which we used to estimate PIC concentrations in the patch. We were confronted by signal to noise issues by the second day in the Jordan Basin patch but we still were able to locate the patch.

We steamed to the southern slope station on 11/13/01, with promises of improving weather conditions (albeit heavy swell). We indeed found fair-sky conditions, so we proceeded with the standard "Pre-Chalk" survey from 1200 on 11/14/01 through 0400 of 11/15/01. As of 0500 on 11/15, we began spreading chalk. The mixed layer was 60 m deep, but with low winds for 2 d, the water-column was beginning to stratify. This provided just enough stability to provide us with a chalk patch ~1.5 km by 0.75 km, with initial b_b values up to 0.08 per m. The patch was complete by ~1000 h under completely sunny skies, in time for the MODIS overpass. Some high cirrus clouds were visible for the MODIS overpass, and a few more by the SeaWiFS overpass. Nevertheless, the patch was visible in the MODIS 1km resolution data (551nm; Figure 3), 0.5 km resolution data (555 nm) and 0.25 km resolution imagery (648 nm) the day that the patch was made. The patch was also visible in the 1 km resolution image the day after it was created. After getting some spectacular data on our ScanFish surveys, we put up a surveillance balloon, and acquired real-time video imagery with a video camera, telemetered to the ship from ~ 1500 ft altitude. We also were able to snap still photos to record the shape of the patch, which allowed us to design our ship surveys better (which, in the end, allowed us to better estimate PIC mass balance of the irregularly-shaped patch).

Along with the optical measurements, Al Plueddemann (WHOI) deployed Lagrangian drifters for estimates of vertical and horizontal mixing. A fully instrumented Hydro drifter recorded changes in stratification and mixing. Cindy Pilskaln (BLOS) deployed Lagrangian sediment traps for collecting the sinking chalk and associated particulate material. Hans Dam and George McManus (UConn) have been looking at grazing and aggregation of the chalk particles as they sink downwards. Overall, our most exposed site (southern site) was the best, and we traced the chalk for 3 d as it spread horizontally and mixed downward. Our last day in the southern site had gale-force conditions, and we were able to watch the patch erode. We returned to Portland on the morning of 20 November.

Validation of global PIC and coccolithophore pigment data

For the 36km global data, there is no comparable sea-truth data available at this time; thus, we compare the statistics of the global values with statistics of regional field surveys or global models. We have focused on processing monthly global PIC fields and examining their associated statistics (Figure 4). Five monthly PIC images were available which showed a 10% coefficient of variation, suggesting that the global features are stable over 30 d time scales, and not dominated by pixel-to-pixel noise. We also examined the latitudinal distribution of PIC, and estimated the global standing stock of PIC for comparison to other published estimates. A global estimate of surface PIC can be made based on the work of Milliman (Milliman, 1993). The former reference provides an estimate of the annual global sinking flux of PIC (in g m^{-2} y^{-1}) and this requires an estimate of the average sinking velocity of particles in order to derive standing stock (=flux/sinking velocity). The modeled average PIC concentration is 1.85 µg PIC l^{-1} (or ~65 Mt PIC with error of ~ one order of magnitude). MODIS-derived monthly averages ranged from 15-55 Mt PIC (Table 1). While these estimates are within the error limits of the modeled values, due to the current reprocessing of all the ocean data with Version 3.4 code, we will have to re-do this analysis when re-processing is completed.

Globally, the coccolith pigment product is well correlated to the MODIS pigment product (MODIS Ocean Products 15; Coccolith Pigment = exp(-0.1214*MODIS pigment$^{0.93}$); r^2=0.89). The data are well centered on the 1:1 line. Regionally, within the Gulf of Maine, however, the correlation is best at high pigment concentrations; at low concentrations, coccolithophore pigment concentration is systematically less than the MODIS pigment value (Coccolith Pigment = exp(-0.188*MODIS pigment$^{1.125}$); r^2=0.91. The ratio of MODIS pigment/Coccolithophore pigment was plotted against the MODIS PIC in order to see how PIC concentrations affected the ratio of the ratio of the two pigment products. The results suggest that as PIC concentrations approach to ~ 5 µg l^{-1}, the mean ratio approaches 1, and indeed could become < 1 at high PIC levels. Given that we expect most of the satellite-derived blooms of coccolithophores to be *E. huxleyi*, we also would expect the band-ratio algorithms to *underestimate* the pigment concentration for suspensions of these small coccoliths. Thus, we suggest using the MODIS pigment product for PIC values up to 5 µg PIC l^{-1}, above which, the coccolithophore pigment values should be used. Given the accuracy of the algorithm, the threshold value of 5 µg PIC l^{-1} is also reasonable. With the success of our recent Chalk-Ex experiment, we also will check the coccolith pigment algorithm within the patch.

Cautions When Using coccolith/PIC data products

The coccolithophore data products should be treated as "preliminary," until the re-processing with Version 3.4 code is complete, and data are re-checked against shipboard validation samples. Note, it is expected that if east-west problems indeed are resolved, we will have many more samples to include in the validation figure (Figure 2). From the validation work done so far, if validation data are available on the same day as the MODIS measurements, the accuracy can be expected to be as good as 0.2 mg PIC m^{-3}. If

no validation data are available, then one can assume a best-case accuracy of ± 2 mg PIC m^{-3}. Moreover, with the polarization and response versus scan angle problems inherent with Versions 3.2 and 3.3 of the processing code, we do not recommend using these MODIS coccolithophore data products unless they are from the western third of the MODIS swath. We also caution using these data from shallow ocean regions, particularly near carbonate banks (e.g. Grand Bahamas), where bottom reflectance will appear as a high-reflectance coccolithophore bloom (presumably such pixels would be flagged due to their shallowness). Moreover, near river mouths and in shallow waters, resuspended sediments (of non-calcite origin) may appear as high suspended calcite concentrations. Only use these data if the waters are sufficiently deep to not have such bottom resuspension or direct river impact. Beware that MODIS-derived coccolith concentrations assume that the coccoliths are from the prymnesiophyte, *E. huxleyi*. If this is not true, then inaccuracies will increase although the errors are not expected to be large. Even when using the data in units of mg m^{-3}, they nevertheless assume a constant backscattering cross-section for *E. huxleyi*, which is known to vary with the size of the calcite particle.

Web Links to Relevant Information

The algorithm theoretical basis document for the coccolithophore products can be found at: http://modis.gsfc.nasa.gov/MODIS/ATBD/atbd_mod23.pdf

More information about the algorithm and inputs can be found in:

Esaias, W., et al., 1998, Overview of MODIS Capabilities for Ocean Science Observations, *IEEE Transactions on Geoscience and Remote Sensing*, **36**, 1250—1265.

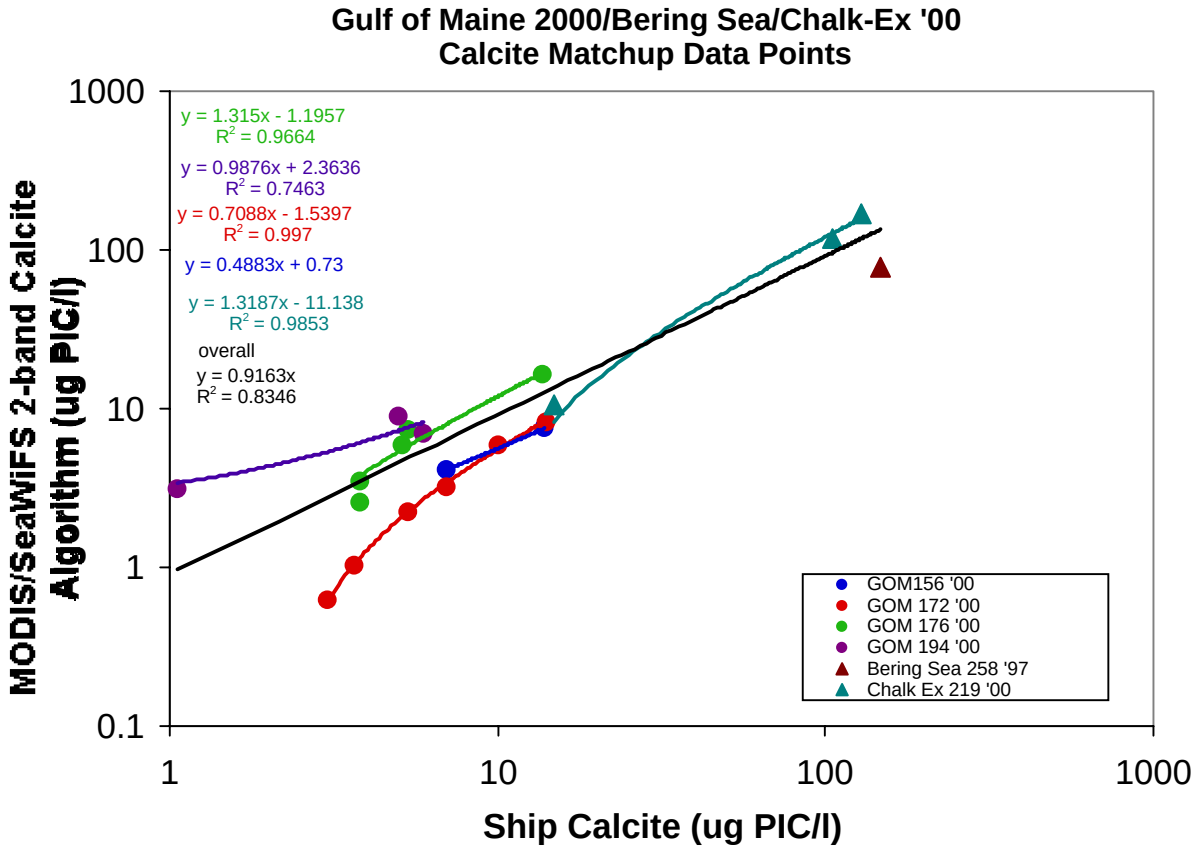

Figure 2. MODIS 2-band suspended PIC values versus ship-derived PIC values. Results taken from Gulf of Maine, 2000, when ship was on west side of MODIS swath. Statistical results: Day 156 (only two data points, no statistics available); Day 172-SE of derived PIC = ± 0.18 µg PIC l^{-1}; Day 176-SE of derived PIC = ± 1.17 µg PIC l^{-1}; Day 194-SE of derived PIC = ± 2.10 µg PIC l^{-1}; All data combined-SE of derived PIC = ± 2.85 µg PIC l^{-1}. Also shown for comparison are data from a Bering Sea coccolithophore bloom (day 258 of 1997) and the Chalk-Ex calcite patch (August '00). The Bering Sea data, shipboard PIC concentrations were based on coccolith counts converted to PIC, (using a conversion factor of 0.2 pg PIC coccolith^{-1}), and satellite PIC estimates based on SeaWiFS data. For the Chalk-Ex data (also using SeaWiFS), backscattering was measured, and converted to PIC concentrations using laboratory-derived results on the backscattering cross-section of $CaCO_3$.

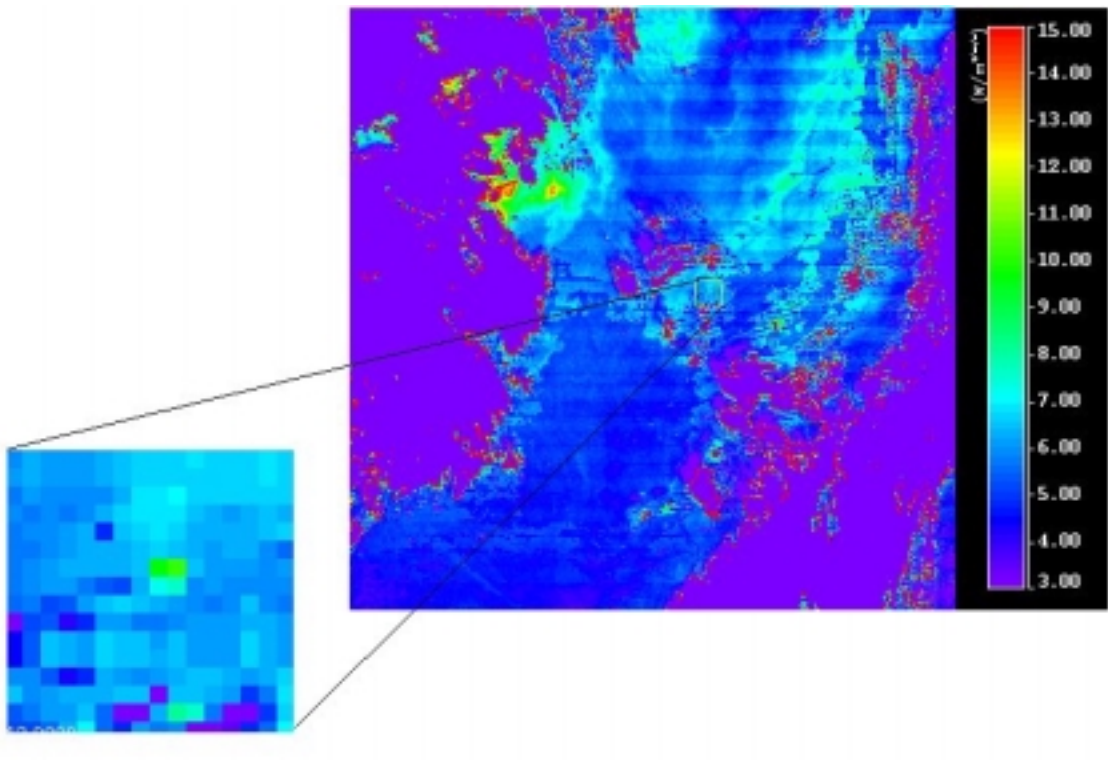

Figure 3. MODIS 1 km data from 15 November, 2001 Chalk-Ex experiment. Clouds are visible to the NE and SW of the patch. The patch region is shown as an inset, with water-leaving radiance values higher than the surrounding water. The patch position and orientation exactly matches that observed from the ship using the Global Positioning System.

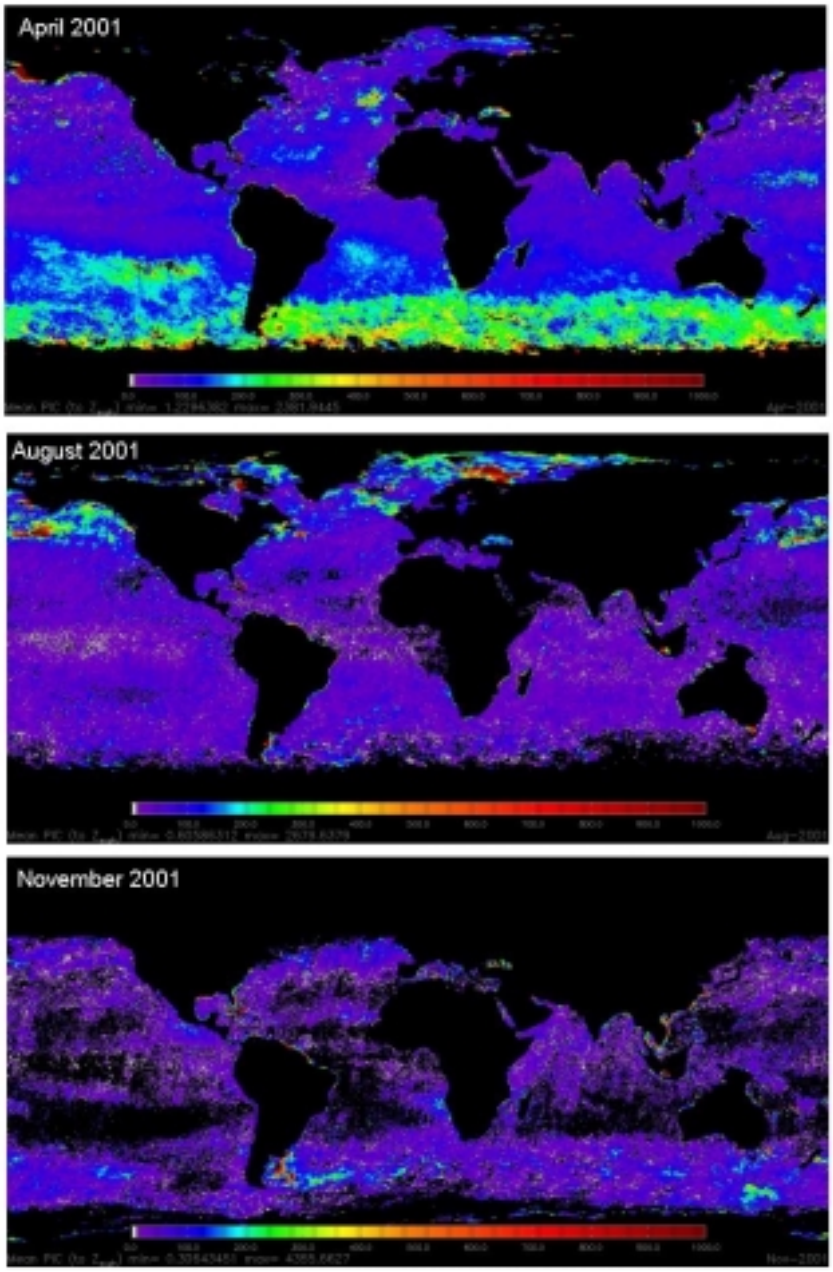

Figure 4. MODIS global images of PIC. Data represent the 36 km monthly averages, as processed with Versions 3.2 and 3.3 of the MODIS ocean code. Coefficient of variation of these data is ~ 10%.

Table 1. Global euphotic estimates of PIC (Mt), POC (Mt) and PIC:POC ratio based on 5 months of 36 km MODIS data. PIC determined as described in text using Versions 3.2 and 3.3 of the MODIS ocean code. POC estimates based on algorithm of Morel (1988) which relates chlorophyll to POC. Both PIC and POC integrated to base of euphotic zone using estimates of Kpar (also based on Morel (1988) chlorophyll vs. Kpar relationship). Average values of the five months of data given at bottom of table.

	PIC (Mt)	POC (Mt)	PIC/POC
April	51.56	1030.75	5.00%
May	52.42	958.83	5.47%
August	23.30	1028.14	2.27%
October	15.90	990.54	1.61%
November	15.04	955.89	1.57%
Average	31.64	992.83	3.19%

Anticipated future efforts:

We will spend the first half of 2002 doing post cruise data processing for the November Chalk-Ex experiment. We are currently processing all PIC samples from last year's Gulf of Maine and Chalk-Ex work which will have to be cross-registered with re-processed MODIS data after it becomes available. Moreover, we will continue working on the Gulf of Maine coccolithophore bloom results for publication. As noted above, the three-band algorithm for determining suspended calcite concentration has the added advantage that chlorophyll does not interfere with the acquisition of the PIC. Data checks are ongoing before this algorithm will be considered fully validated within the MODIS data stream. The principal difficulty in PIC validation work is the simultaneous acquisition of coccolithophore data and satellite imagery (because of the ephemeral nature of coccolithophore blooms). We shall continue validating the new coccolithophore algorithm with MODIS data as they become available in our ongoing Gulf of Maine and Southern Ocean work during '02.

Referencing Data in Journal Articles

Results derived from this algorithm should cite the paper of Gordon et al.(Gordon et al., 1988) for the original discussion, and (Balch et al., 1999; Balch et al., 1996) for field data on the backscattering cross-section of calcite.

Citations

Balch, W.M., Drapeau, D., Fritz, J., Bowler, B. and Nolan, J., 2001. Optical backscatering in the Arabian Sea-continuous underway measurements of particulate inorganic and organic carbon. *Deep Sea Research I* 48, 2423-2452.

Balch, W.M., Drapeau, D.T., Cucci, T.L., Vaillancourt, R.D., Kilpatrick, K.A. and Fritz, J.J., 1999. Optical backscattering by calcifying algae--Separating the contribution by particulate inorganic and organic carbon fractions. *Journal of Geophysical Research* 104, 1541-1558.

Balch, W.M., Kilpatrick, K., Holligan, P.M., Harbour, D. and Fernandez, E., 1996. The 1991 coccolithophore bloom in the central north Atlantic. II. Relating optics to coccolith concentration. *Limnology and Oceanography* 41, 1684-1696.

Gordon, H.R., Brown, O.B., Evans, R.H., Brown, J.W., Smith, R.C., Baker, K.S. and Clark, D.K., 1988. A semianalytic radiance model of ocean color. *Journal of Geophysical Research* 93, 10909-10924.

Milliman, J., 1993. Production and accumulation of calcium carbonate in the ocean: Budget of a nonsteady state. *Global Biogeochemical Cycles* 7, 927-957.

Additional Developments

The following presentations were made at the December 2001 MODIS Science Team Meeting at the BWI Marriott:

Balch, W.M., D. Drapeau, B. Bowler, A. Ashe, J. Goes, E. Scally, H. Gordon, K. Kilpatrick, and R. Evans. Validation of the MODIS suspended calcite product.

H.R. Gordon, R. Evans, E. Kearns, K. Kilpatrick, K. Voss, and the RSMAS Remote Sensing Laboratory staff. MOD 18 Normalized Water-leaving Radiance.

CY 2001 PUBLICATIONS

(NAS5-31363 Personnel bold highlighted)

Balch, W.M., D. Drapeau, B. Bowler and J. Fritz, Continuous measurements of calcite-dependent light scattering in the Arabian Sea, *Deep Sea Research I*, **48**, 2423—2452 (2001).

Chomko, R.M. and **H.R. Gordon**, Atmospheric correction of ocean color imagery: Test of the spectral optimization algorithm with SeaWiFS, *Applied Optics*, **40**, 2973—2984 (2001).

Gordon, H.R., **G.C. Boynton**, **W.M. Balch**, S.B. Groom, D.S. Harbour, and T.J. Smyth, Retrieval of Coccolithophore Calcite Concentration from SeaWiFS Imagery, *Geophysical Research Letters* , **28**: 1587—1590 (2001).

Holben, B.N., D.Tanre, A.Smirnov, T.F.Eck, I.Slutsker, N.Abuhassan, W.W.Newcomb, J.Schafer, B.Chatenet, F.Lavenue, Y.J.Kaufman, J.Vande Castle, A.Setzer, B.Markham, D.Clark, R.Frouin, R.Halthore, A.Karnieli, N.T.O'Neill, C.Pietras, R.T.Pinker, **K.Voss**, G.Zibordi, An emerging ground-based aerosol climatology: Aerosol Optical Depth from AERONET, *Journal of Geophysical Research,* **106D**, 12067—12097 (2001).

Moulin, C., **H.R. Gordon**, **R.M. Chomko**, **V.F. Banzon**, and R.H. Evans, Atmospheric correction of ocean color imagery through thick layers of Saharan dust, *Geophysical Research Letters*, **28**, 5—8 (2001).

Moulin, C., **H.R. Gordon**, **V.F. Banzon**, and R.H. Evans, Assessment of Saharan dust absorption in the visible to improve ocean color retrievals and dust radiative forcing estimates from SeaWiFS, *Journal of Geophysical Research*, **106D**, 18,239—18,249 (2001).

Quinn, P. K., D. J. Coffman, T. S. Bates, T. L. Miller, J. E. Johnson, **K. J. Voss**, **E. J. Welton**, C. Neusüss, Dominant Aerosol Chemical Components and Their Contribution to Extinction During the Aerosols99 Cruise Across the Atlantic, *Journal of Geophysical Research,* **106D**, 20783—20810 (2001).

Voss, K. J., **E. J. Welton**, P. K. Quinn, R. Frouin, M. Reynolds, and M. Miller, Aerosol Optical Depth Measurements During the Aerosols99 Experiment, *Journal of Geophysical Research,* **106D**, 20811—20820 (2001).

Voss, K. J., **E. J. Welton**, J. Johnson, A. Thompson, P. K. Quinn, and **H. R. Gordon**, Lidar Measurements During Aerosols99, *Journal of Geophysical Research* **106D**, 20821—20832 (2001).

Quinn, P. K. , D.J. Coffman, T.S. Bates, T.L. Miller, J.E. Johnson, **E.J. Welton**, C. Neusüss, M. Miller, and P. J. Sheridan, Aerosol Optical Properties during INDOEX 1999: Means, Variability, and Controlling Factors, *Journal of Geophysical Research* (In Press).

Welton, E. J., P. J. Flatau, **K. J. Voss**, **H. R. Gordon**, K. Markowicz, J. R. Campbell, and J. D. Spinhirne, Micro-pulse Lidar Measurements of Aerosols and Clouds During INDOEX 1999, *Journal of Geophysical Research* (In Press).

APPENDIX I

NASA/GSFC Contract No. NAS5-31363

OCEAN OBSERVATIONS WITH EOS/MODIS
Algorithm Development and Post Launch Studies

Howard R. Gordon
University of Miami
Department of Physics
Coral Gables, FL 33124

Plans for FY 01

Preamble

This document describes plans for Fiscal Year 2001 regarding two MODIS Ocean-related algorithms.

A. Retrieval of the Normalized Water-Leaving Radiance (Atmospheric Correction).

B. Retrieval of the Detached Coccolith/Calcite Concentration

Fiscal Year 2001 will be heavily focused on the evaluation and validation of MODIS-derived products. However, as we already know (from theoretical studies and from SeaWiFS) that there are certain situations in which the algorithms are unable to perform properly or that there are items that have not been included in the initial implementation, a portion of our effort will be directed toward algorithm improvement. Thus, we break our effort into two broad components for each algorithm:

- Algorithm Improvement/Enhancement;
- Validation of MODIS Algorithms and Products.

These components will overlap in some instances.

RETREIVAL OF NORMALIZED WATER-LEAVING RADIANCE (ATMOSPHERIC CORRECTION)

Algorithm Evaluation/Improvement

1. *Evaluation/Tuning of Algorithm Performance*

Now that MODIS imagery has become available the process of evaluation of the MODIS performance is underway. Examination of the imagery shows several major challenges that must be dealt with before the imagery can be usefully employed for ocean studies. Among these difficulties are the fact that

- the imagery is striped suggesting that the individual detectors in each band have different sensitivities,
- that the severity of the striping appears to depend on the scan angle, and
- that there is excessive sun glint in the imagery in the tropics.

We have been working with R. Evans and the RSMAS group to alleviate these problems. This collaboration will continue. Once the principal radiometric challanges are overcome, we will use the MOBY and MOCE-6 data to initialize the overall radiometric calibration. After this initialization procedure, the imagery will be examined on a regular basis to ensure that the algorithms and the instrument are operating properly. Specifically, the sensor-algorithms should provide the expected "clear water radiances" [Gordon and Clark, "Clear water radiances for atmospheric correction of coastal zone color scanner imagery," *Applied Optics*, **20**, 4175-4180, 1981] in the blue-green region of the spectrum, and should retrieve water-leaving radiances that agree with measurements at the MOBY site [Clark *et al.*, "Validation of Atmospheric Correction over the Oceans," *Jour. Geophys. Res.*, **102D**, 17209-17217, 1997]. Any deviation from expectation or measurement must be reconciled. Deviations could be due to time dependence of the sensor calibration coefficients (i.e., instability in the sensor's radiometric response), improper initialization, improper correction for the sensor's polarization sensitivity, etc. Such analysis of necessity involves a statistical study of the derived water-leaving radiances with sufficient observations to unravel possible effects due to viewing angle, solar zenith angle, and other factors that could influence the retrievals. In addition, the performance of the atmospheric correction algorithm will be carefully studied. For example, does the algorithm choose candidate aerosol models that do not vary significantly from pixel to pixel? Such variation could indicate poor performance of the sensor in the NIR. Do the models that are chosen suggest that $\varepsilon(749,869)$ is undergoing a systematic variation with time? Such a variation would indicate that the radiometric response of the sensor is varying in time.

These studies will enable the algorithms to be tuned to the sensor and, in the event of an expected degradation in the sensor response, provide the necessary corrections to the response.

2*. Implement the Initial Algorithm Enhancements*

Several algorithm enhancements were planned for implementation into the processing stream in the immediate post-lanch era. Among those implemented since launch are

1. the addition of wind-induced surface roughness effects in the computation of the Rayleigh-scattering contribution to the top-of-atmosphere radiance, and
2. our correction of the MODIS residual polarization sensitivity [Gordon, Du, and Zhang, "Atmospheric correction of ocean color sensors: analysis of the effects of residual instrument polarization sensitivity," *Applied Optics*, **36**, 6938-6948] using MCST/SBRS-supplied MODIS polarization sensitivity characterization data.

As mentioned in Section 1, examination of MODIS imagery $\pm 20° - 30°$ from the solar equator reveals significant contamination due to sun glitter, even outside what would normally be considered to be the "glitter pattern." This high glint contribution is particularly troublesome at the MOBY site, which is used to monitor the performance and calibration of MODIS. Thus to fully utilize the MOBY site, and to extend the usefulness of MODIS imagery in these areas, we need to remove as much of the sun glint contribution as possible. At present the glitter pattern is masked using computations described in our ATBD. This mask needs to be refined into a validated scheme for removing sun glint. This will be a major focus of our enhancement effort.

3. Study Future Enhancements

The principal focus of enhancing the basic algorithms are absorbing aerosols. We consider correcting for absorbing aerosols to be the most important of the unsolved atmospheric correction issues because it has such a significant impact in many geographical areas. Algorithms to effect such correction are under intense development now. Among the possibilities we are studying are the spectral matching algorithm (SMA) [Gordon, Du, and Zhang, "Remote sensing ocean color and aerosol properties: resolving the issue of aerosol absorption," *Applied Optics*, **36**, 8670-8684 (1997)], the spectral optimization algorithm SOA [Chomko and Gordon, "Atmospheric correction of ocean color imagery: Use of the Junge power-law aerosol size distribution with variable refractive index to handle aerosol absorption," *Applied Optics* , **37**, 5560-5572 (1998)], and application of a model of Saharan dust transported over the ocean by the winds that is currently in the testing phase (Moulin *et al.*, in preparation).

The SMA is now being studied extensively because it can be added to the present MODIS algorithm with minor impact, as it uses the same look-up-tables (LUTs) as the existing algorithm. Another attractive feature is that it is completely compatible with our present plans for dealing with wind-blown desert dust. We plan to implement this algorithm in phases. In the first phase, the algorithm will be used to provide a flag that signals the presence of absorbing aerosols. In the second phase, the SMA will actually perform the atmospheric correction and retrieve the ocean products. In the third phase, it will be applied to wind-blown dust. Our goal is to implement all three phases during FY00. A question that needs to be resolved is whether or not the SMA, which employs a semi-analytic model of ocean color [Gordon *et al.*, "A Semi-Analytic Radiance Model of Ocean Color," *Jour. Geophys. Res.*, **93D**, 10909-10924, 1988], is compatible with more sophisticated ocean color models, e.g., Lee *et al.* ["Method to derive ocean absorption coefficients from remote sensing reflectance," *Applied Optics*, **35**, 453—462, 1996] or Garver and Seigel ["Inherent optical property inversion of ocean color spectra and its biogeochemical interpretation: 1 time series from the Sargasso Sea," *Geophys. Res.*, **102C**, 18607—18625, 1997].

The SOA is attractive in that it does not require detailed aerosol models to effect atmospheric correction and it has been successfully operated off the U.S. East Coast using the Garver and Seigel [1997] model for the ocean's reflectance. Unfortunately, its efficacy in dealing with wind-blown desert dust, which displays absorption that varies strongly with wavelength, is unclear. The performance of this algorithm will be studied in parallel with the SMA development.

There are two additional enhancements that are now in the research phase: (1) developing an accurate model of the subsurface upwelling radiance distribution as a function of view angle, sun angle, and pigment concentration, and (2) evaluating the performance of the SMA and SOA algorithms in the presence of high concentrations of colored dissolved organic matter (CDOM). The study of these will continue during FY 2000.

Most validation measurements of upwelled spectral radiance (BRDF) in the water are made viewing in the nadir direction. In contrast, ocean color sensors are usually non-nadir viewing. Thus, an important question is how does one validate the sensor performance when the quantity being measured differs from the quantity being sensed? Obviously, one must either correct the validation measurement to the correct viewing angle of the sensor, or correct the sensor observation to what it would be if the view were nadir. Either strategy requires a model of the subsurface radiance distribution. We are using measurements made near the MOBY site to develop such a model. We started using the model of Morel and Gentili ["Diffuse reflectance of oceanic waters. II. Bidirectional aspects," *Applied Optics*, **32**, 6864—6879 (1993)]; however, that model did not agree well with the experimental results. We are now trying to understand the source of the disagreement by examining processes left out of the computation of the radiance distribution, such as instrument self-shadowing and polarization. Once a model of the BRDF is available, we will use it to correct the diffuse transmittance for BRDF effects as described by Yang and Gordon ["Remote sensing of ocean color: Assessment of the

water-leaving radiance bidirectional effects on the atmospheric diffuse transmittance," *Applied Optics*, **36**, 7887-7897 (1997)].

Initial work with MODIS imagery shows a pronounced asymmetry in the normalized water-leaving radiance in the visible across the scan (higher on the east). This is exactly what might be expected from water BRDF affects. Thus the BRDF will be given more attention than we felt was justified prior to acquiring the initial MODIS imagery.

The SMA and the SOA identify the presence of absorbing aerosols by using the full spectrum of radiance at the top of the atmosphere (TOA). Typically, absorbing aerosols cause a depression of the TOA radiance in the blue portion of the spectrum. Unfortunately, CDOM in the water leads to a depression in the blue. We are examining the interference of these two effects. Strong interference could limit the usefulness of ocean color sensors in coastal waters where CDOM is high and absorbing aerosols (from urban pollution) are likely to be present.

Validation of MODIS Algorithms and Products

Our participation in validation and initialization exercises requires that an array of instrumentation be maintained and fully operational at all times. Furthermore, data analysis skills need to be maintained as well. Personnel for such maintenance are included in our cost estimates.

4. Participate in MODIS Validation Campaigns

Present plans developed by D. Clark are to have a short validation field campaign in December 2000, followed by a major campaign in the spring of 2001. We will participate in these campaigns by providing several data sets: (1) we shall use our whitecap radiometer [K.D. Moore, K.J. Voss, and H.R. Gordon, "Spectral reflectance of whitecaps: Instrumentation, calibration, and performance in coastal waters," *Jour. Atmos. Ocean. Tech*., **15**, 496-509 (1998)] to measure the augmented reflectance of the water due to the presence of whitecaps; (2) we shall use our radiance distribution camera system (RADS) to measure the BRDF of the subsurface reflectance; (3) we shall employ our micro pulse lidar (MPL) to measure the vertical distribution of the aerosol (of critical importance when absorbing aerosols are present); (4) we shall use our solar aureole cameras and all-sky radiance camera (SkyRADS) to measure the sky radiance distribution to provide the aerosol scattering phase function; and (5) we will measure the aerosol optical depth (AOD). All measurements will be carried out at the station locations with the exception of the MPL which will operate continuously during the campaign. This data will be combined with the data from MOBY to fine tune the sensor and algorithms.

In addition, we will continue to operate our CIMEL station in the Dry Tortugas as part of the Aeronet Network [Holben, *et al*., "AERONET--A federated instrument network and data archive for aerosol characterization," *Remote Sensing of Environment*, **66**. 1-16].

Data from this site will be used to validate MODIS-derived AOD and possibly provide a means to examine the calibration of the near infrared (NIR) spectral bands.

5. Complete Analysis of SeaWiFS Validation Campaign (MOCE-5) Data

We will complete our analysis of the MOCE-5 data acquired in the fall of 1999 simultaneously with SeaWiFS imagery. This data set will serve as a validation platform of the MODIS atmospheric correction algorithm, and a test bed for the more advanced algorithms described in Section 3.

Retrieval of the Detached Coccolith/Calcite Concentration

Algorithm Evaluation/Improvement

1. Evaluation/Tuning of Algorithm Performance

Evaluation of the coccolith/calcite concentration has focused on two sets of observations: a) a coccolithophore bloom which occurred in the Gulf of Maine during the summer of 2000, and b) a large-scale manipulation experiment performed in August, in which 25 tons of coccolith chalk was disseminated into a patch (initial size = $3km^2$). As with the retrieval of normalized water-leaving radiance (above), the coccolith algorithm suffers from the striping and sun glint issues. The Gulf of Maine coccolithophore bloom of 2000 formed in June, and extended well into July. We first observed it during our NASA SIMBIOS cruises aboard the M/S Scotia Prince ferry. During these trips, the acid-labile backscattering increased significantly (to ~50% of the total backscattering). MODIS imagery from this bloom (Fig. 1) showed remarkable detail, and a first look at the acid-labile backscattering values (and assumed calcite-specific backscattering coefficients of the coccoliths) revealed that the algorithm-derived calcite concentrations were reasonable. The true test, however, will await final processing of our coccolith count samples, and suspended calcite analyses (being done by Scripps Analytical Facility on their inductively-coupled atomic absorption spectrometer). These will then be directly compared to the MODIS imagery.

The second part of the algorithm tuning work involved "Chalk-Ex", a large-scale manipulation experiment in which finely ground coccolith chalk was spread into a patch. The ship work was done aboard the R/*V Cape Hatteras* from 4-10 August, 2000. Twenty five cubic yards of the chalk particles (median size = 2µm--the same size as coccoliths) were mixed with seawater, and dispersed into the wake of the research vessel, as it steamed in widening circles. The weather was excellent for the dispersal, with almost completely clear skies, and low winds. The patch was finished late morning on 6 August 2000, and was ~3km in diameter.

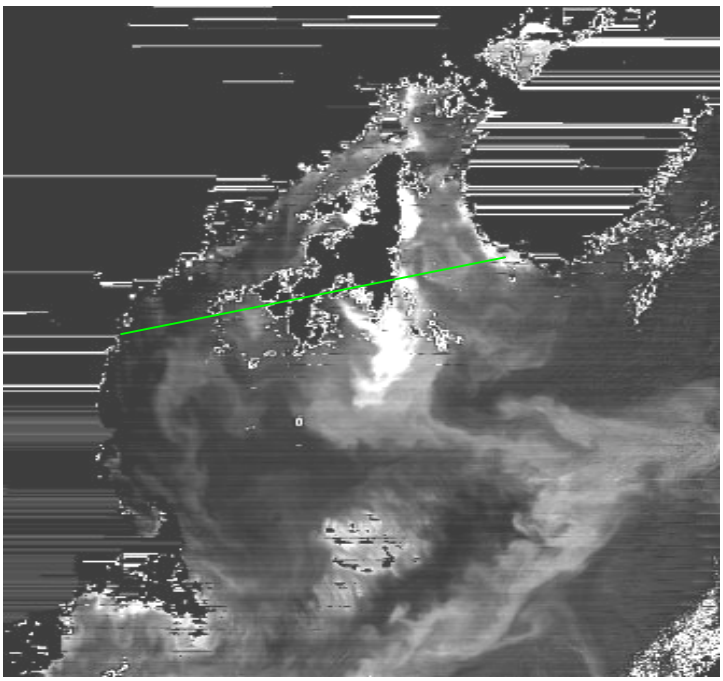

Figure 1- MODIS image of PIC concentration in Gulf of Maine from June 20, 2000. Note advection of coccoliths around northern flank of Georges Bank, with fine-scale eddy structure along the frontal boundary. Scale- White = 3 x 10^{-3} moles PIC m^{-3} ; light grey =2 x 10^{-3} moles PIC m^{-3}; dark grey = 0.75x10^{-3} moles PIC m^{-3}; black = 0-0.1 x 10^{-3} moles PIC m^{-3}. Ferry track is shown with green line.

Unfortunately for Chalk-Ex, there was an unexpected formatting problem aboard MODIS 10h before chalk deployment was to begin (~1800 EDT 5 August). The MODIS operations team discovered that the formatter circuitry was resetting itself (~ 330 resets were observed). There was a mixture of valid and invalid data packets observed for some time afterwhich no valid data packets were sent (6:21 PM EDT (22:21 Zulu)). At approximately 11:30 EDT (August 6, 2000 03:30 Zulu; ~1 hour before the first valid MODIS overpass) MODIS was placed in low power mode with the mirror stopped and survival heaters turned on. The instrument was not turned on again until several days following the mishap, thus, no MODIS imagery was collected of the chalk patch. Fortunately, the chalk patch was observed with SeaWiFS and analyses of the derived backscattering values are being done at this time.

2. Implement the Initial Algorithm Enhancements

The initial coccolith algorithm has been implemented with MODIS data. Gordon et al (1988) first described the scheme to derive coccolith concentrations from estimates

of blue and green water-leaving radiance. The technique essentially uses a ratio algorithm (Gordon and Morel, 1983) to provide a first guess of chlorophyll concentration. Next, for each unique water-leaving radiance and chlorophyll level, a look-up table is consulted (derived from the specific scattering coefficient of calcite coccoliths and chlorophyll, as well as the specific absorption of chlorophyll) which provides an estimate of the $CaCO_3$ concentration. The process is iterated several times until stable chlorophyll and $CaCO_3$ concentration are achieved. This approach has been implemented after MODIS launch and global maps of suspended CaCO3 concentration are now available.

A new three-band algorithm for deriving suspended CaCO3 concentration has been submitted to *Geophysical Research Letters* for publication:

H. R. Gordon, G. C. Boynton, **W. M. Balch**, S. B. Groom, D. S. Harbour , and T. J. Smyth. Retrieval of Coccolithophore Calcite Concentration from SeaWiFS Imagery. *Geophysical Research Letters* (Submitted)

This paper examines blooms of the coccolithophorid *E. huxleyi*, observed in SeaWiFS imagery, with a new algorithm for the retrieval of detached coccolith concentration. The algorithm uses only bands in the red and near infrared (NIR) bands to minimize the influence of the chlorophyll and dissolved organic absorption. We used published experimental determinations of the calcite specific backscattering and its spectral dependence, and assumed that the absorption coefficient of the medium was that of pure water, to estimate the marine contribution to the SeaWiFS radiance. The aerosol (and Rayleigh-aerosol interaction) contribution to the radiance was modeled as an exponential function of wavelength. These allow derivation of the coccolith concentration on a pixel-by-pixel basis from SeaWiFS or MODIS imagery. Application to a July 30, 1999 SeaWiFS image of a bloom south of Plymouth, England indicates that the SeaWiFS estimates are in good agreement with surface measurements of coccolith concentration.

3. Study Future Enhancements

It is anticipated that, provided future algorithm performance is adequately validated, the three-band algorithm will be implemented for use with MODIS data rather than the two band approach (since it is not affected by chlorophyll and dissolved organic matter).

4. Participate in MODIS Validation Campaigns

We plan to continue MODIS-validation work in ’01. At this time, we are planning two 13 ton Chalk-Ex deployments in the summer of 2001. One will be in blue water, SE of Georges Bank. The other patch will be created in a more productive part of the Gulf of Maine (yet to be determined). MODIS will pay for 3d of this cruise, while the Navy will cover the other 11d. A second cruise is planned for November 2001, in which two more 13 ton patches will be deployed in the same locations as during the first cruise. Ship time for the second cruise will be provided completely by the Office of Naval Research. We also will monitor ocean color imagery for Gulf of Maine Blooms. In the event a Gulf of

Maine feature is observed, we will endeavor to sample it. Our ferry program is currently under review to the NASA SeaWiFS program. If funded, we will collect more coccolithophore data from the ferry during twelve cruises in 2001. These data will be used in MODIS validation.

APPENDIX II

MOD 18 Normalized Water-leaving Radiance

Howard R. Gordon and Many Others*

University of Miami

MODIS SCIENCE TEAM MEETING Dec. 2001

*R. Evans, E. Kearns, K. Kilpatrick, and RSMAS Remote Sensing Laboratory staff.

MOD 18 Normalized Water-leaving Radiance

Howard R. Gordon and Many Others*

University of Miami

MODIS SCIENCE TEAM MEETING Dec. 2001

R. E*vans, E. Kearns, K. Kilpatrick, K. Voss and RSMAS Remote Sensing Laboratory staff.

Atmospheric Correction

$$\rho_t(\lambda) = \rho_r(\lambda) + \rho_{A(\lambda)} + t(\lambda)\rho_w(\lambda)$$

Note: $\rho_w(765) \approx \rho_w(865) \approx 0$, and define

$$\varepsilon^{MS}(765,865) = \frac{\rho_t(765) - \rho_r(765)}{\rho_t(865) - \rho_r(865)}$$

The correction algorithm then does the following

$$\varepsilon^{MS}(765,865) \Rightarrow \varepsilon^{SS}(765,865) \Rightarrow \textit{Aerosol Model}$$
$$\Rightarrow \varepsilon^{SS}(\lambda,865) \Rightarrow \varepsilon^{MS}(\lambda,865)$$

$$\rho_{A(\lambda)} = \varepsilon^{MS}(\lambda,865)\rho_{A(865)}$$

Also,

$$\textit{Aerosol Model and } \rho_t(865) - \rho_r(865) \Rightarrow t(\lambda),$$

so

$$\rho_W(\lambda) = t^{-1}(\lambda)\left[\rho_t(\lambda) - \rho_r(\lambda) - \rho_A(\lambda)\right]$$

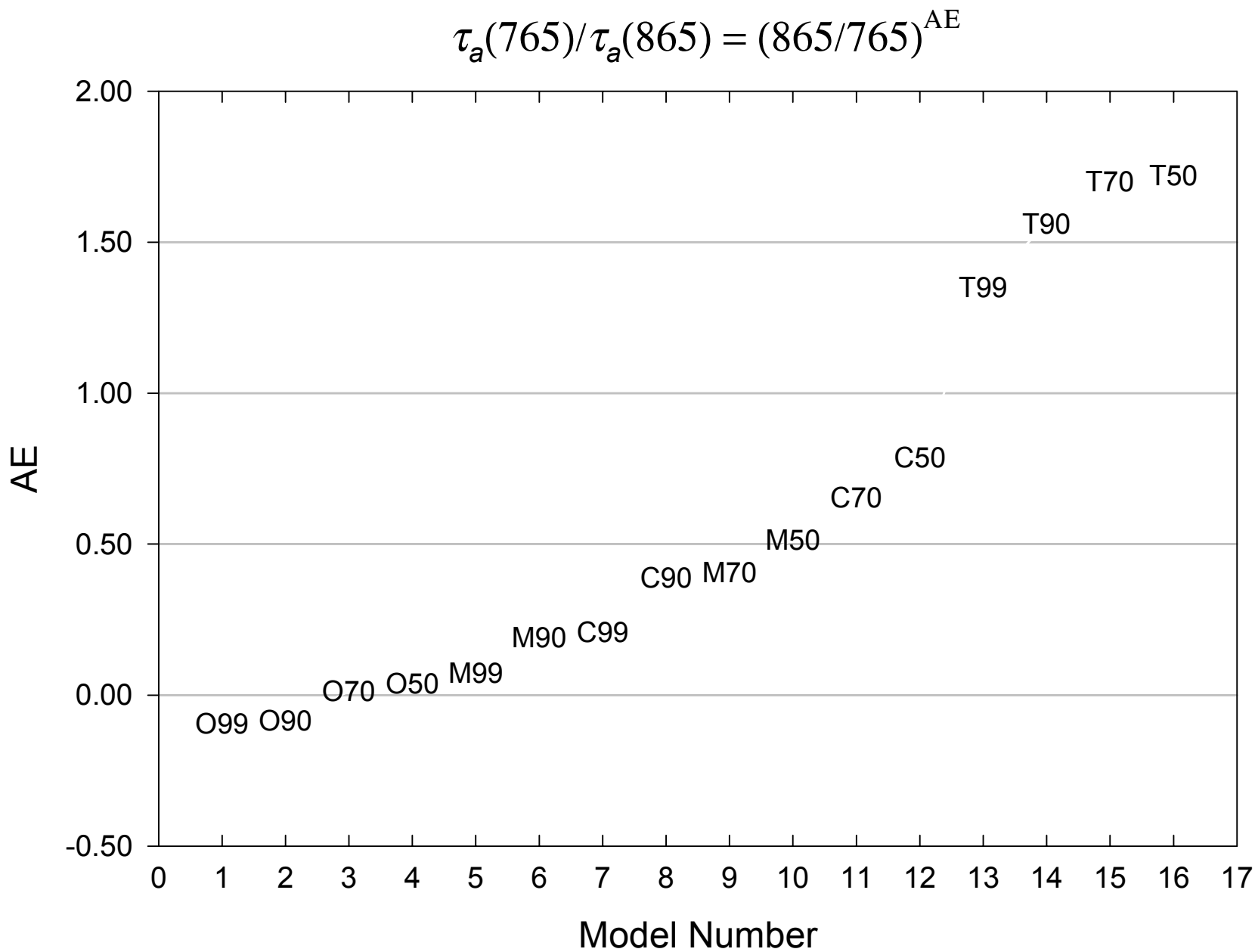
$\tau_a(765)/\tau_a(865) = (865/765)^{AE}$
AE
2.00
1.50
1.00
0.50
0.00
-0.50
0 1 2 3 4 5 6 7 8 9 10 11 12 13 14 15 16 17
Model Number
T70 T50
T90
T99
C50
C70
M50
C90 M70
M90 C99
M99
O70 O50
O99 O90

GOOD CALIBRATION IS REQUIRED

Typical values (clear atmosphere)

λ	$\rho_t(\lambda)$	$\rho_w(\lambda)$
412	0.34	0.040
443	0.29	0.038
488	0.23	0.024
531	0.19	0.009
551	0.15	0.005
670	0.10	0.0004

$\Rightarrow$ Successful operation requires excellent *relative* calibration

POLARIZATON

MODIS polarization sensitivity can lead to significant error:

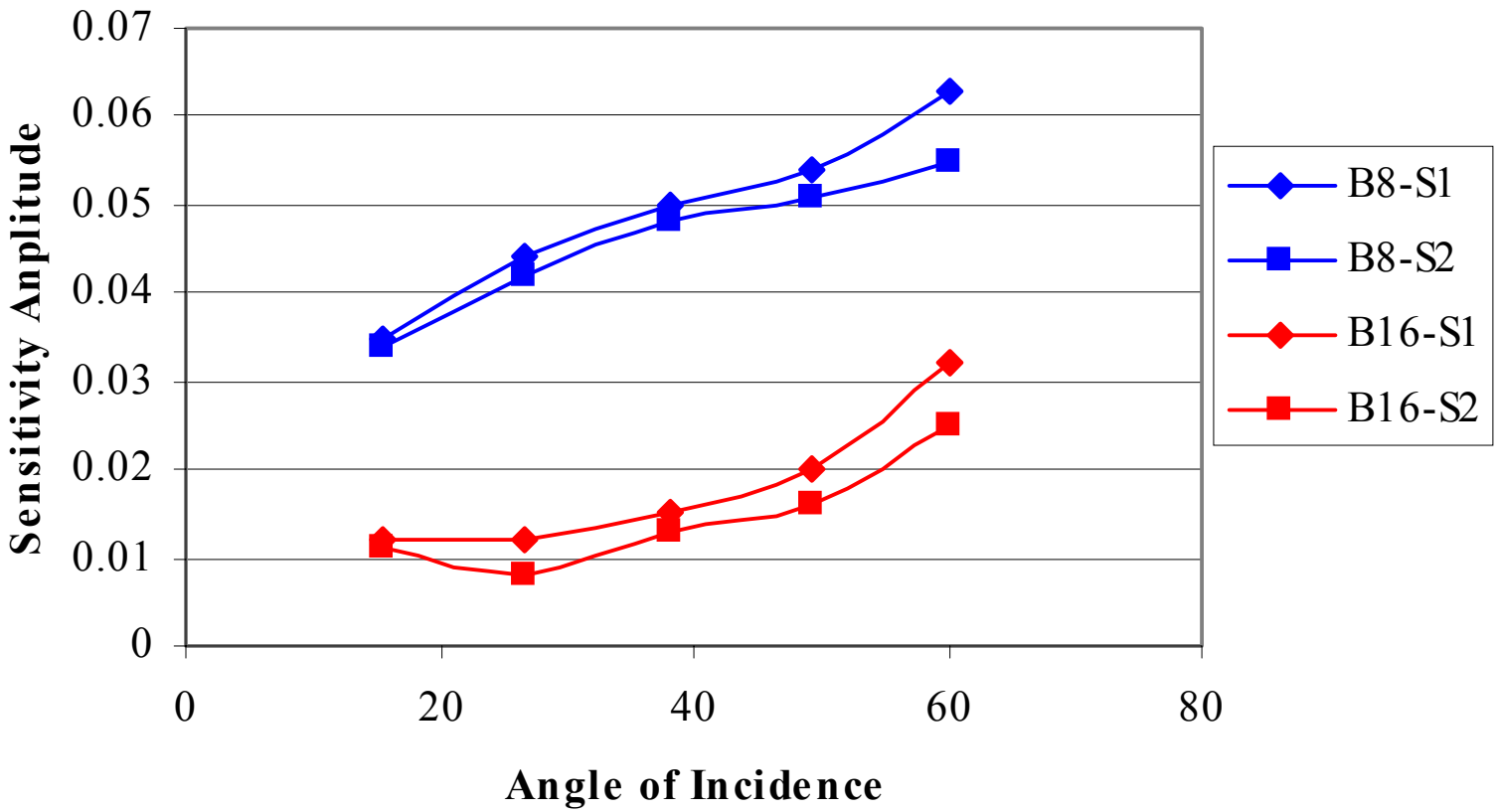

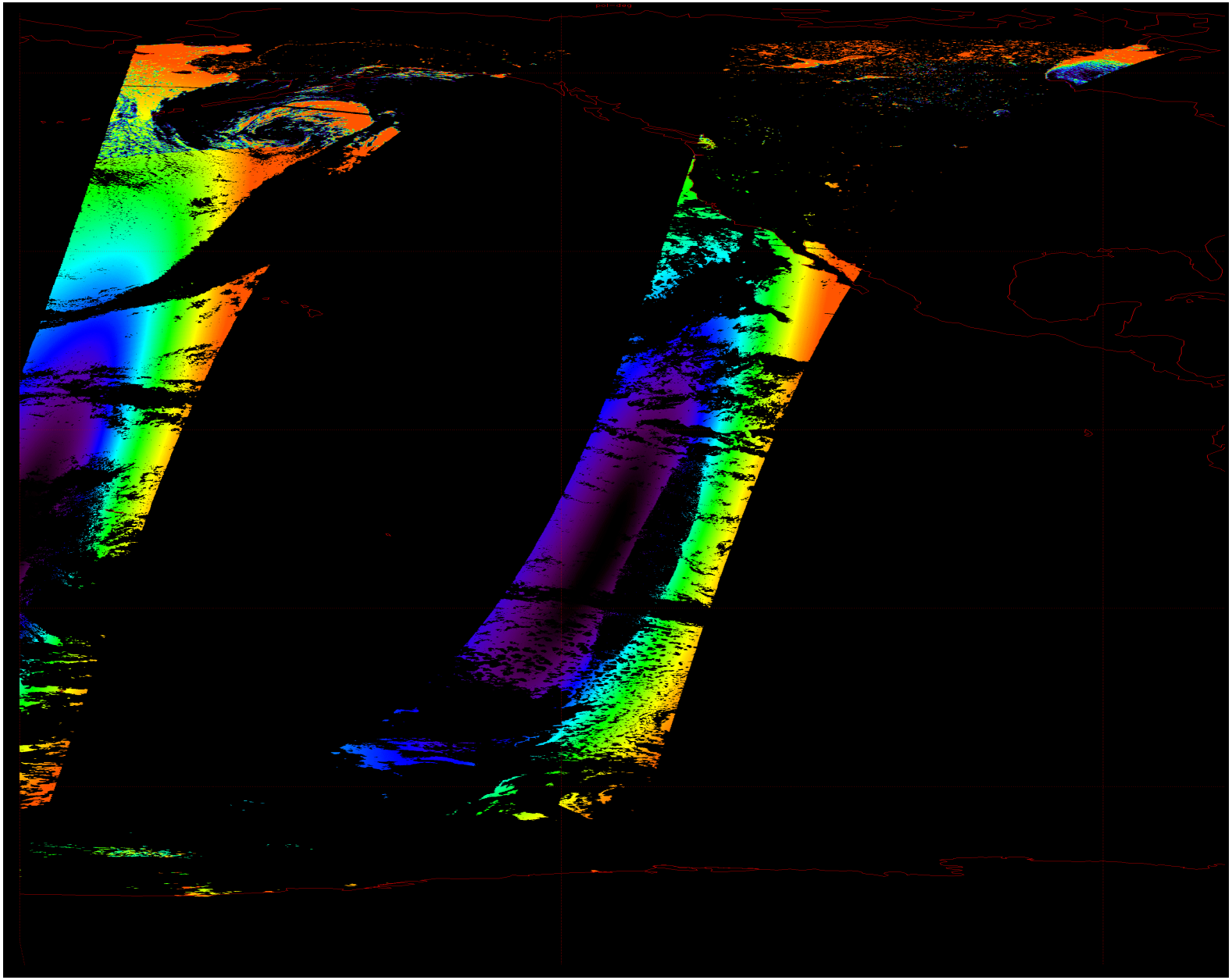

Degree of Polarization (December)

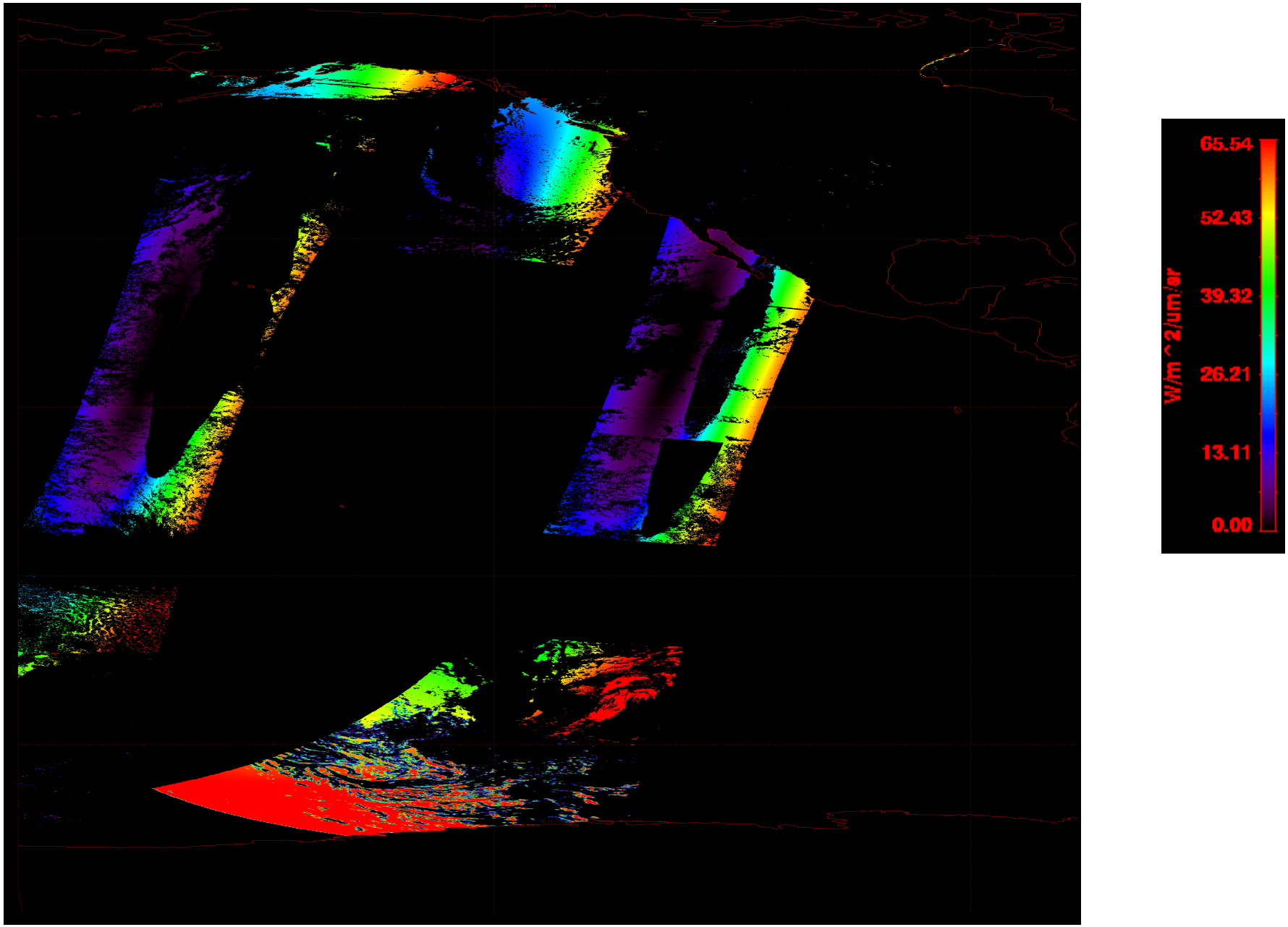

Degree of Polarization (April)

- Original Polarization Sensitivity Correction:
  Assume that $\rho_t(\lambda)$ is polarized in a manner identical to the Rayleigh component $\rho_r(\lambda)$

- Revised Polarization Sensitivity Correction:
  Assume that all of the components of $\rho_t(\lambda)$, other than $\rho_r(\lambda)$, i.e., $\rho_A(\lambda)$ and $\rho_w(\lambda)$, are completely unpolarized.

INDICIA OF ALGORITHM PERFORMANCE

1. Variation of $\varepsilon^{SS}(765,865)$ across the MODIS scan

At a given location and time, $\varepsilon^{SS}(765,865)$ varies in a systematic manner across the scan that is characteristic of each of the candidate aerosol models.

How does $\varepsilon^{SS}(765,865)$ vary across the MODIS scan?

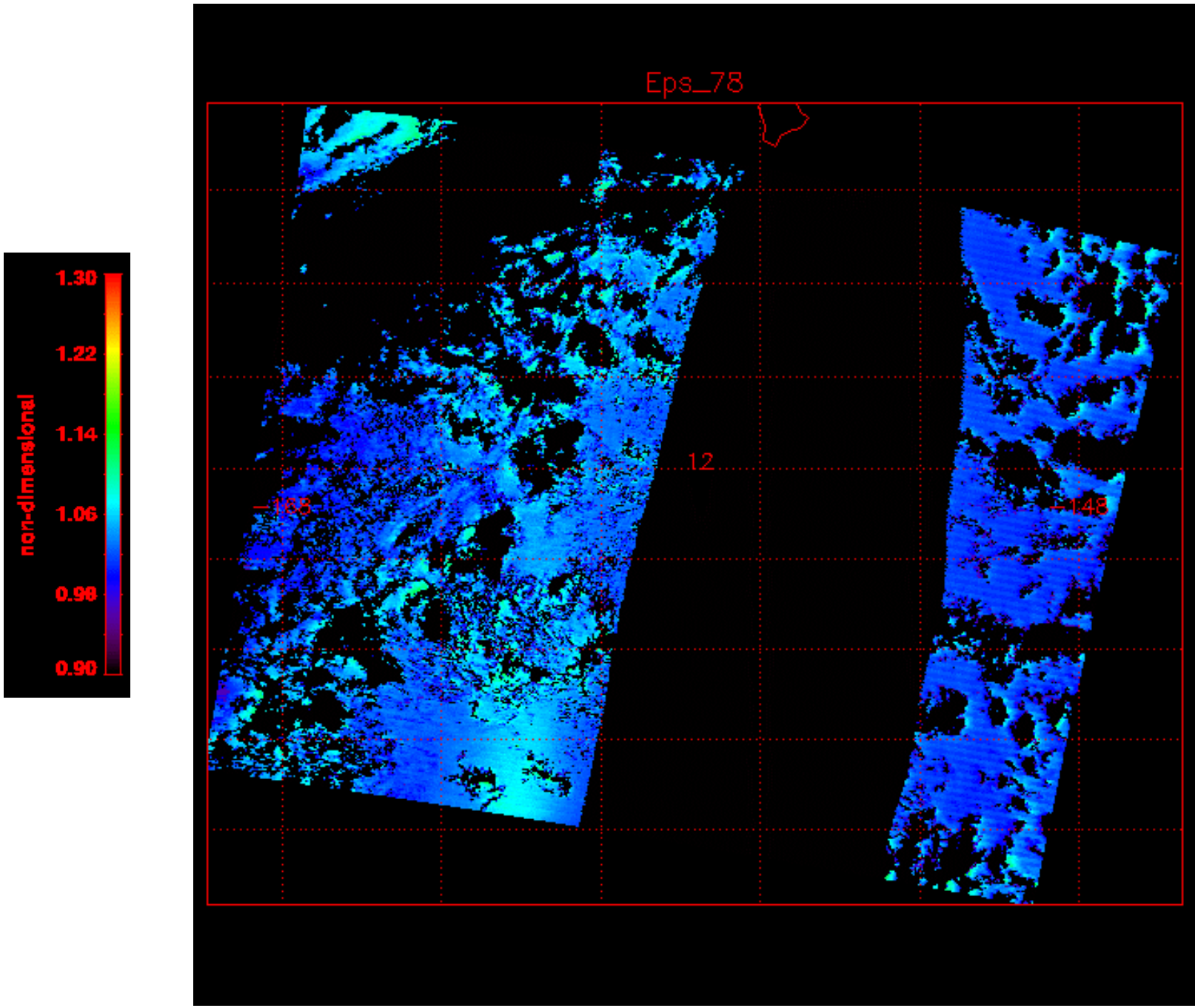
Eps_78
1.30
1.22
1.14
1.06
0.98
0.90
non-dimensional
12
-165
-148

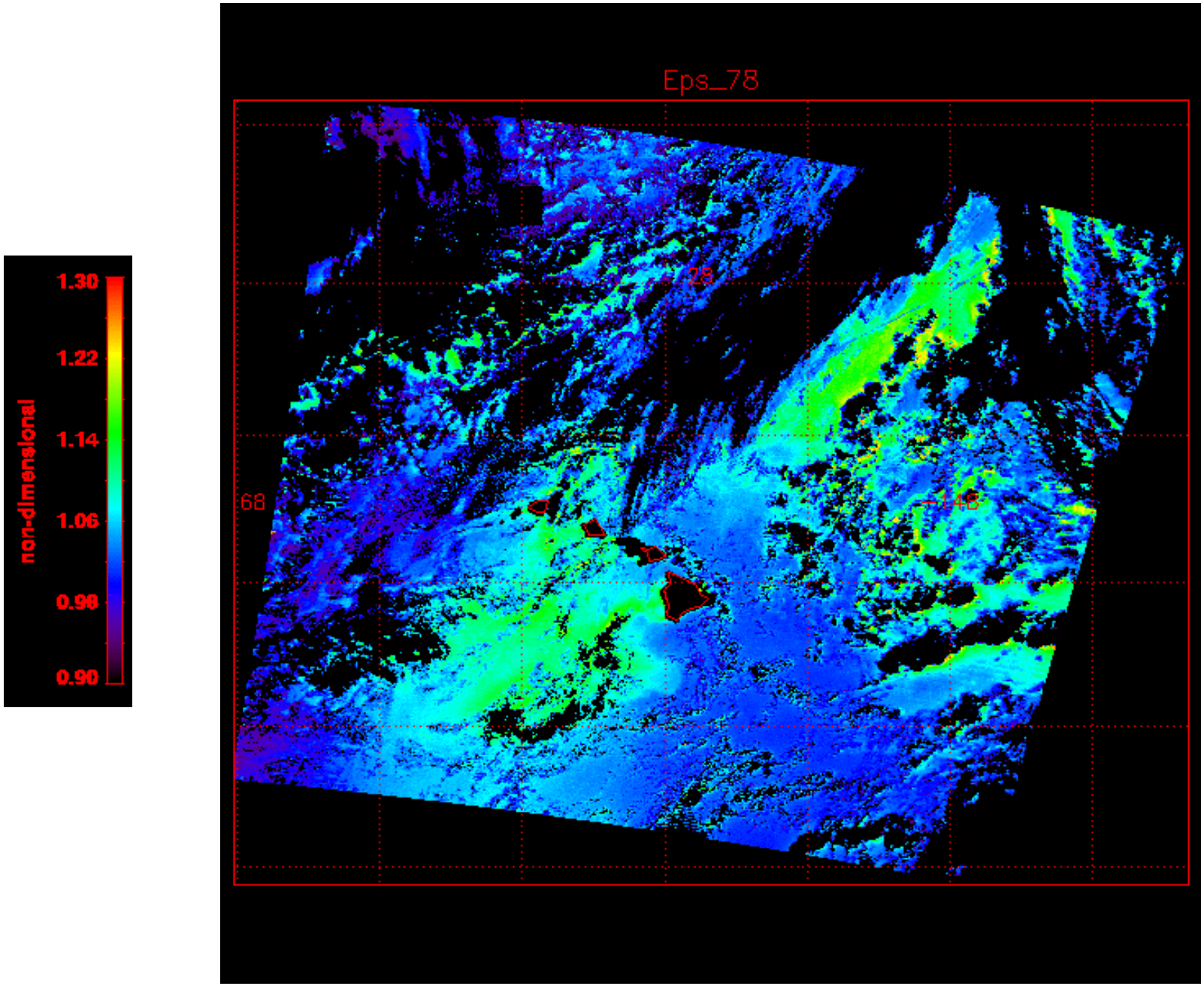
Eps_78
1.30
1.22
1.14
1.06
0.98
0.90
non-dimensional
68

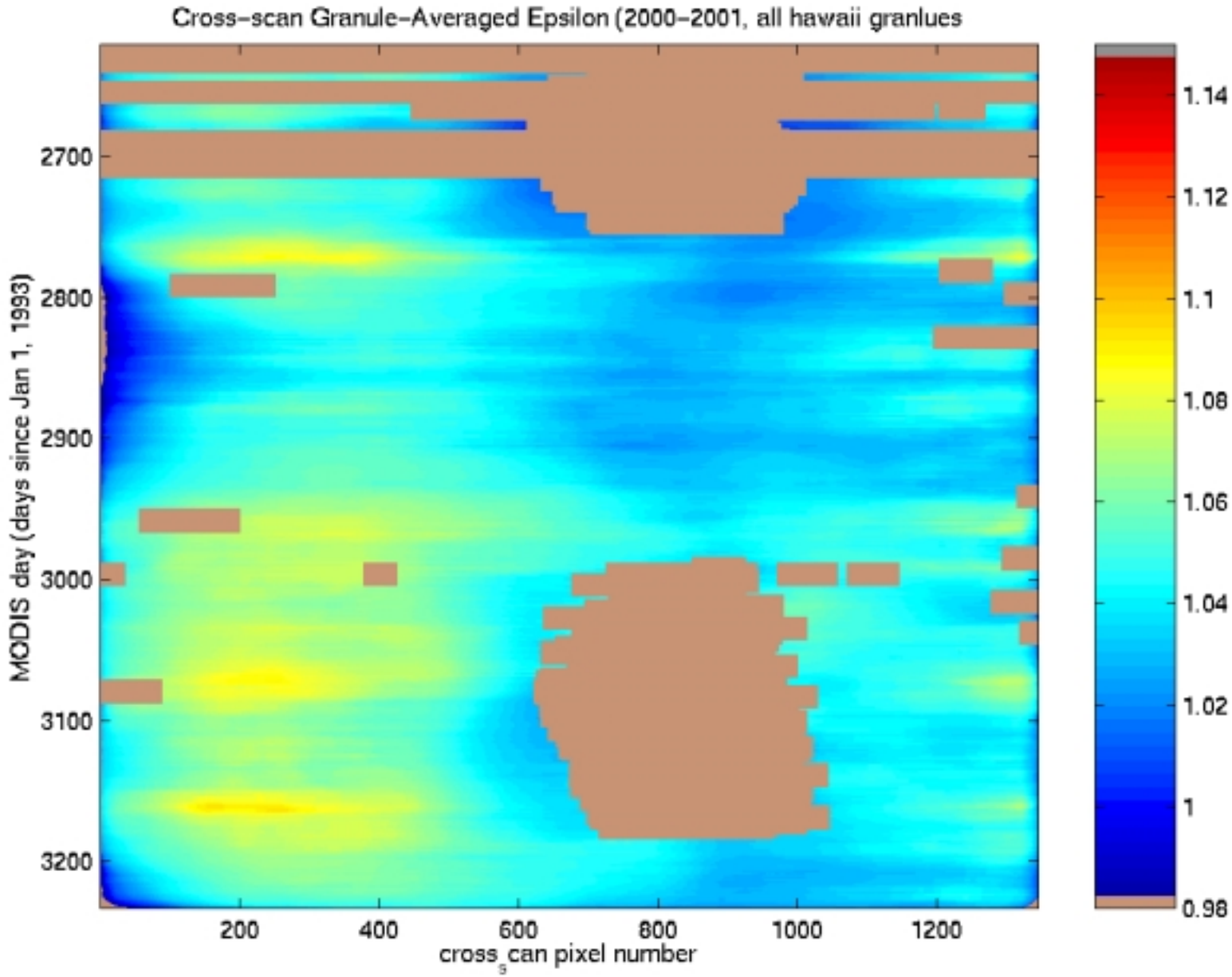
Cross-scan Granule-Averaged Epsilon (2000-2001, all hawaii granlues
MODIS day (days since Jan 1, 1993)
2700
2800
2900
3000
3100
3200
200
400
600
800
1000
1200
cross scan pixel number
1.14
1.12
1.1
1.08
1.06
1.04
1.02
1
0.98

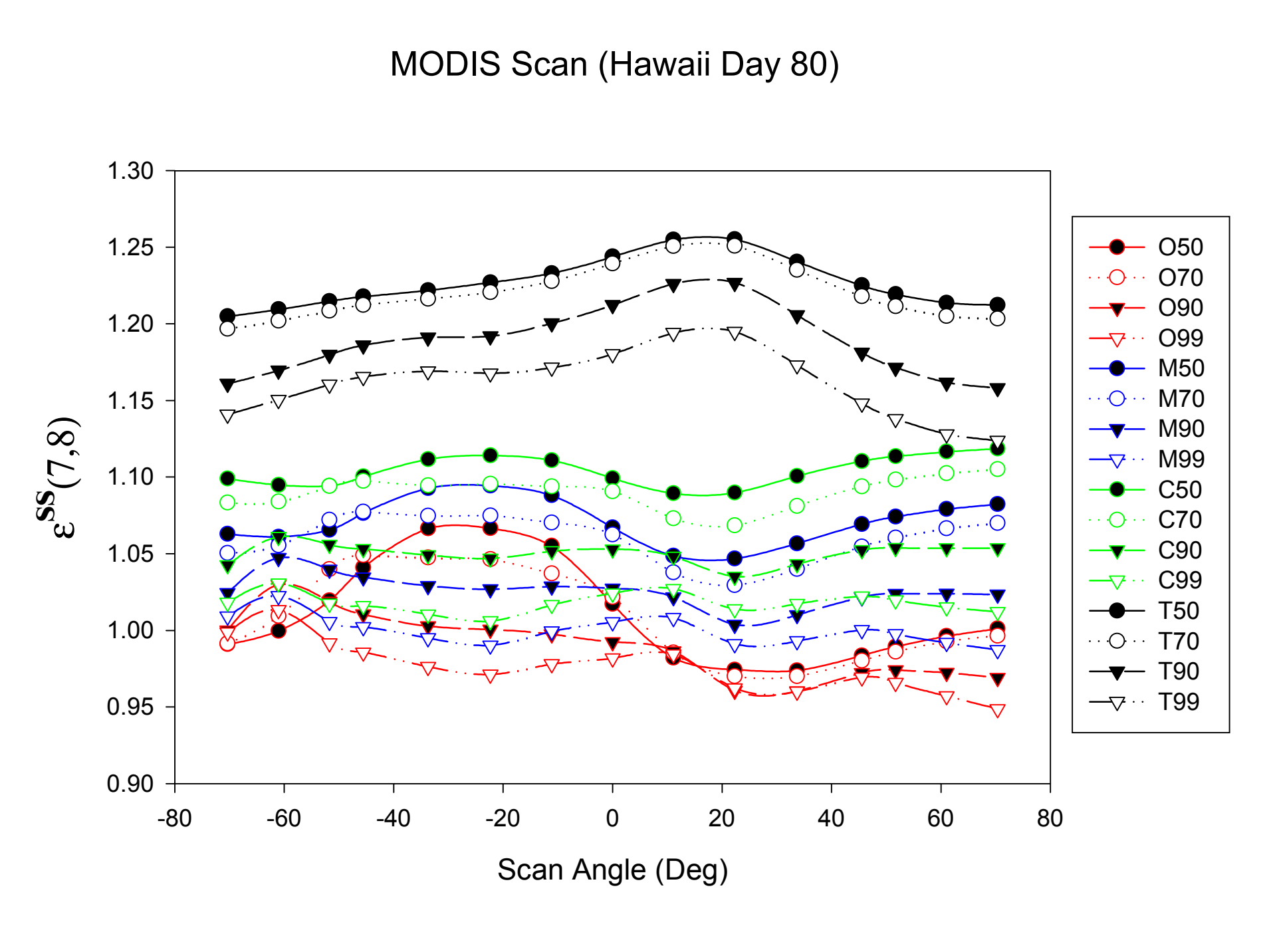
MODIS Scan (Hawaii Day 80)
1.30
1.25
1.20
1.15
1.10
1.05
1.00
0.95
0.90
$\varepsilon^{ss}(7,8)$
-80
-60
-40
-20
0
20
40
60
80
Scan Angle (Deg)
O50
O70
O90
O99
M50
M70
M90
M99
C50
C70
C90
C99
T50
T70
T90
T99

- The fact that $\varepsilon^{SS}(765,865)$ shows the predicted behavior across the scan suggests that the relative calibration of Bands 15 and 16 are very close to correct.

- However, the absolute values of $\varepsilon^{SS}(765,865)$ are a little higher than the range of the models, suggesting that the calibration factor (counts to radiance) of the 765 nm band may be a little too large relative to the 865 nm band.

- Note that changing the relative calibration factors of these two bands will necessitate recalibrating the others as well.

2. Comparison of water-leaving radiance with SeaWiFS

Look at 2000129 off U.S. East Coast

SeaWiFS
Chl *a*

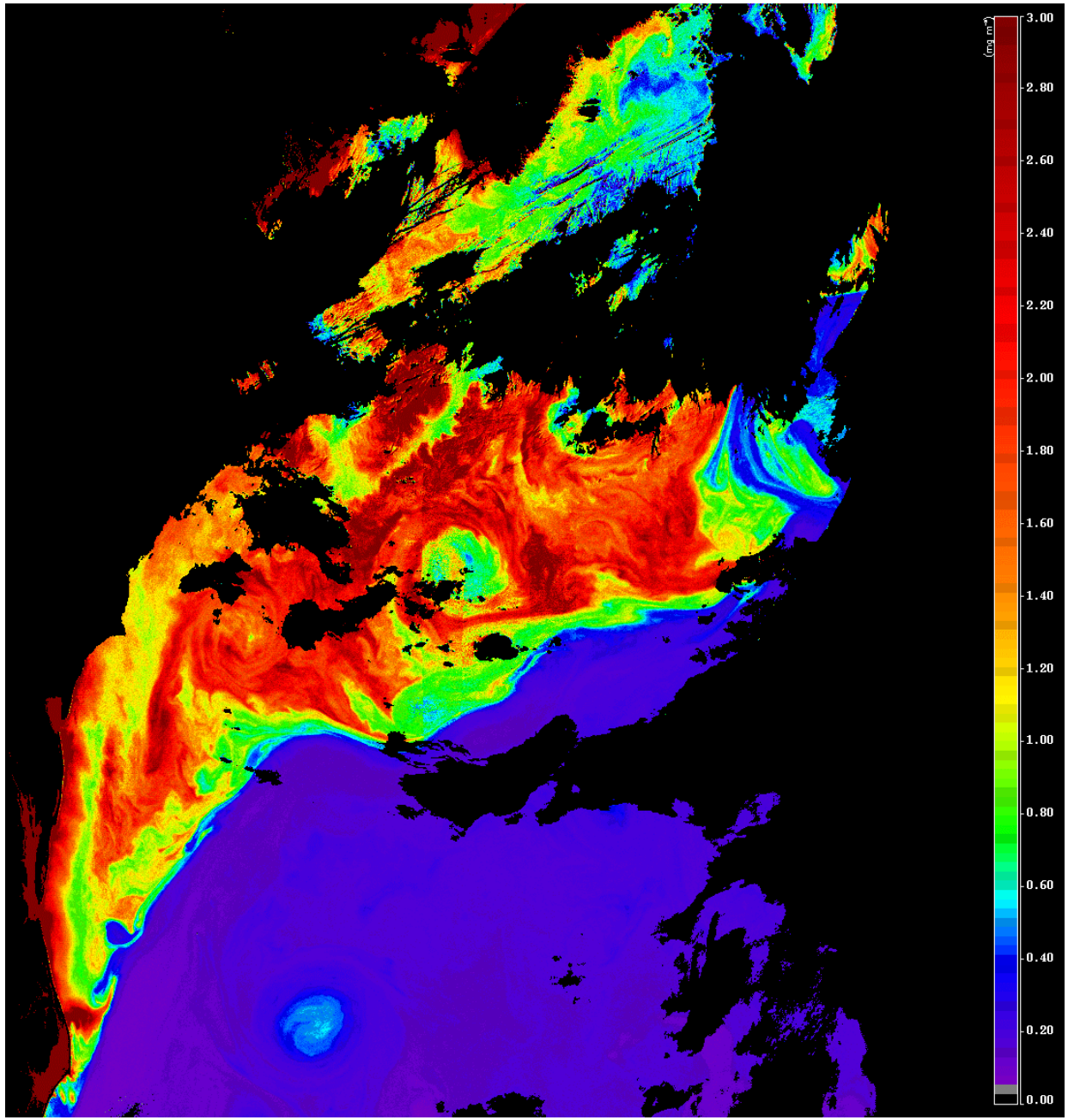

3.00

2.00

1.00

0.00

SeaWiFS

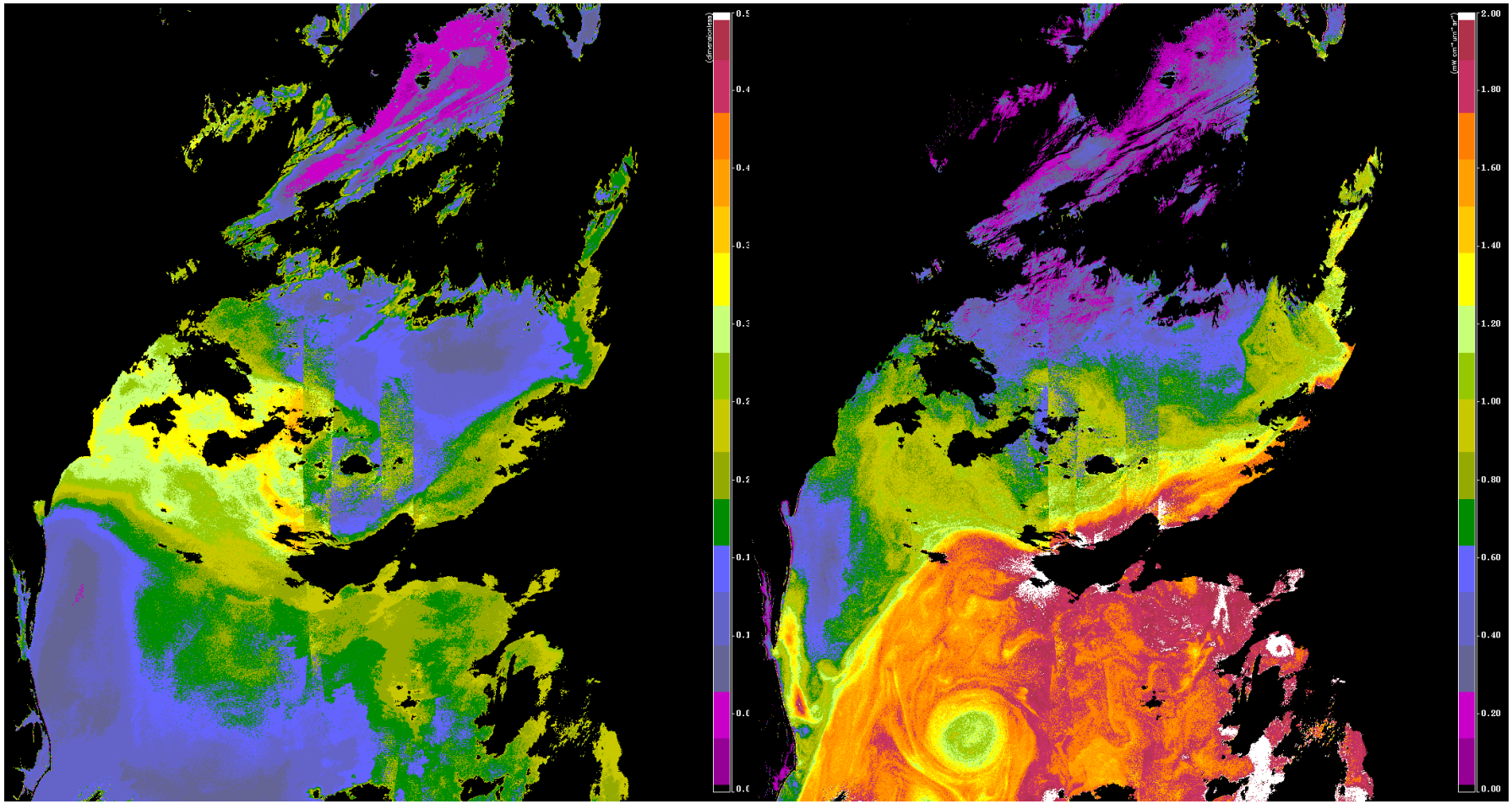

nLw(443)

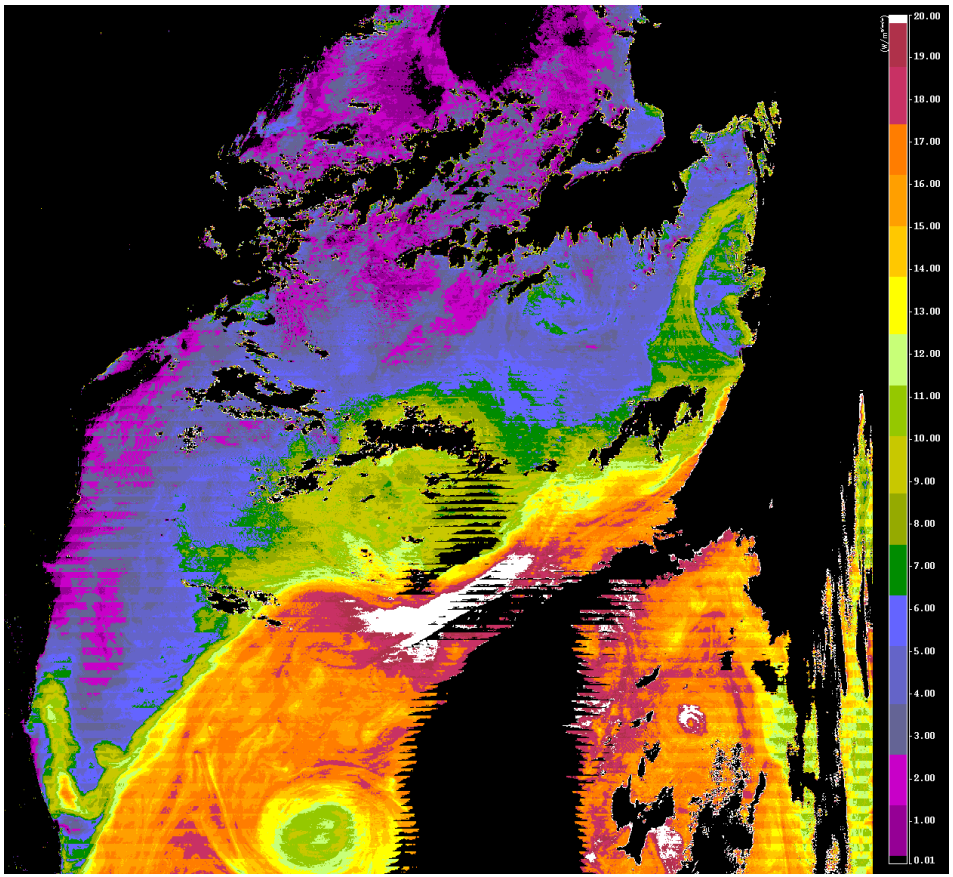

MODIS

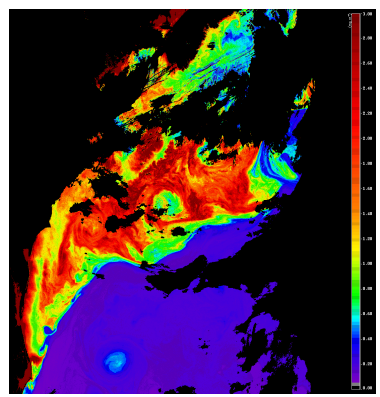

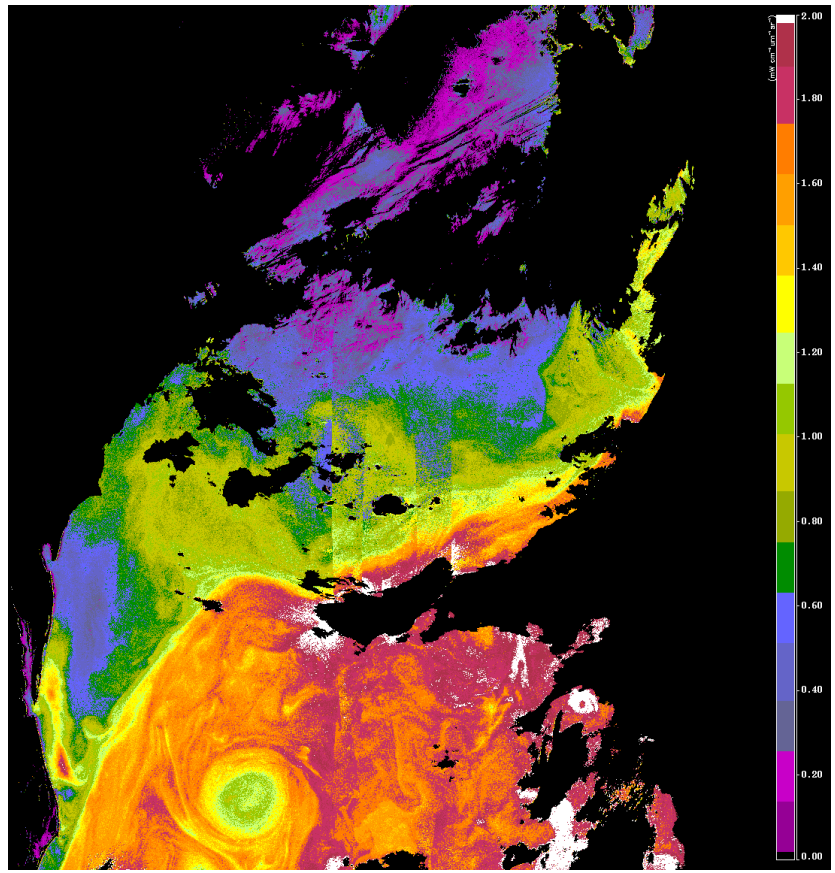

SeaWiFS

MODIS nLw(551)

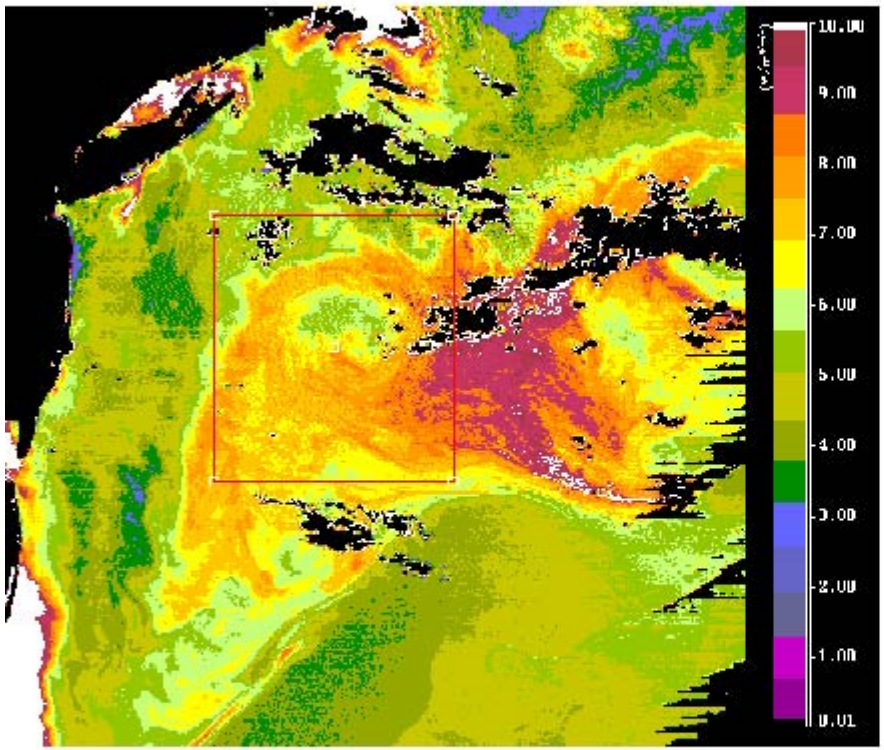

M

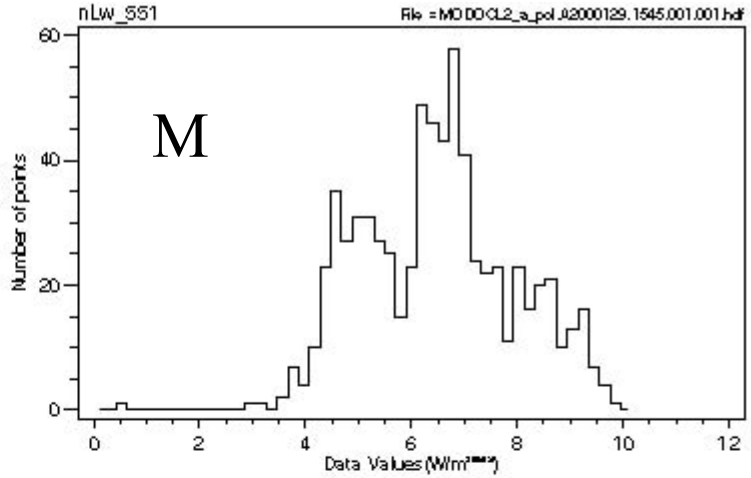

Min : 0.4800
Max : 9.8150
Median: 6.5000

Mean: 6.4849
STD : 1.4340
Mode : 6.8105

Bin size : 0.203000, No. of bins : 50
No. pts selected/No. pts in area : 711/746 (95.3083%)
Area : Blotch = 1

S

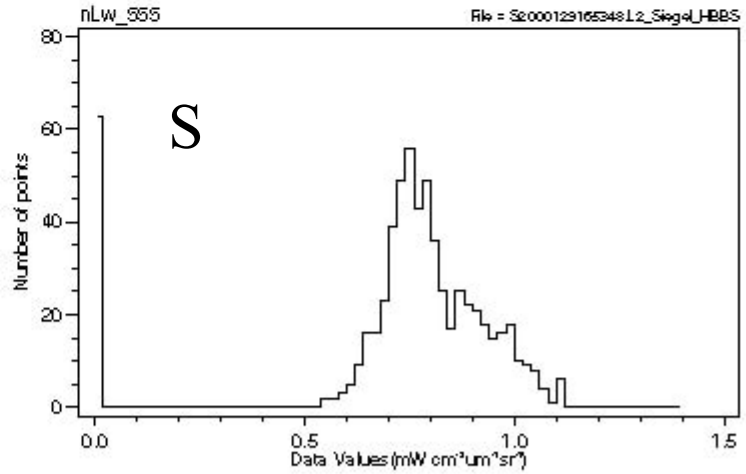

Min : 0.0000
Max : 1.1100
Median: 0.7720

Mean: 0.7285
STD : 0.2662
Mode : 0.0100

Bin size : 0.0200000, No. of bins : 70
No. pts selected/No. pts in area : 626/626 (100.000%)
Area : Blotch = 1

MODIS nLw(551)

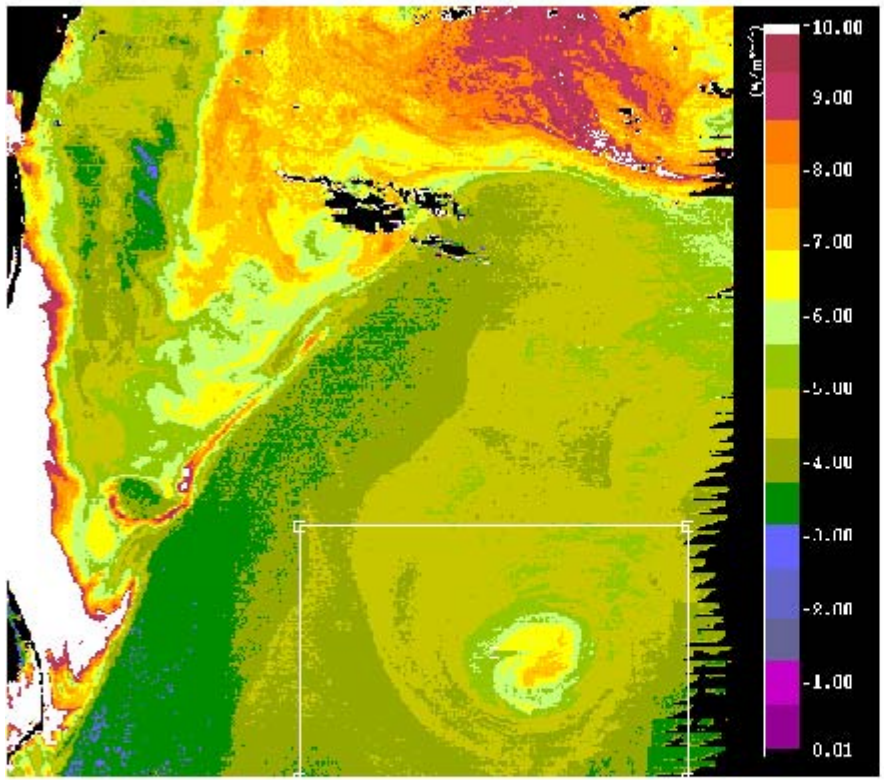

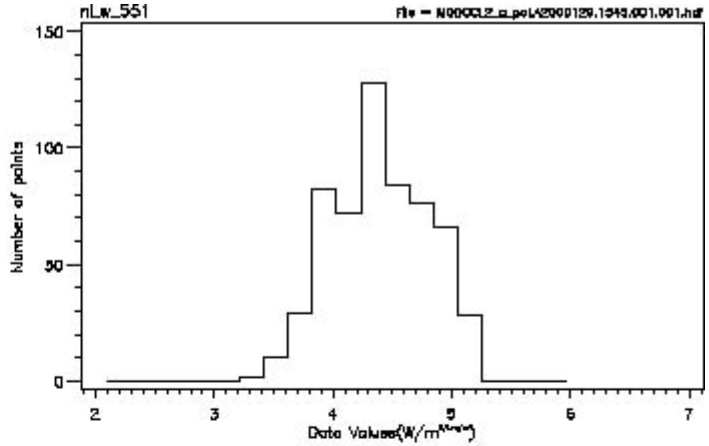

Min : 3.3920
Max : 5.1810
Median: 4.3790
Mean: 4.3988
STD : 0.3992
Mode : 4.3345

Binsize : 0.203000, No. of bins : 20
No. pts selected/No. pts in area : 577/606 (95.2145%)
Area : Blotch color = 7

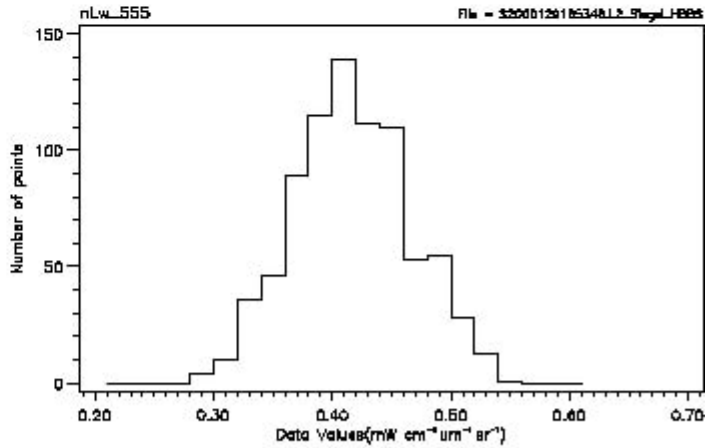

Min : 0.2870
Max : 0.5560
Median: 0.4150
Mean: 0.4173
STD : 0.0489
Mode : 0.4100

Binsize : 0.0200000, No. of bins : 21
No. pts selected/No. pts in area : 810/810 (100.000%)
Area : Blotch color = 7

MODIS nLw(443)

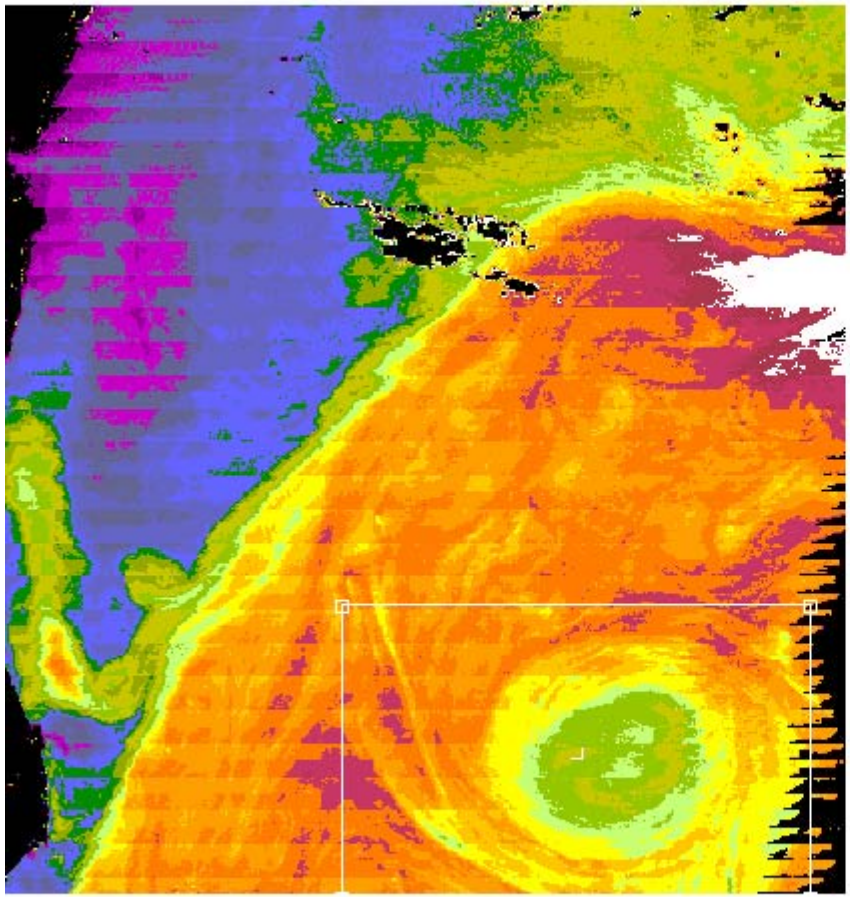

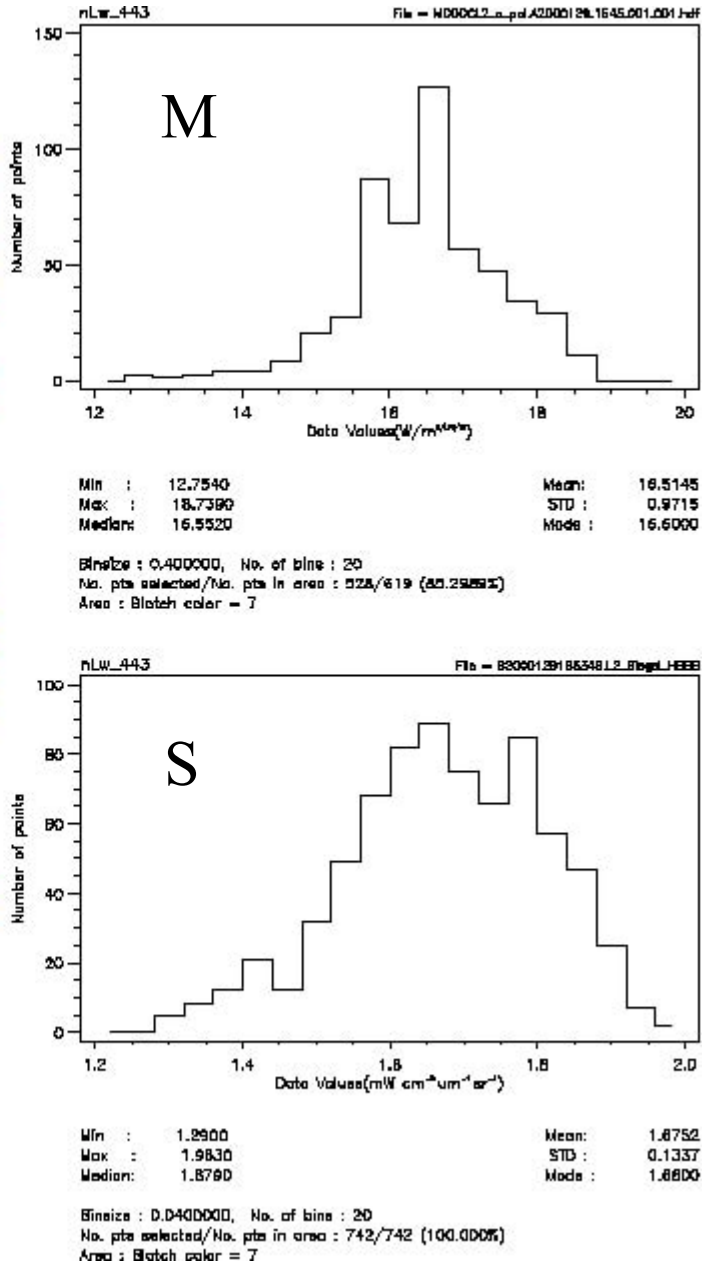

- When AOD(865) < 0.20, there is good agreement between SeaWiFS and MODIS. This implies that the MODIS calibration is very close to being correct.

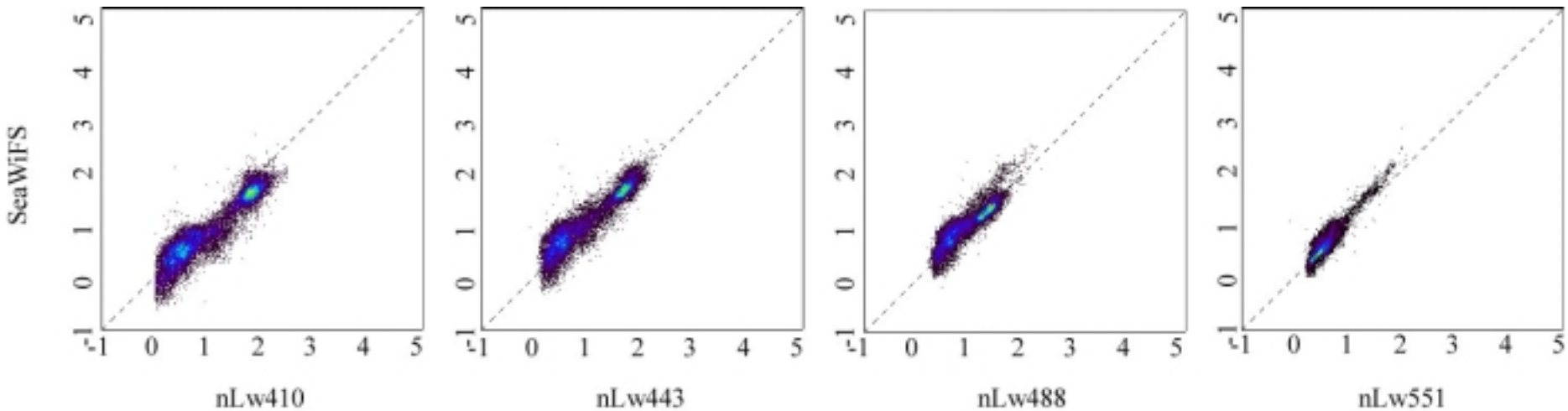

MODIS scene A2000.129.1545
SeaWiFS scene S2000129165158

5apol
Quality 0

$\varepsilon^{SS}(765,865)$

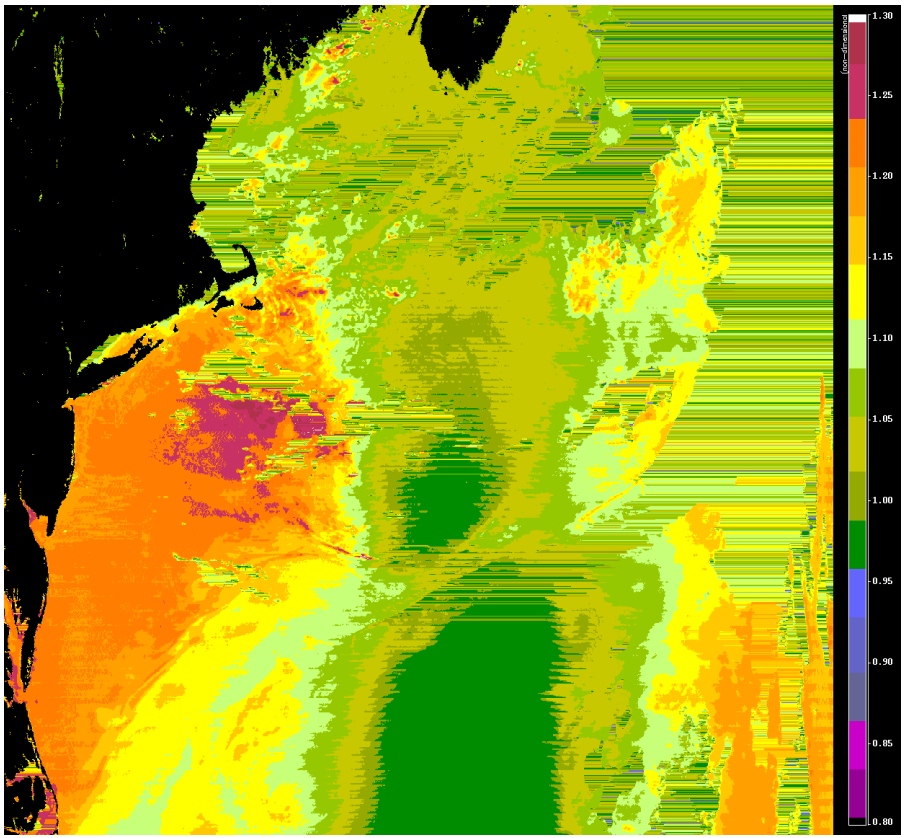

MODIS

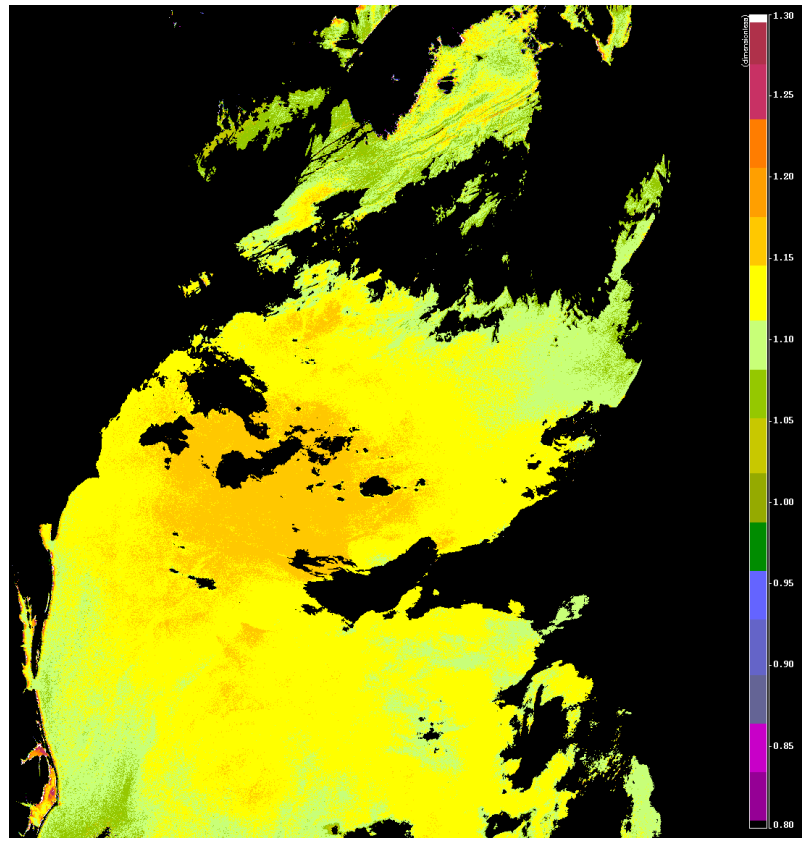

SeaWiFS

1.30

1.05

0.80

AOD(865)

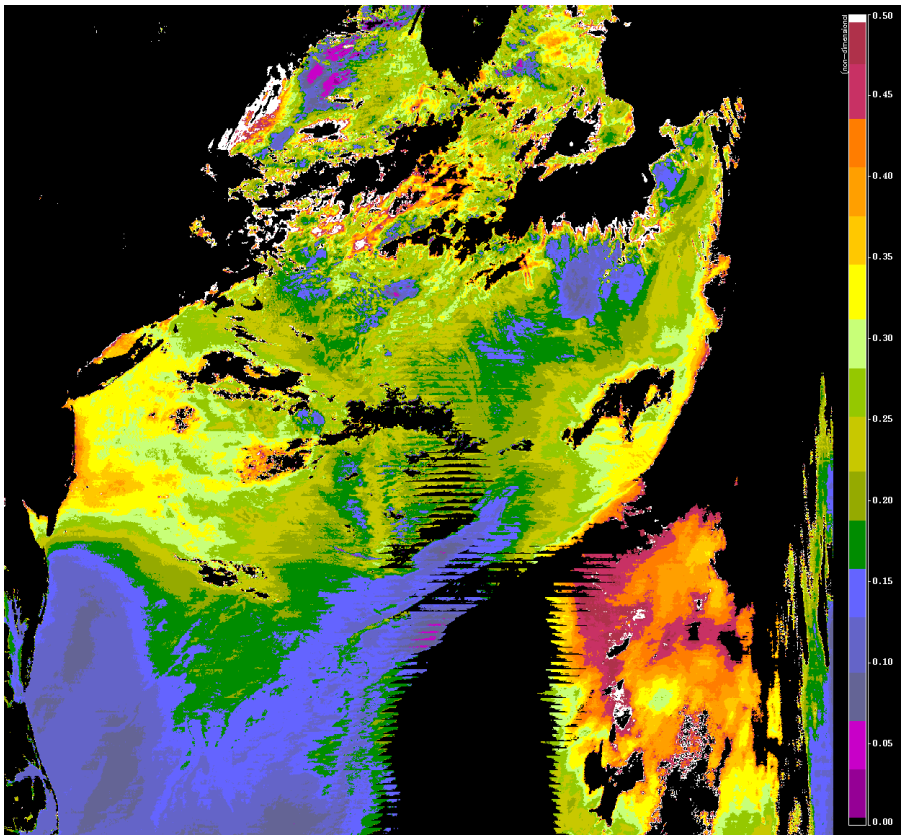

MODIS

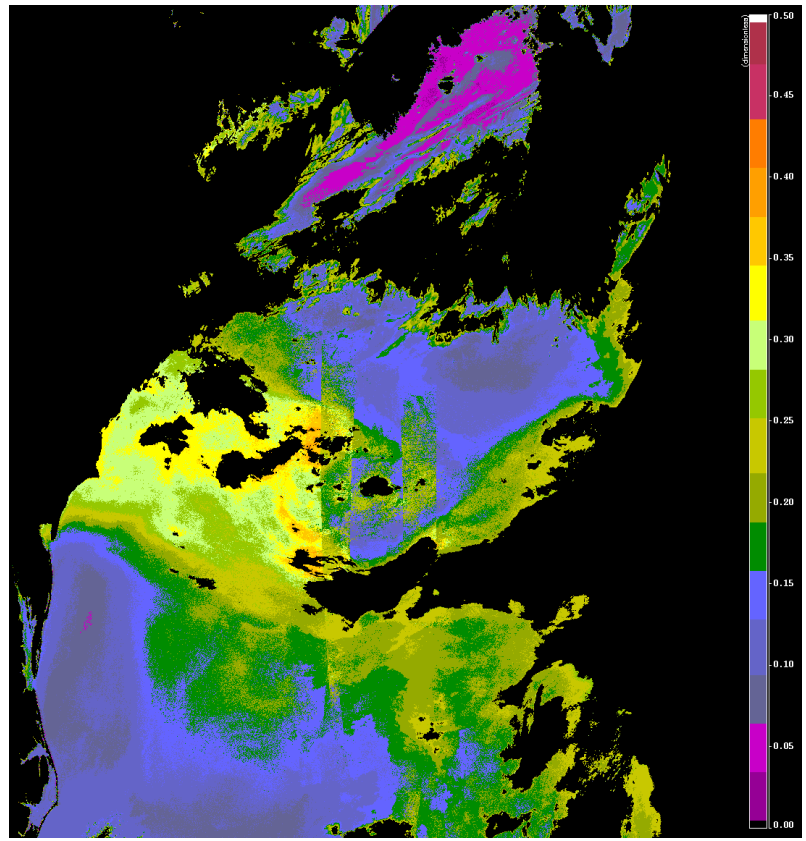

SeaWiFS

0.50

0.25

0.00

- The fact that $\varepsilon^{SS}(765,865)$ shows water structure in 2000129 indicates that there is residual water radiance in the NIR. *Add a correction to the* $\rho_w(765) \approx \rho_w(865) \approx 0$ *assumption. Note, this may increase the processing time.*

- MODIS AOD(865) compares reasonably well with SeaWiFS except in the vicinity of the sun glint.

3. Global Behavior of *nLw*(λ)

- Do the *nLw*'s vary from orbit-to-orbit in an expected manner?

nLw(412) Apr. Quality “All”

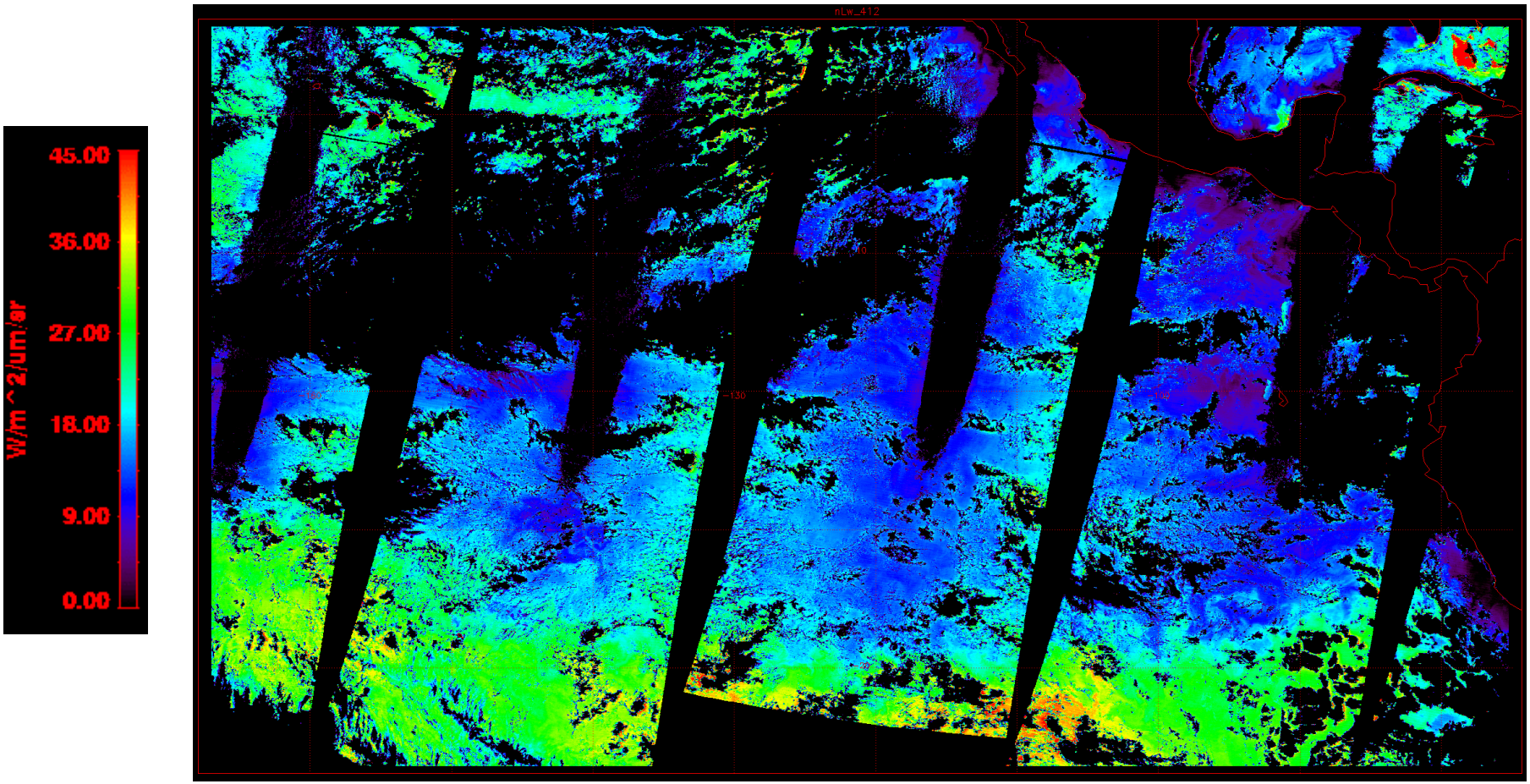

nLw(412) Jun. Quality “All”

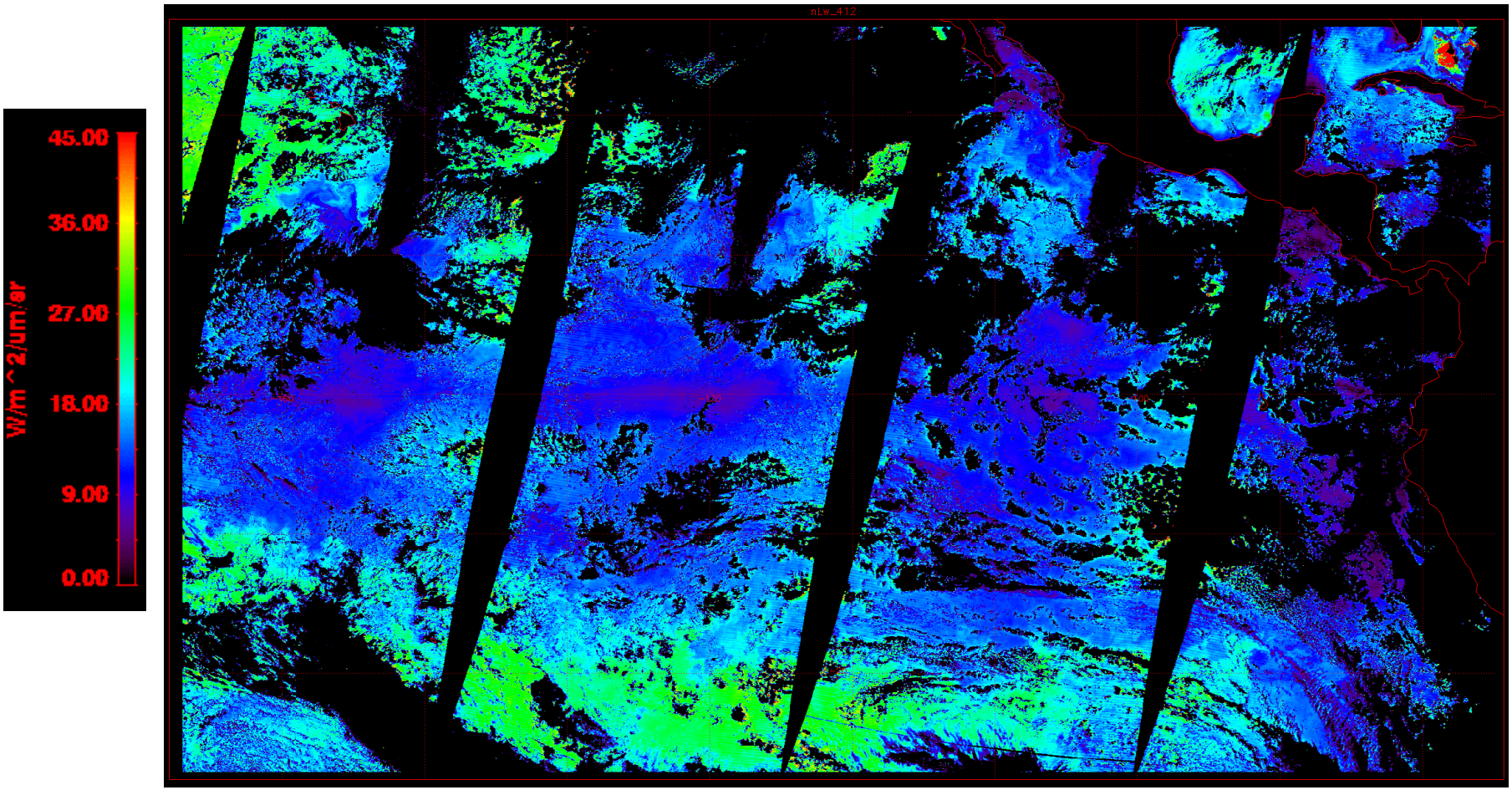

nLw(551) Apr. Quality “All”

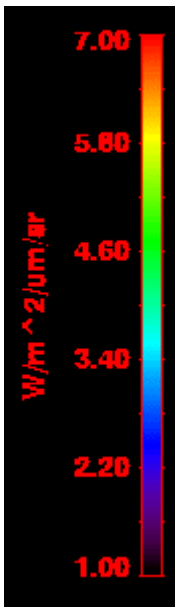

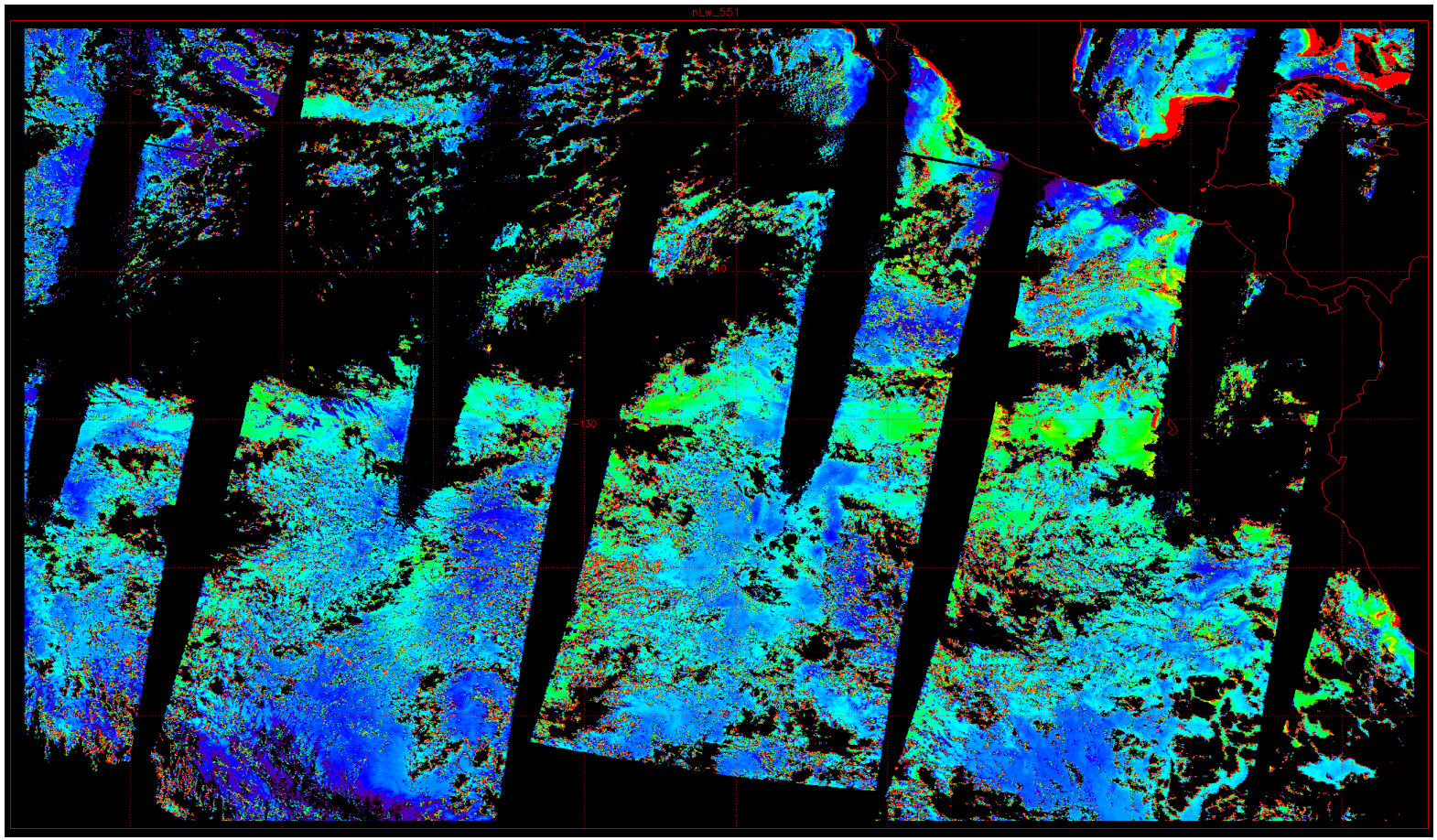

nLw(551) Jun. Quality “All”

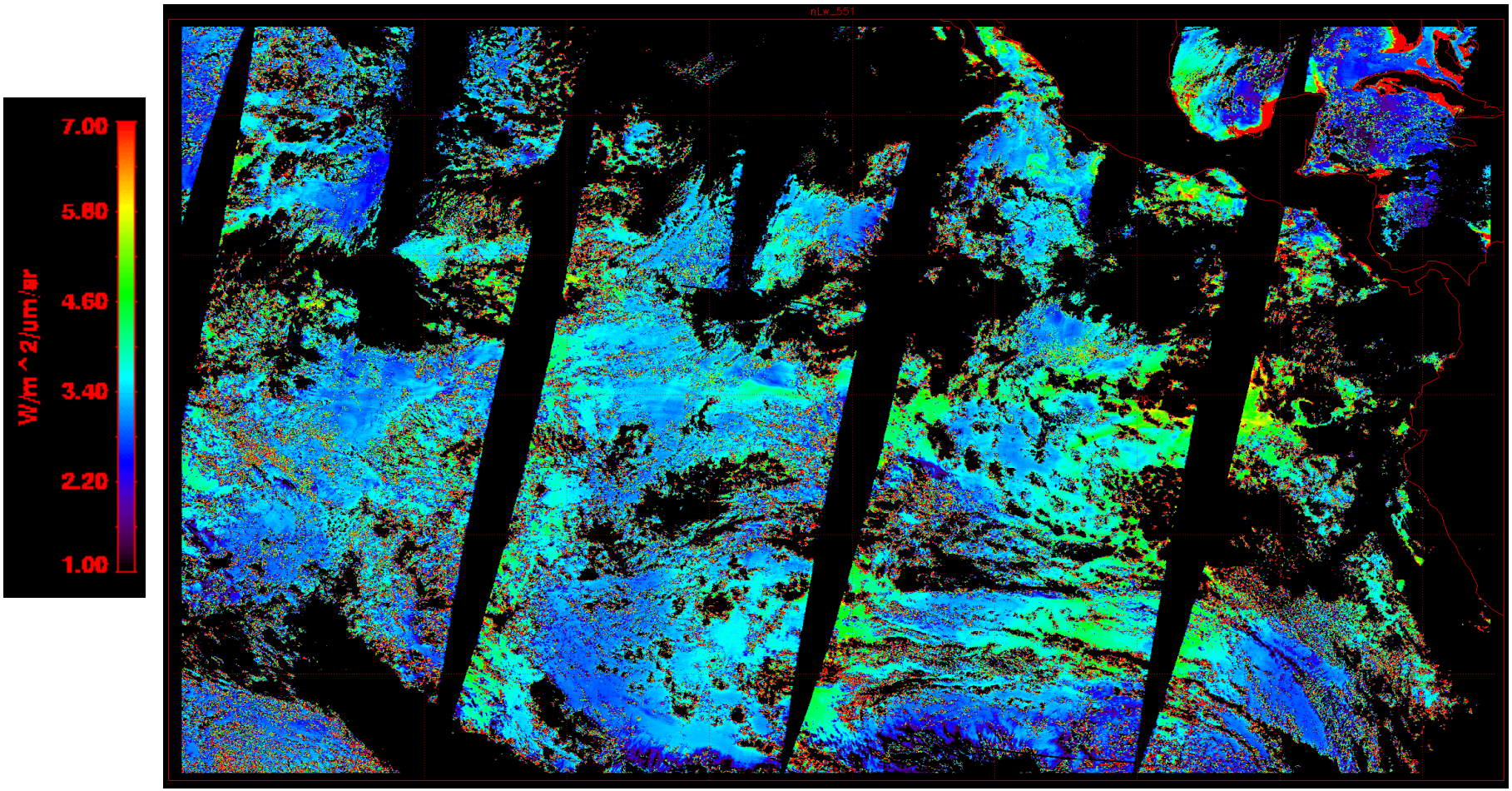

- Cross-scan and orbit-to-orbit behavior of *nLw*(412) is now excellent.

- Cross-scan and orbit-to-orbit behavior of *nLw*(551) implies that more work is required for this band.

Next Steps (Near Term)

- Refine calibration in NIR and then visible
- Add routine to include estimate of ρ_w in the NIR
- Adjust calibration of the fluorescence bands using an ocean-atmosphere model in the red and NIR.
- Add BRDF correction for a better comparison with SeaWiFS

Our intention is to have the first three in place for the reprocessing software.

Next Steps (Farther Term)

- Retrieval in dust.
- Case 2 waters (coastal)

These require coupled ocean and atmosphere retrievals, and the concomitant significant changes to the structure and speed of the processing algorithms.

APPENDIX III

Simultaneous determination of oceanic and atmospheric parameters for ocean color imagery by spectral optimization: A validation

Simultaneous determination of oceanic and atmospheric parameters for ocean color imagery by spectral optimization: A validation

by

R. M Chomko,[1] H.R. Gordon,[1] S. Maritorena,[2] D.A. Siegel[2,3]

[1]Department of Physics
University of Miami
Coral Gables, FL 33124

[2]Institute for Computational Earth System Science
University of California, Santa Barbara
Santa Barbara, CA 93106

[3]Department of Geography
University of California, Santa Barbara
Santa Barbara, CA 93106

The Aerosol Model

Use a Junge Power-Law Size Distribution

$$\frac{dN}{dD} = 0\,,\ D < D_0,$$

$$\frac{dN}{dD} = \frac{K}{D_1^{\nu+1}}\,,\ D_0 \le D \le D_1,$$

$$\frac{dN}{dD} = \frac{K}{D^{\nu+1}}\,,\ D_1 \le D \le D_2,$$

$$\frac{dN}{dD} = 0\,,\ D > D_2,$$

- $m = m_r - m_I$, where m_r is either 1.50 or 1.333, and m_i = 0, 0.001, 0.003, 0.010, 0.030, and 0.040.
- D_0 = 0.06 μm, D_1 = 0.20 μm, and D_2 = 20 μm.
- ν ranges from 2.0 to 4.5 in steps of 0.5.
- 72 separate aerosol models (2 values of $m_r \times$ 6 values of $m_i \times$ 6 values of ν).

$$\rho_A(G,\lambda,m_r,m_i,\nu) = a(G,\lambda,m_r,m_i,\nu)\tau(\lambda) + b(G,\lambda,m_r,m_i,\nu)\tau^2(\lambda) + c(G,\lambda,m_r,m_i,\nu)\tau^3(\lambda) + d(G,\lambda,m_r,m_i,\nu)\tau^4(\lambda)\,,$$

- Interpolate to essentially give a continuum of models.

Garver and Siegel (1997)

$$\rho_w = \rho_w(b_b/a+b_b)$$

$$a = a_w + a_{ph} + a_{cdm}$$
$$b_b = (b_b)_w + (b_b)_p$$

$$a_{ph}(\lambda) = a_{ph0}(\lambda)\ C$$
$$a_{cdm}(\lambda) = a_{cdm}(443)\ \exp[-0.0206(\lambda - 443)]$$
$$(b_b)_p(\lambda) = (b_b)_{p0}\ [443/\lambda]^{1.03}$$

$$\rho_w = \rho_w(\lambda, C, a_{cdm}(443), (b_b)_{p0})$$

Now optimize on 7 parameters

C, $a_{cdm}(443)$, $(b_b)_{p0}$, ν, $\tau_a(865)$, m_r, and m_I

with 8 spectral bands

Optimization

$$\rho_t(\lambda) = \rho_r(\lambda) + \rho_A(\lambda) + t_v(\lambda)t_s(\lambda)\rho_w(\lambda)\,,$$

$$\rho_{Aw}(G,\lambda,measured) \equiv \rho_A(G,\lambda) + t_v(G,\lambda)t_S(G,\lambda)\rho_W(\lambda)\,.$$

The modeled counterpart of ρ_{Aw}:

$$\hat{\rho}_{Aw}(G,\lambda,m_r,m_i,\nu,\tau_a,C,a_{cdm}(443),(b_b)_{p0}) \equiv \hat{\rho}_A(G,\lambda,m_r,m_i,\nu,\tau_a) + \hat{t}_v(G,\lambda,m_r,m_i,\nu,\tau_a)\hat{t}_S(G,\lambda,m_r,m_i, \times \hat{\rho}_W(\lambda,C,a_{cdm}(443),b_{bp}(443)).$$

Assuming $\rho_A(765)$ and $\rho_A(765) = 0$ gives estimation of the parameters ν and τ_a.

Given ν and τ_a we minimize the quantity

$$\sum_{\lambda_i}\left\{\hat{\rho}_{Aw}(G,\lambda_i,m_r,m_i,\nu,\tau_a,C,a_{cdm}(443),b_{bp}(443)) - \rho_{Aw}(G,\lambda_i,measured)\right\}^2$$

In effect, we have optimized for 7 parameters:

C, $a_{cdm}(443)$, $b_{bp}(443)$, ν, τ_a, m_r, and m_i;

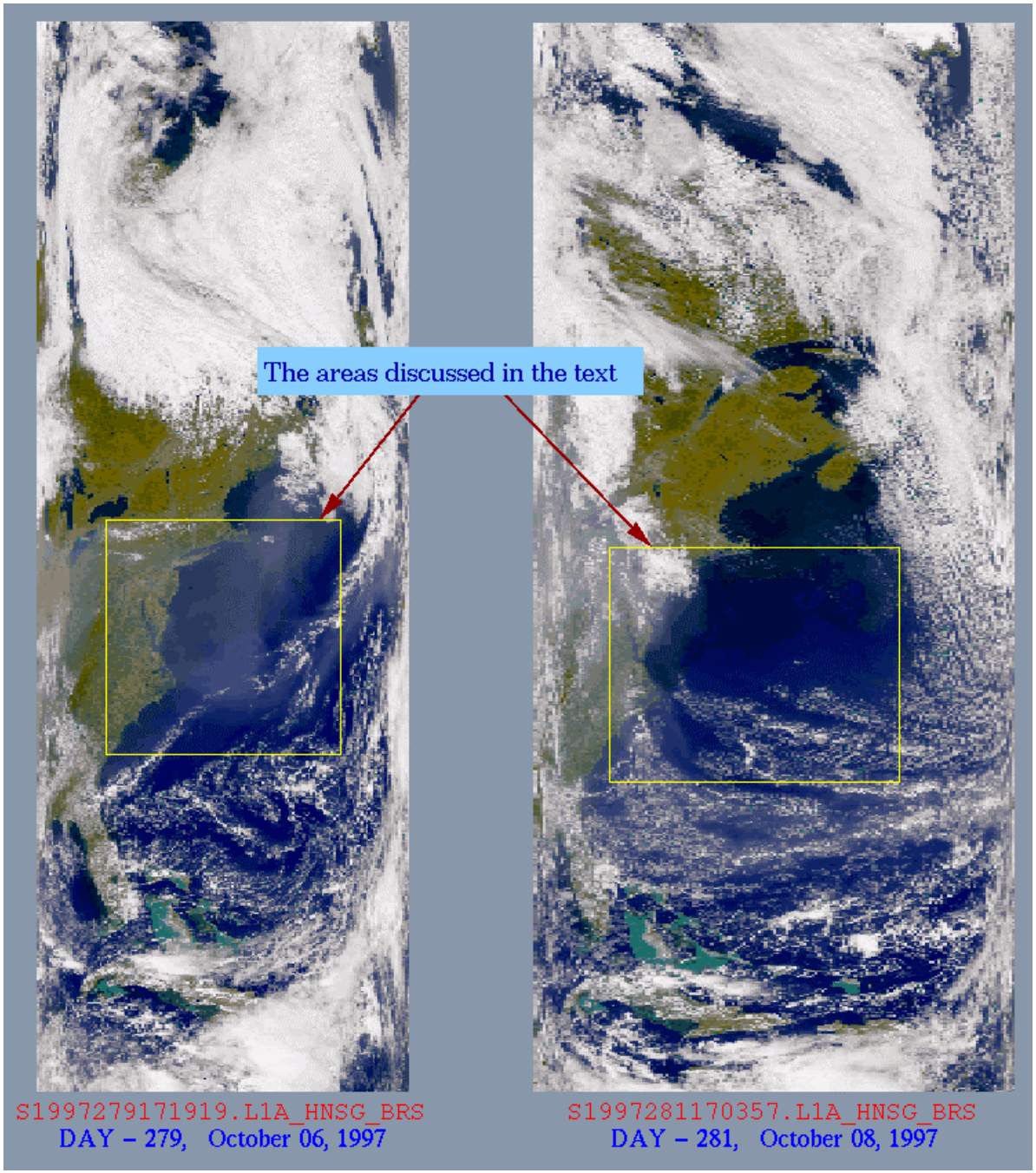
The areas discussed in the text
S1997279171919.L1A_HNSG_BRS
DAY – 279, October 06, 1997
S1997281170357.L1A_HNSG_BRS
DAY – 281, October 08, 1997

SOA $a_{cdm}(443)$ (m^{-1})

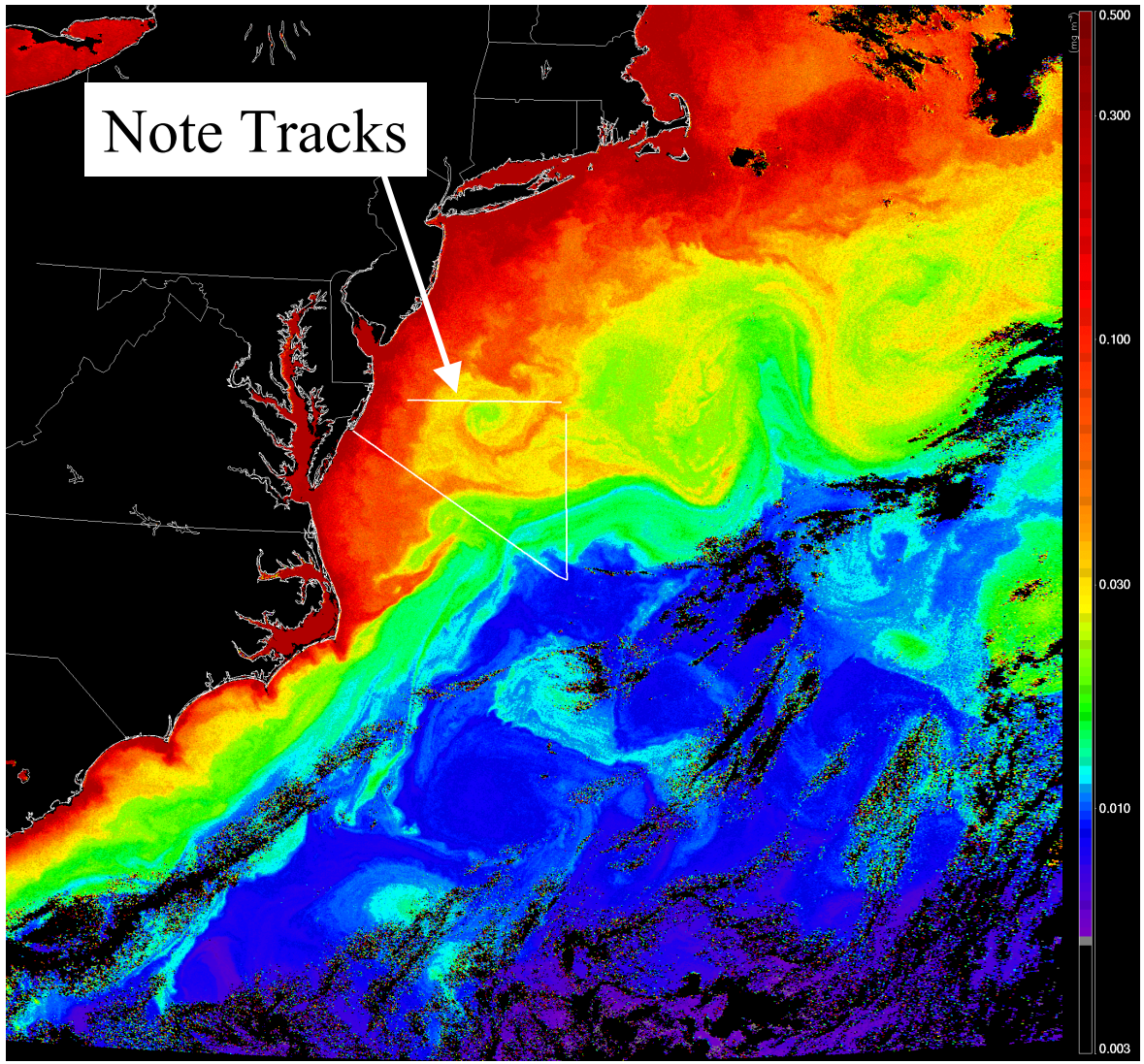

SOA $a_{cdm}(443)$ (m^{-1})

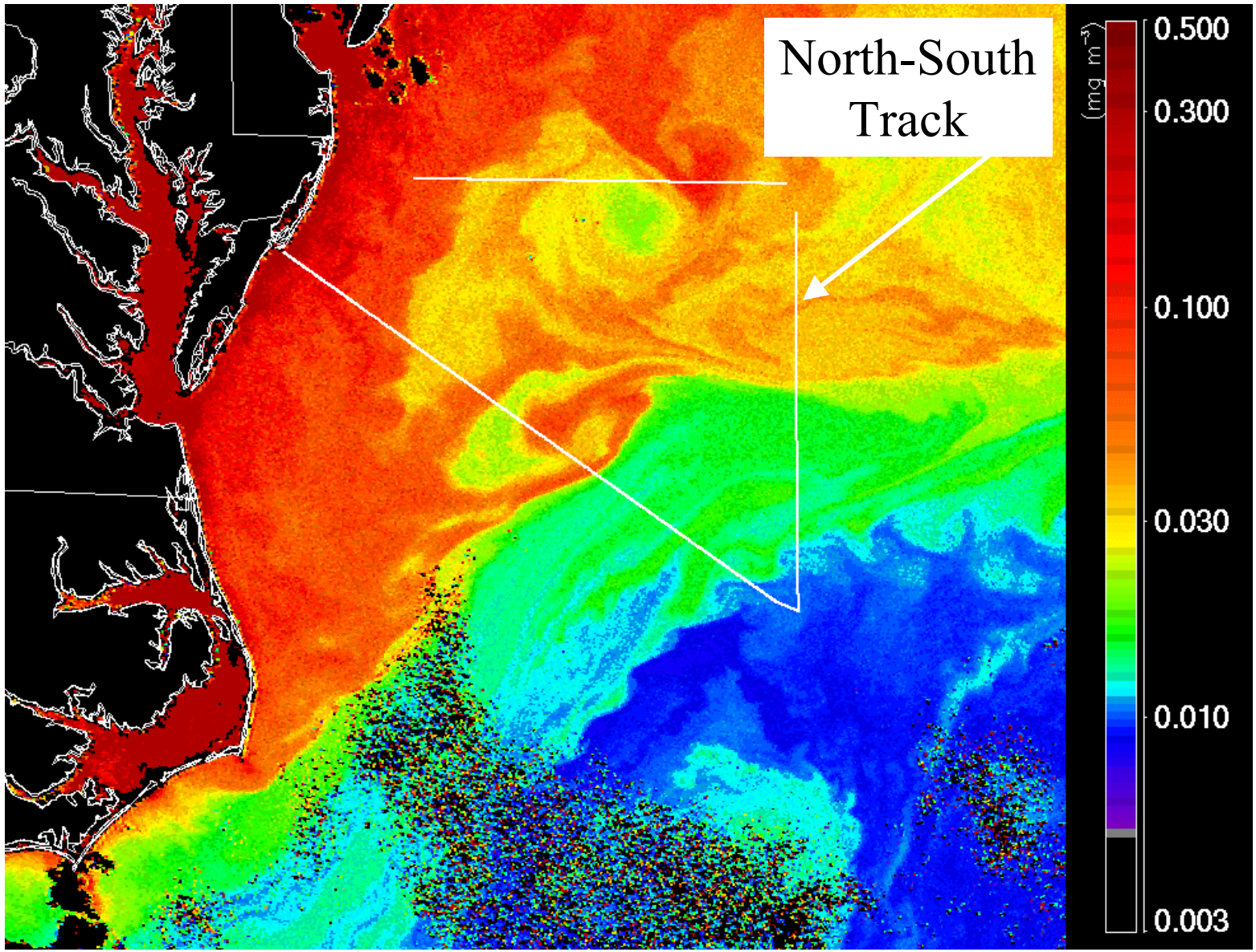

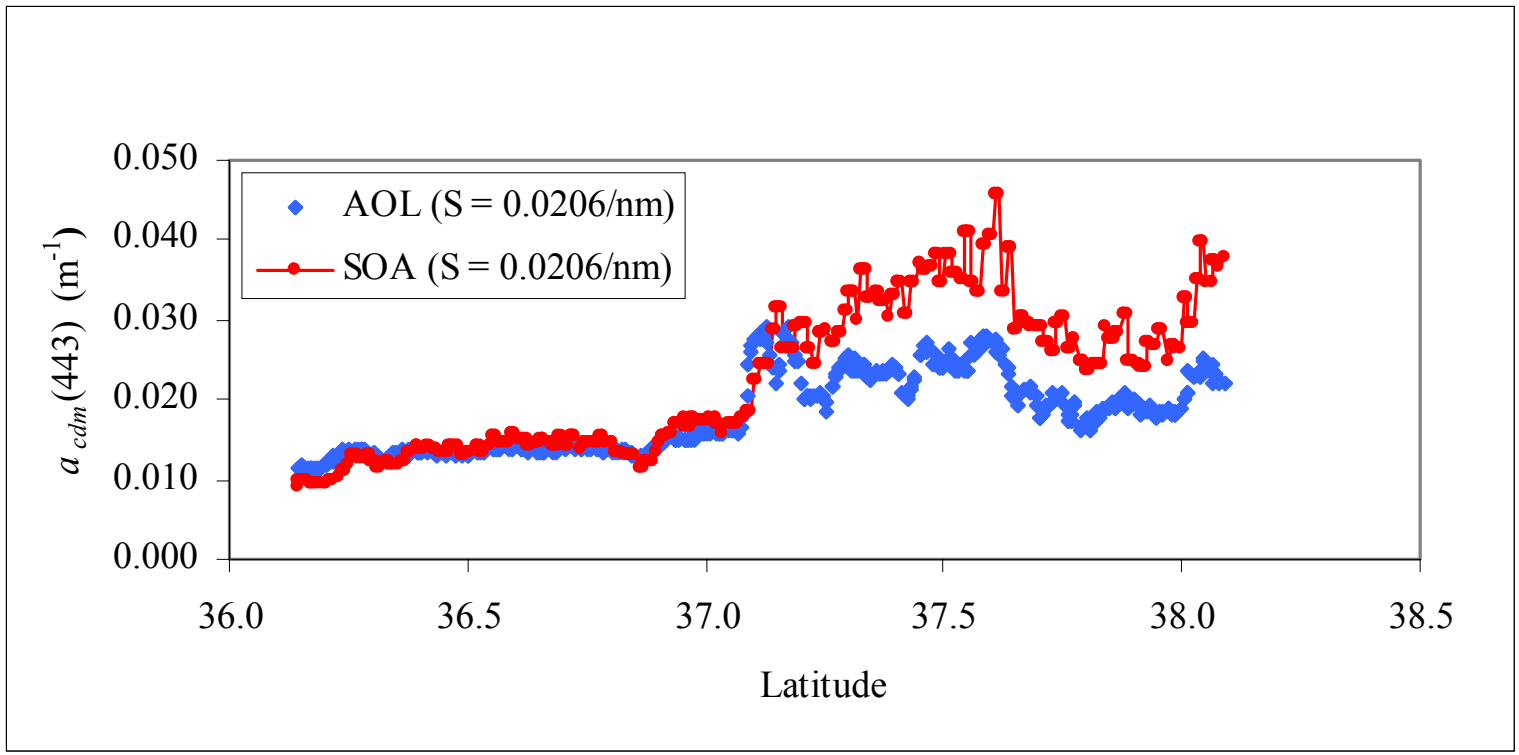

Comparison of SOA and AOL $a_{cdm}(443)$ along the North-South Track

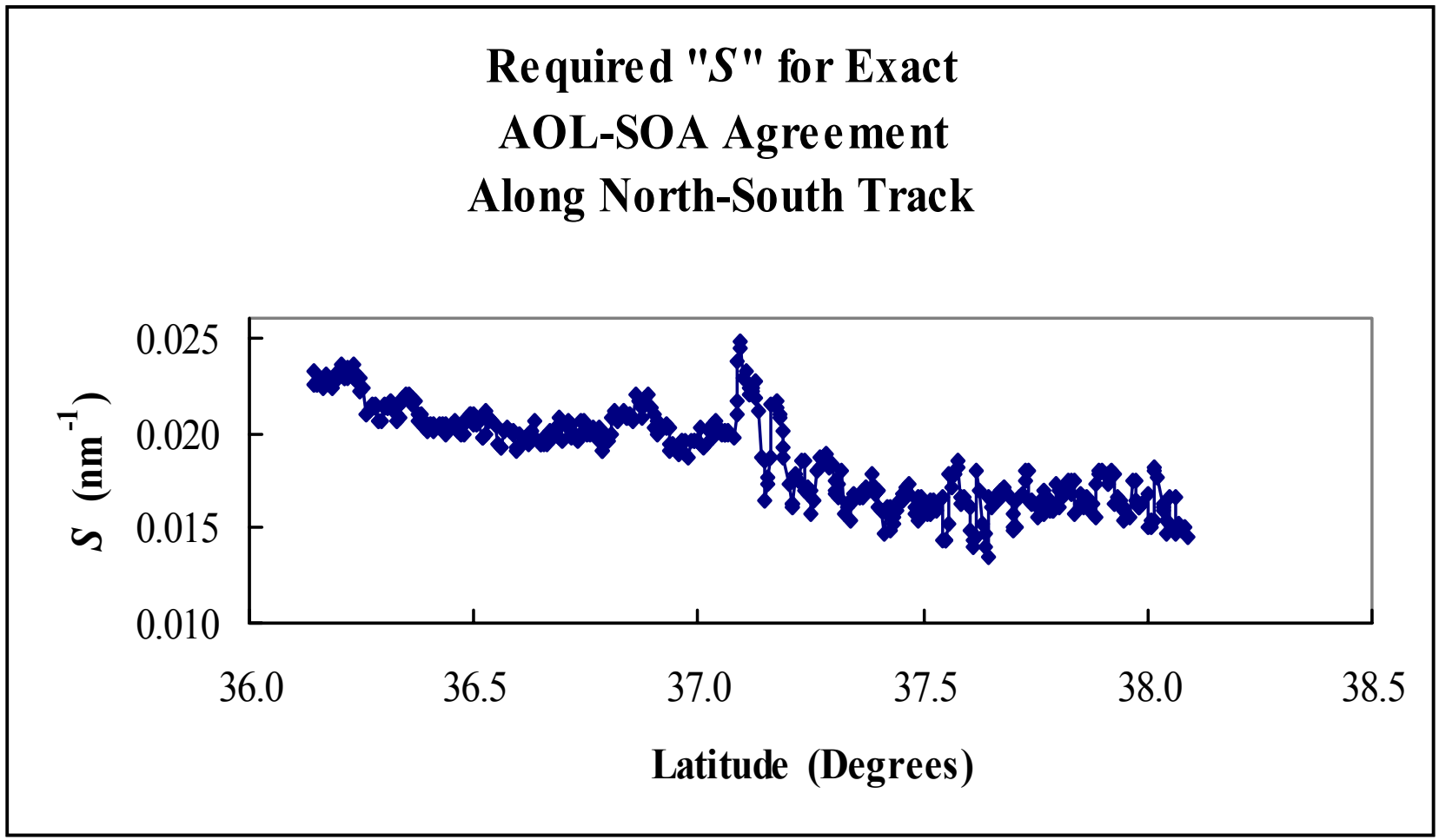
Required "S" for Exact
AOL-SOA Agreement
Along North-South Track
S (nm-1)
0.025
0.020
0.015
0.010
36.0
36.5
37.0
37.5
38.0
38.5
Latitude (Degrees)

SOA *Chl a* (mg/m^3)

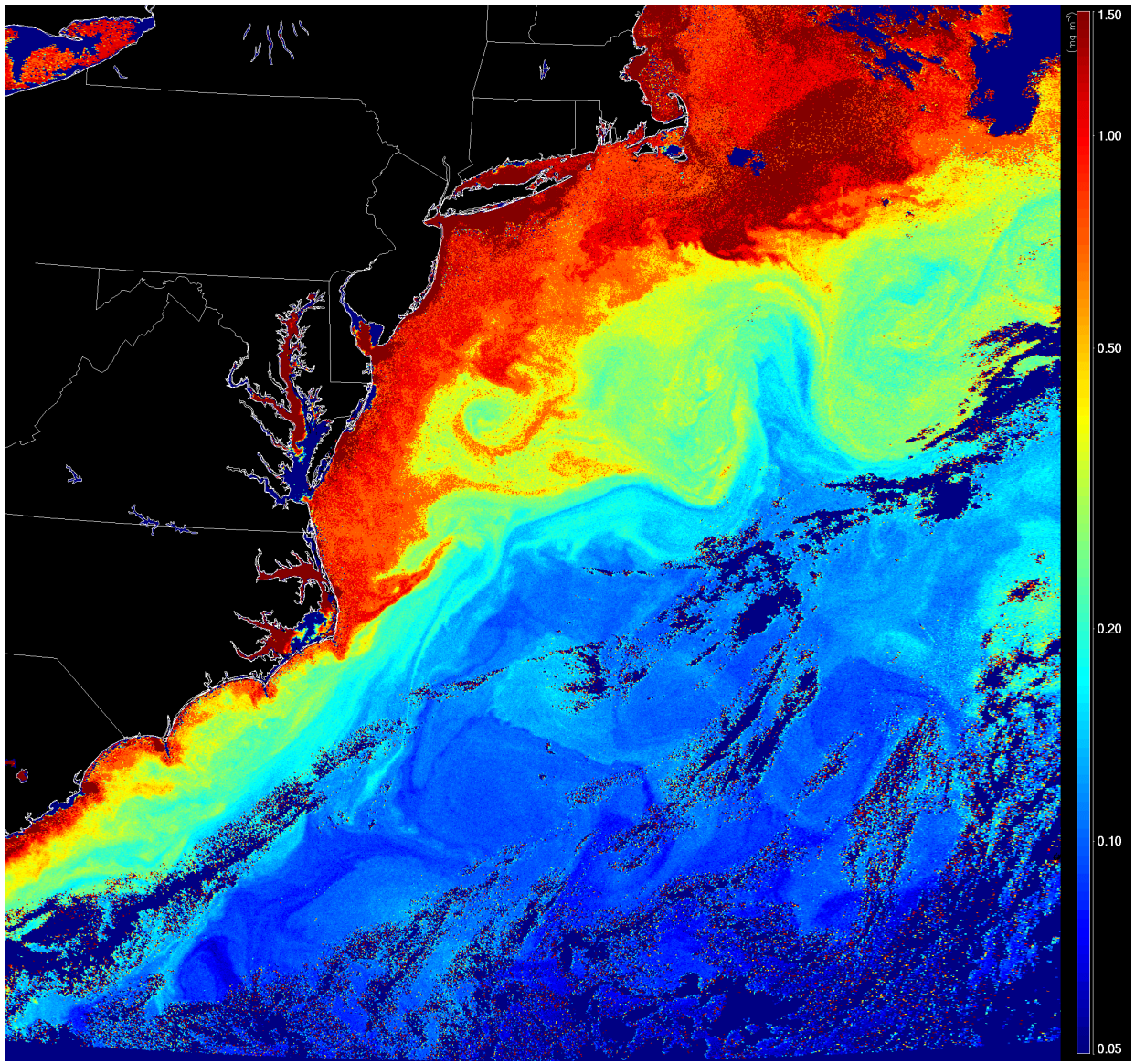

1.50

1.00

0.50

0.10

SeaWiFS 8-day mean *Chl a*

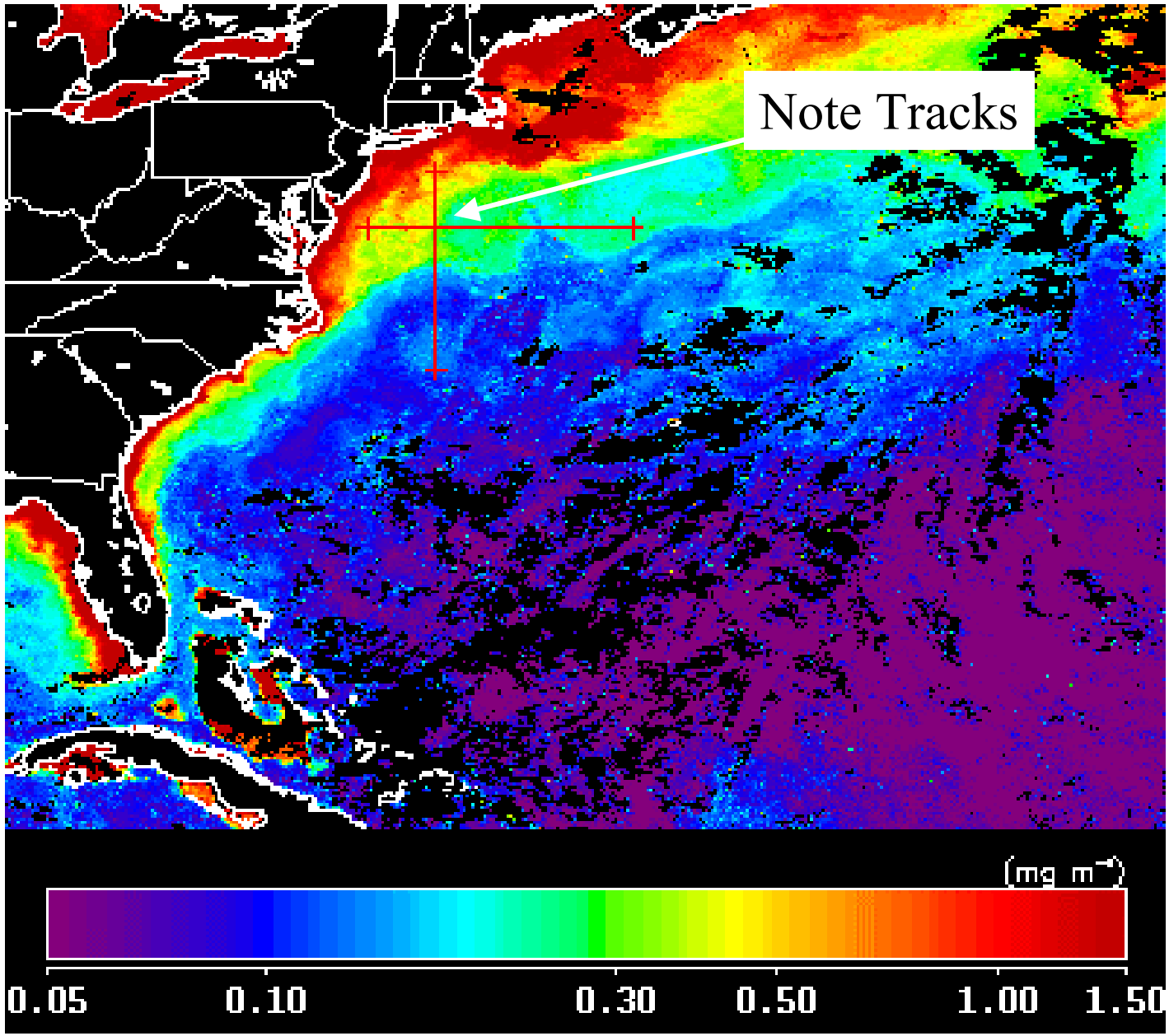

Comparison with SeaWiFS

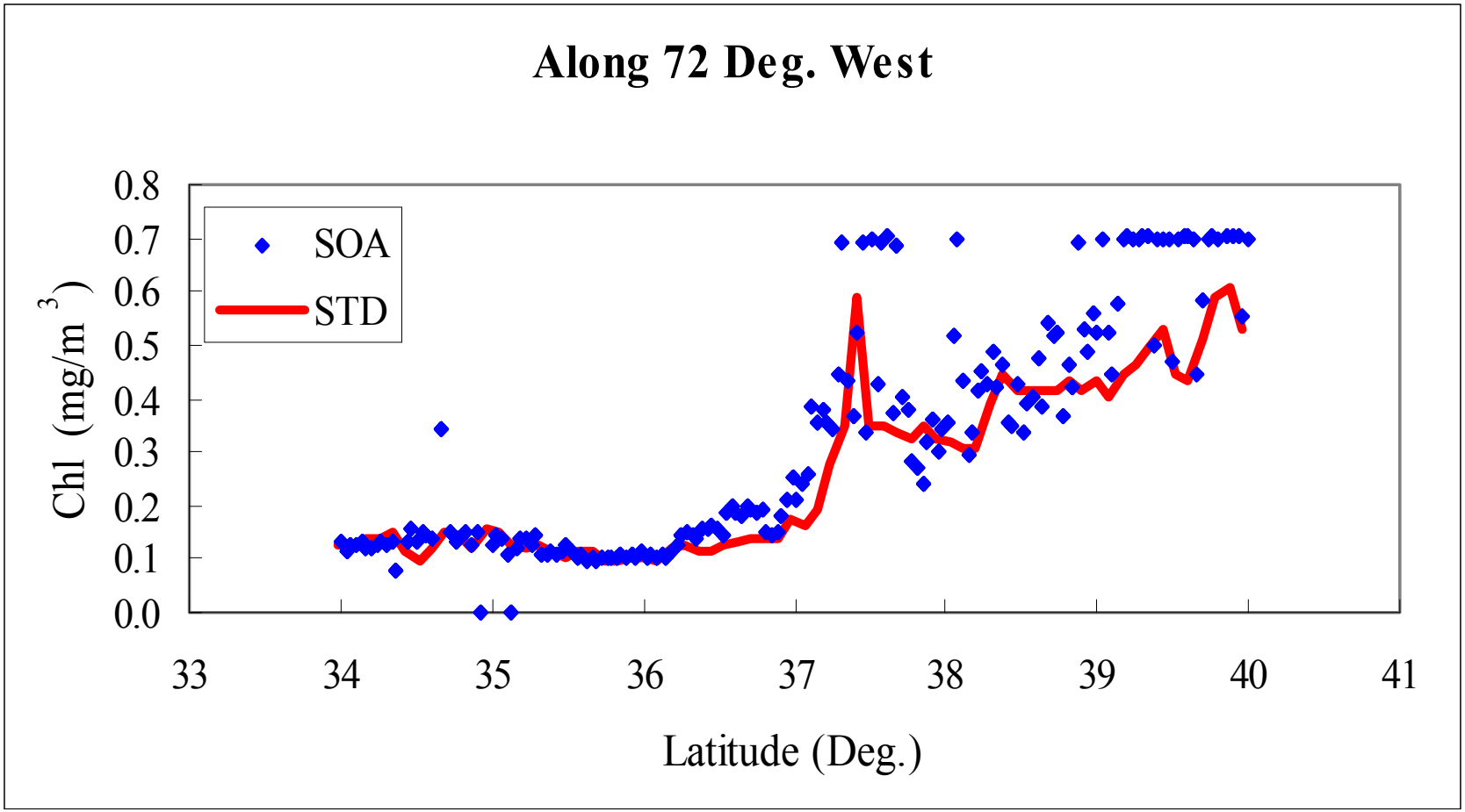

Comparison with SeaWiFS

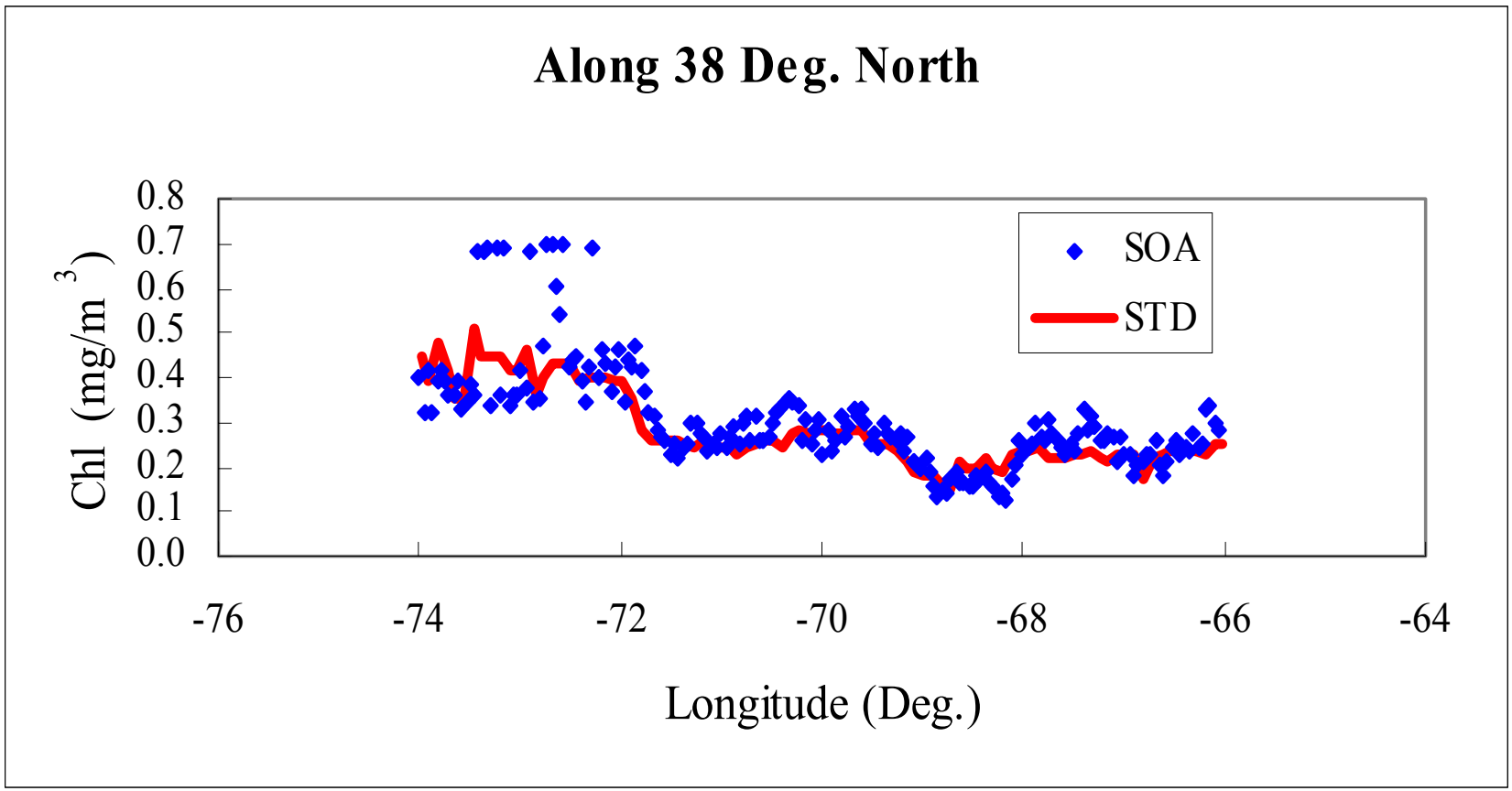

$b_{bp}(443)$ (m^{-1})

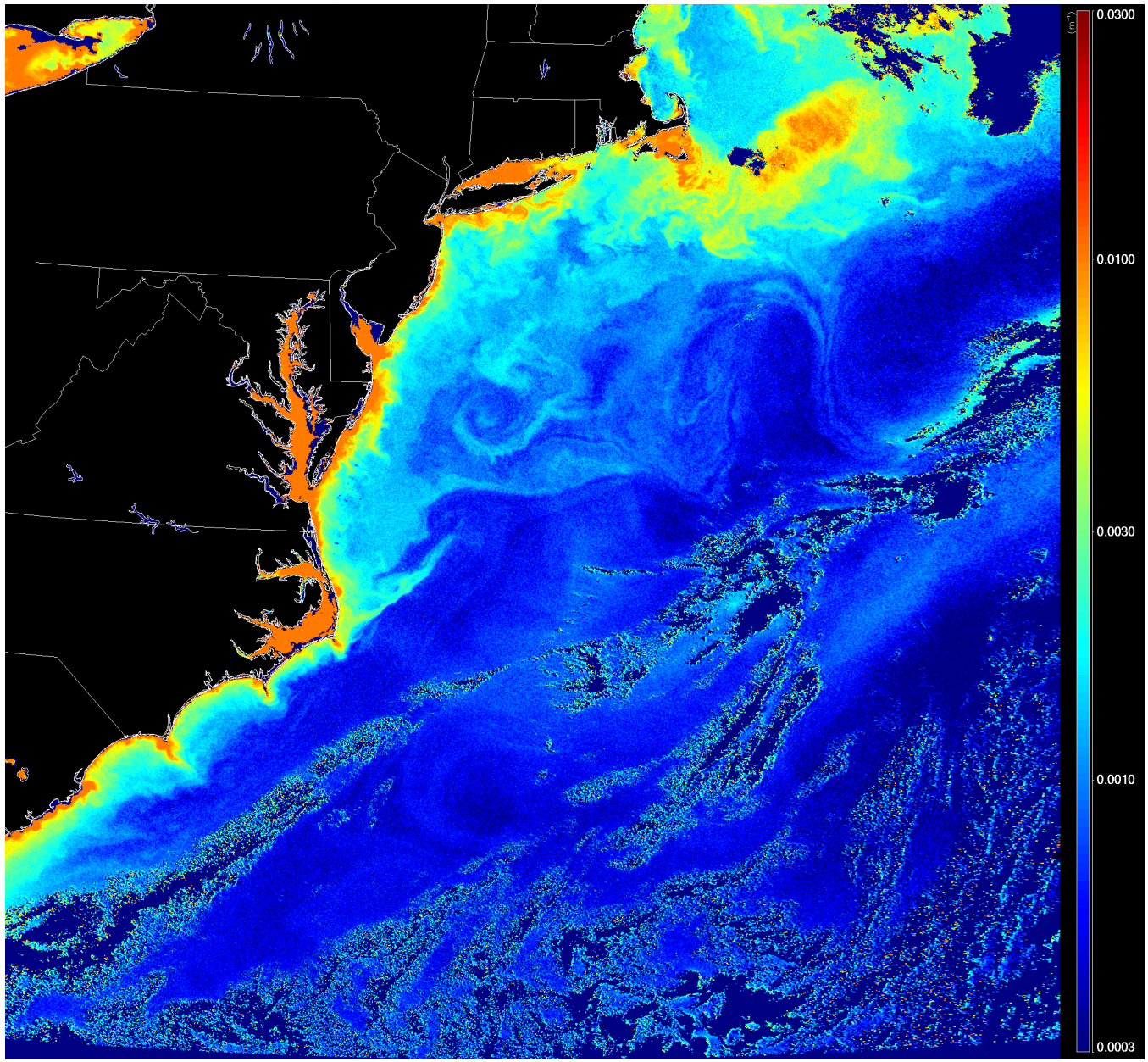

ν

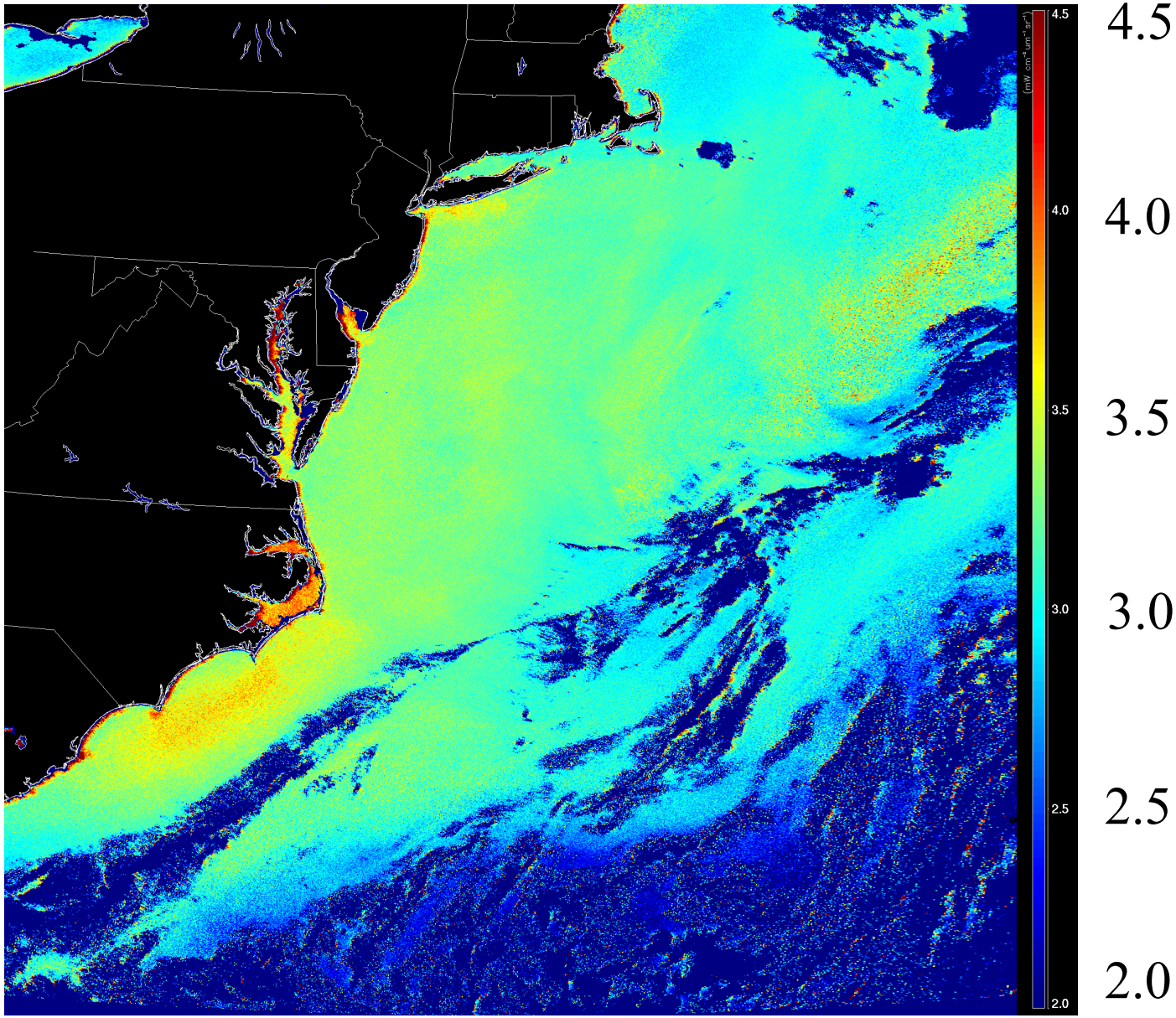

ω_0

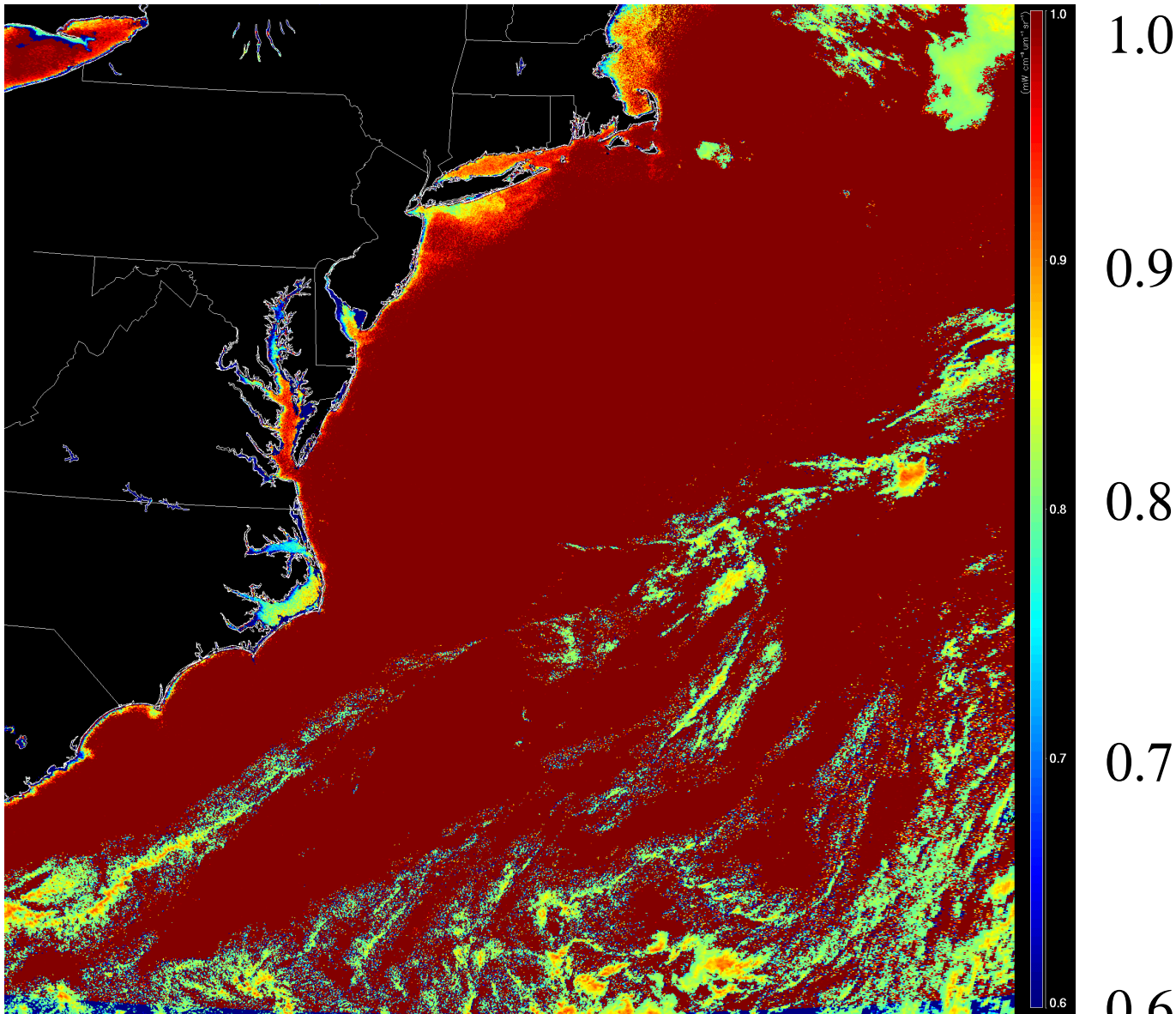

Case 2 Waters

To extend to Case 2 waters, use the retrieved water parameters to estimate ρ_w in the NIR. Then subtract the water contribution from $\rho_t - \rho_r$ in the NIR, and process the pixel again. Keep doing this until stable values of ρ_w in the NIR are obtained. The following slides compare the results for the atmospheric parameters ω_0 and υ with ("as Case 2") and without ("as Case 1") such iteration. The fact that these parameters have similar values in the turbid coastal waters and the offshore oceanic waters show that a realistic atmospheric correction has been achieved.

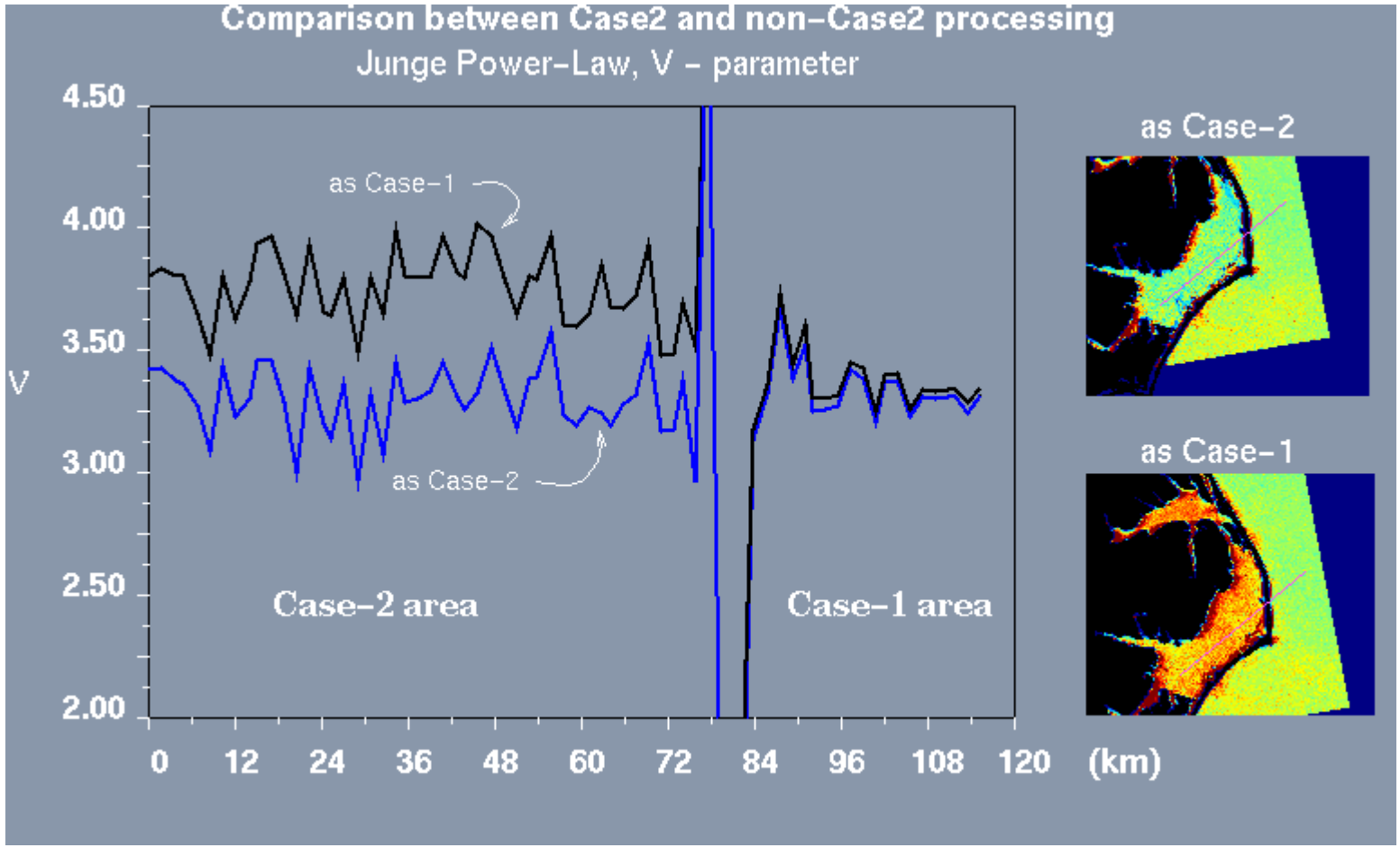
Comparison between Case2 and non-Case2 processing
Junge Power-Law, V - parameter
4.50
4.00
3.50
3.00
2.50
2.00
V
as Case-1
as Case-2
Case-2 area
Case-1 area
0
12
24
36
48
60
72
84
96
108
120
(km)
as Case-2
as Case-1

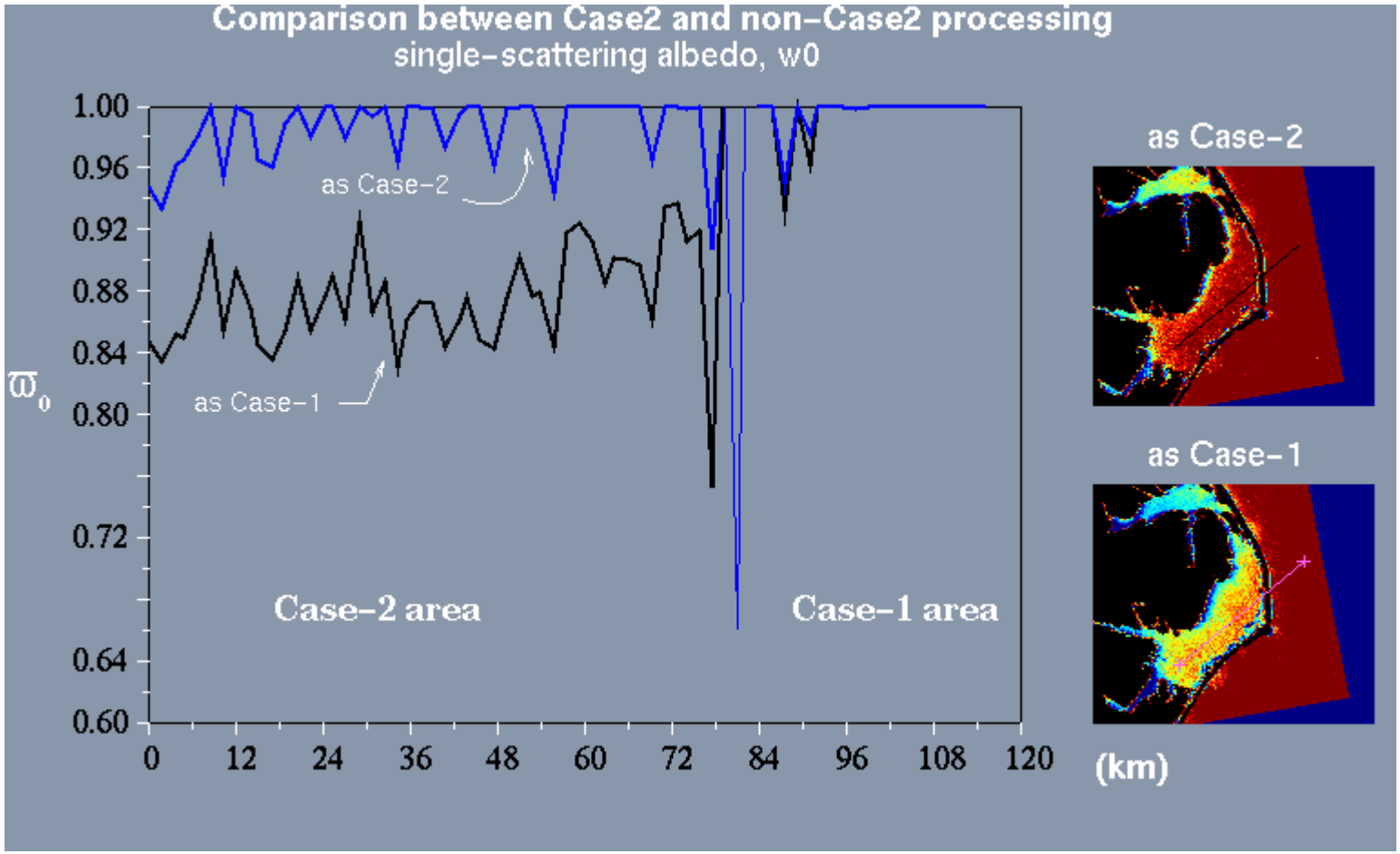
Comparison between Case2 and non-Case2 processing
single-scattering albedo, w0
1.00
0.96
0.92
0.88
0.84
0.80
0.72
0.64
0.60
ω0
as Case-2
as Case-1
Case-2 area
Case-1 area
0
12
24
36
48
60
72
84
96
108
120
(km)
as Case-2
as Case-1

Timing of the SOA applied to Case 2 Waters

Parameter: ω_0

No Iteration 4 Iterations

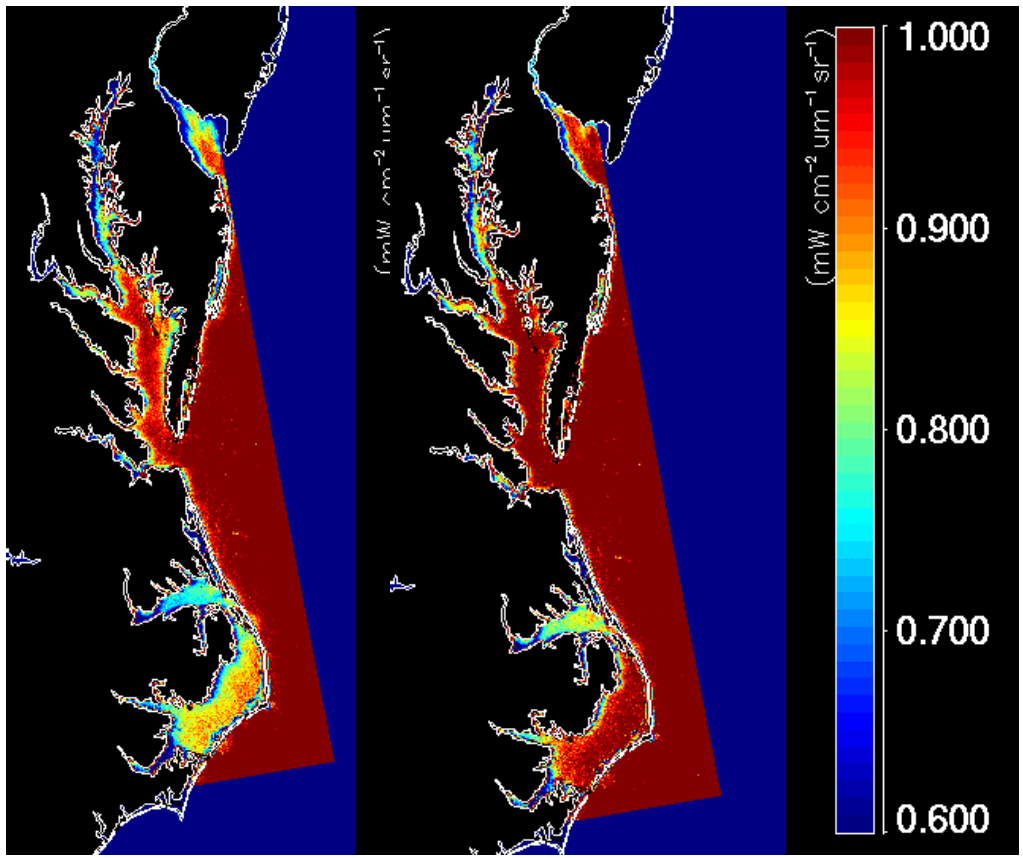

Times correspond to processing the rectangular section of the image.

4,684 Sec 19,476 Sec

Conclusions

- Good agreement between AOL and SOA estimates of $a_{cdm}(443)$.
- Good agreement between SeaWiFS and SOA *Chl a* estimates.
- Extension to Case 2 waters shows promise.

APPENDIX IV

Spectral Matching Algorithm in Wind Blown Dust

The Spectral Matching Algorithm in Wind-blown Dust

R.M. Chomko and H.R. Gordon

- We have added the Garver-Siegel (1997) model for ρ_w into the spectral matching algorithm.
- Here, we compare the retrieved *Chl a* for a single dusty day (Day 276, 1997) with the SeaWiFS 8-day mean.

Aerosol Models for Dust

Moulin, Gordon, Banzon, and Evans (2000)

Size Distribution:

- 3 component log-normal (Shettle 1984)
- Large component ($\times 1$, $\times 10$, $\times 20$)

Absorption Index:

- Patterson (1981)
- "Lower limit" (SeaWiFS)

Vertical Distribution:

- $0 \rightarrow 2$ km
- $0 \rightarrow 4$ km
- $0 \rightarrow 6$ km

Total number of models:

3 sizes $\times$ 2 indices $\times$ 3 vertical Struct. =18

Garver and Siegel (1997)

$$\rho_w = \rho_w(b_b/a+b_b)$$

$$a = a_w + a_{ph} + a_{cdm}$$
$$b_b = (b_b)_w + (b_b)_p$$

$$a_{ph}(\lambda) = a_{ph0}(\lambda)\ C$$
$$a_{cdm}(\lambda) = a_{cdm}(443)\ \exp[-0.0206(\lambda-443)]$$
$$(b_b)_p(\lambda) = (b_b)_{p0}\ [443/\lambda]^{1.03}$$

$$\rho_w = \rho_w(\lambda, C, a_{cdm}(443), (b_b)_{p0})$$

$L_t(865)$ Day 276 (Counts)

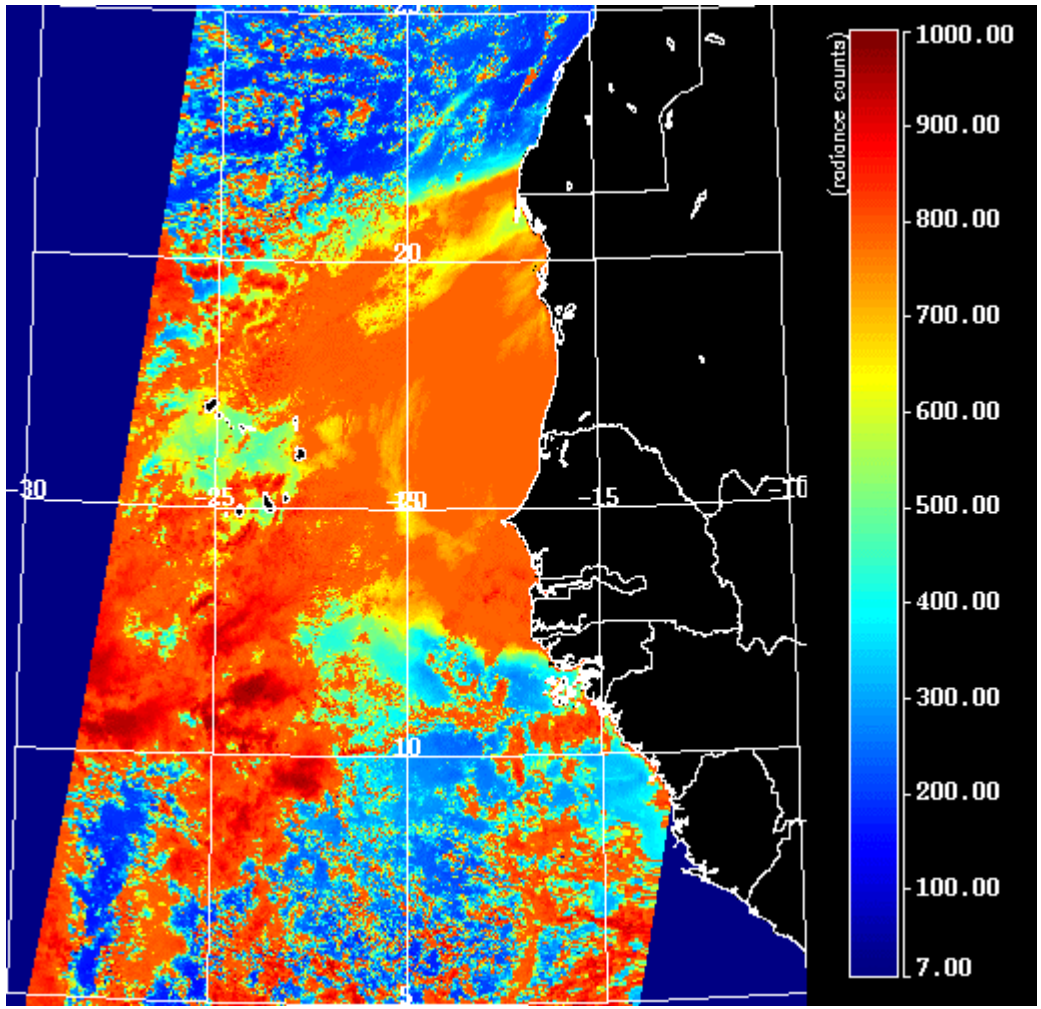

a_{cdm} (m^{-1})

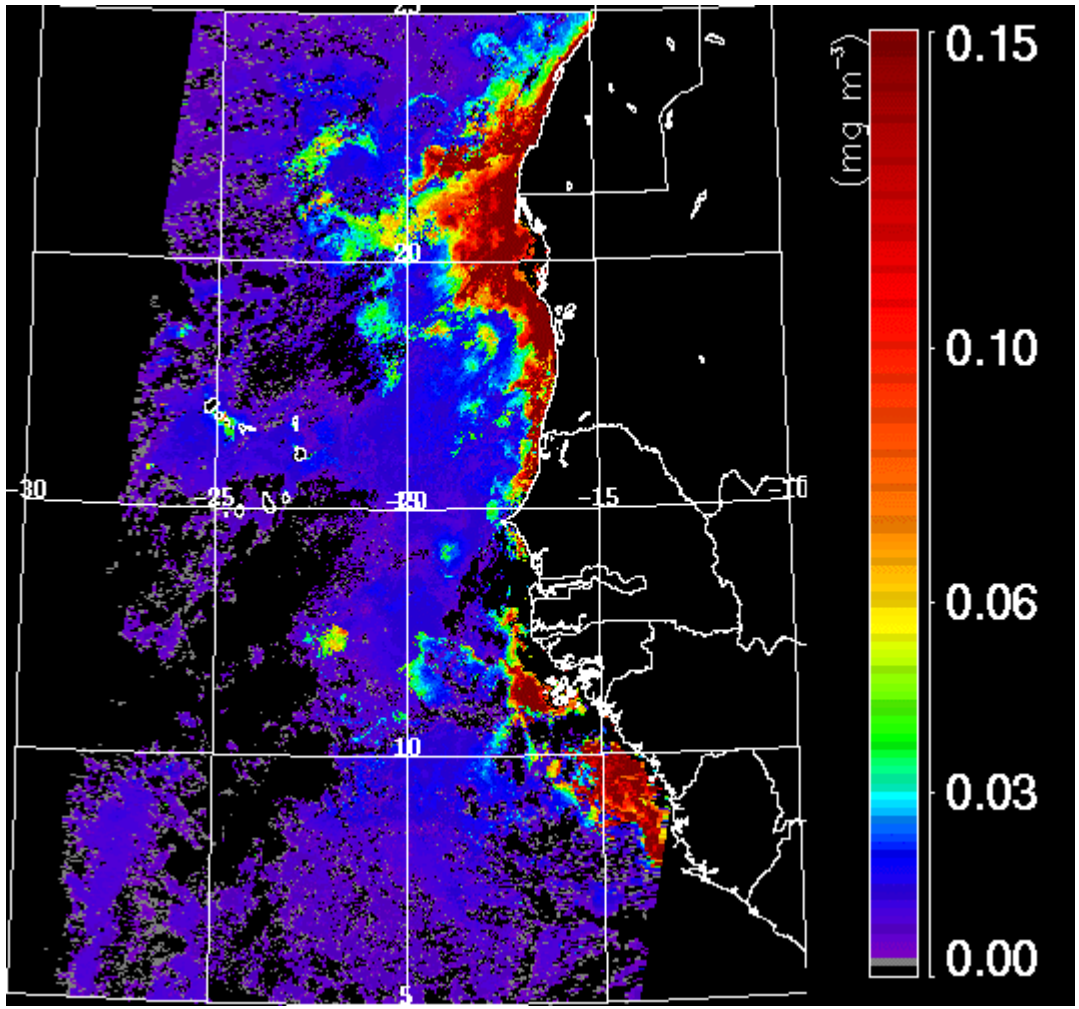

Chl a

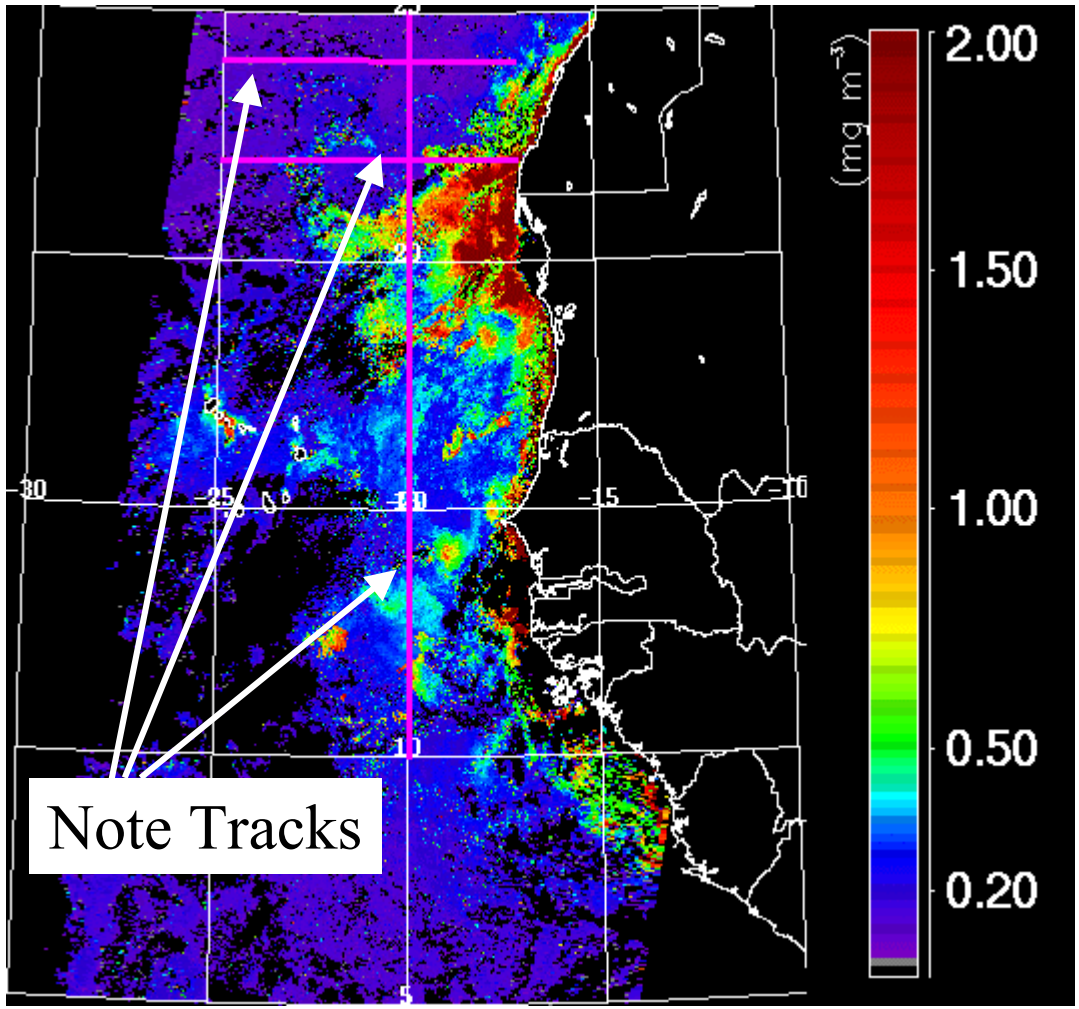

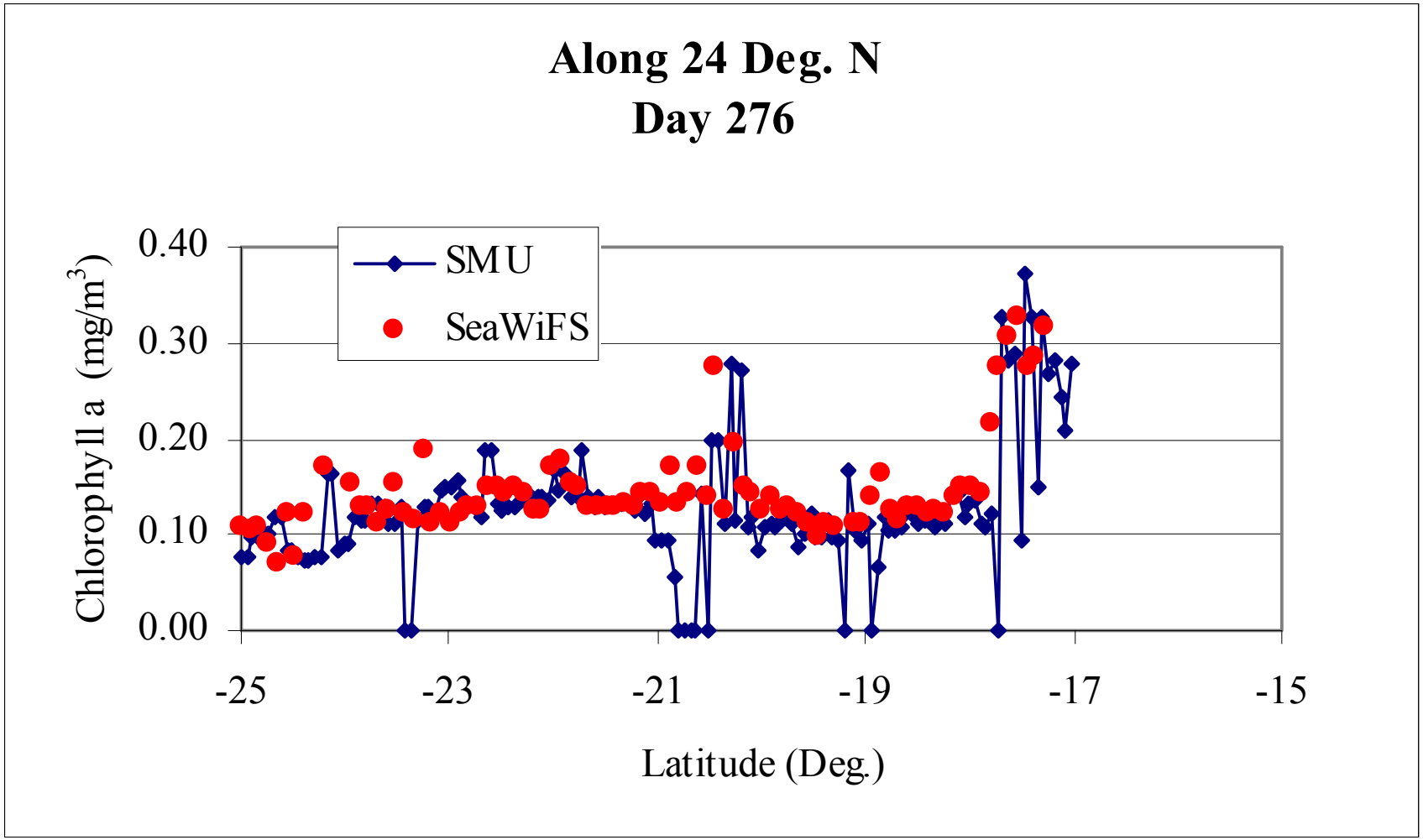
Along 24 Deg. N
Day 276
SMU
SeaWiFS
Chlorophyll a (mg/m3)
0.40
0.30
0.20
0.10
0.00
-25
-23
-21
-19
-17
-15
Latitude (Deg.)

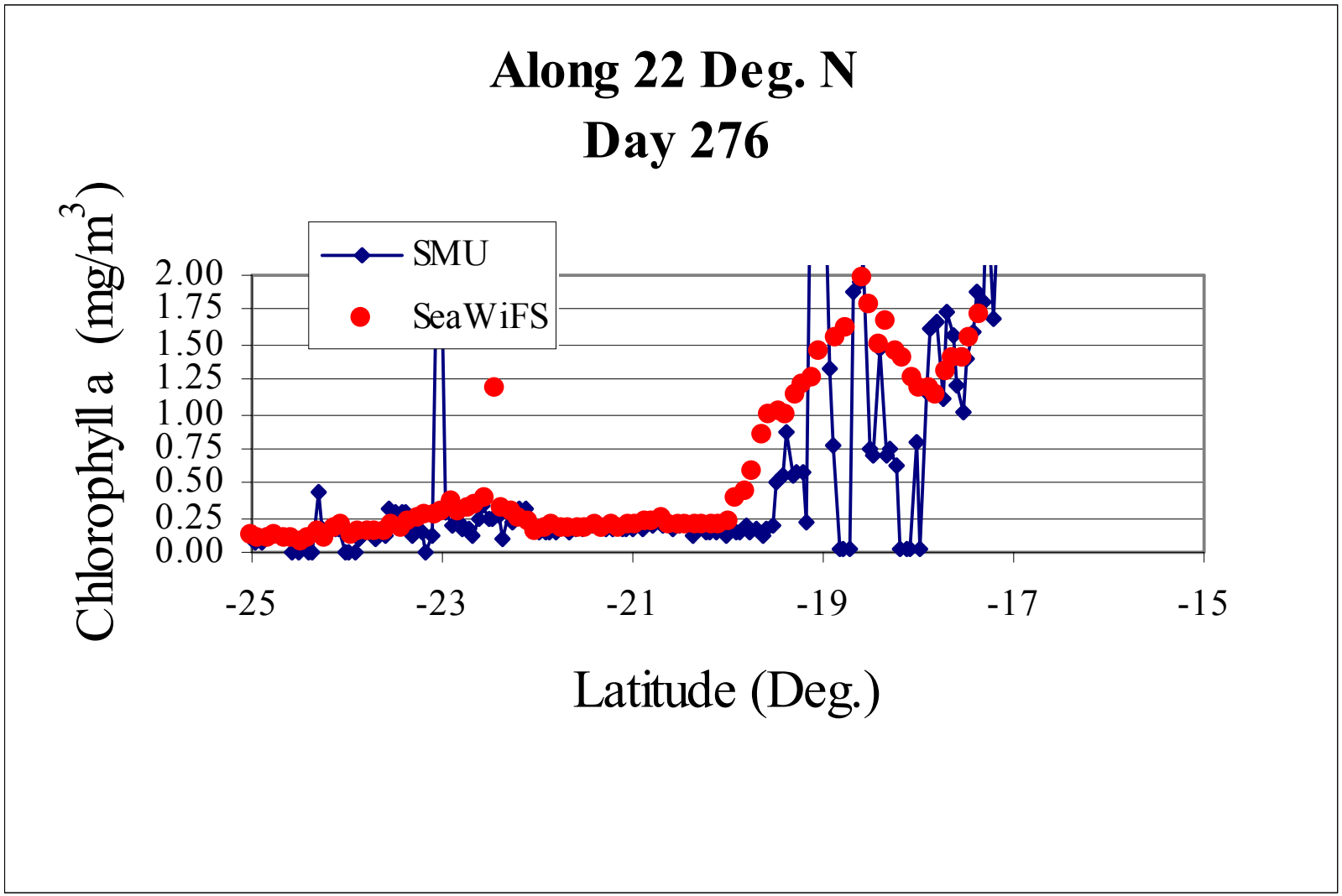
Along 22 Deg. N
Day 276
Chlorophyll a (mg/m3)
SMU
SeaWiFS
2.00
1.75
1.50
1.25
1.00
0.75
0.50
0.25
0.00
-25
-23
-21
-19
-17
-15
Latitude (Deg.)

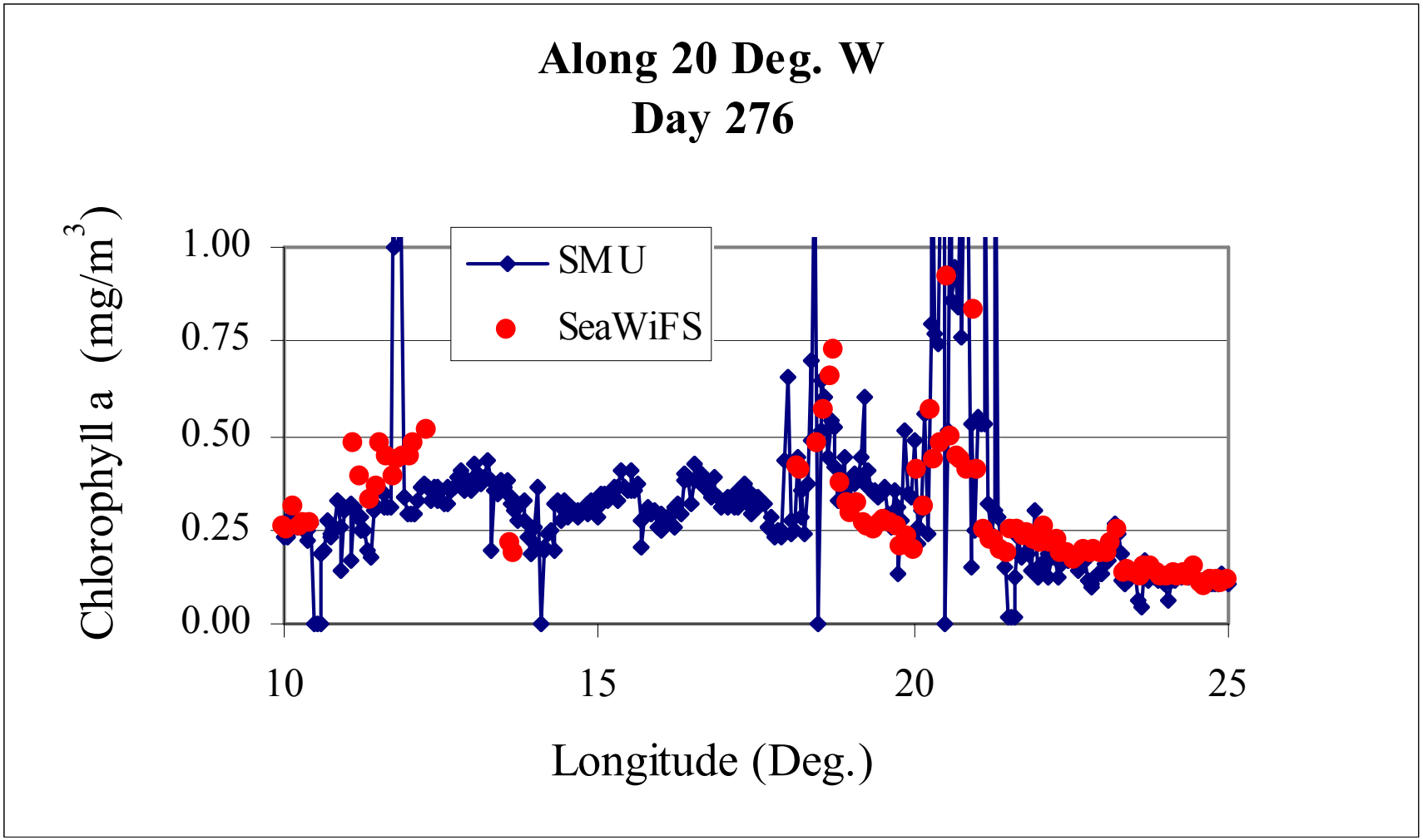
Along 20 Deg. W
Day 276
Chlorophyll a (mg/m3)
1.00
0.75
0.50
0.25
0.00
SMU
SeaWiFS
10
15
20
25
Longitude (Deg.)

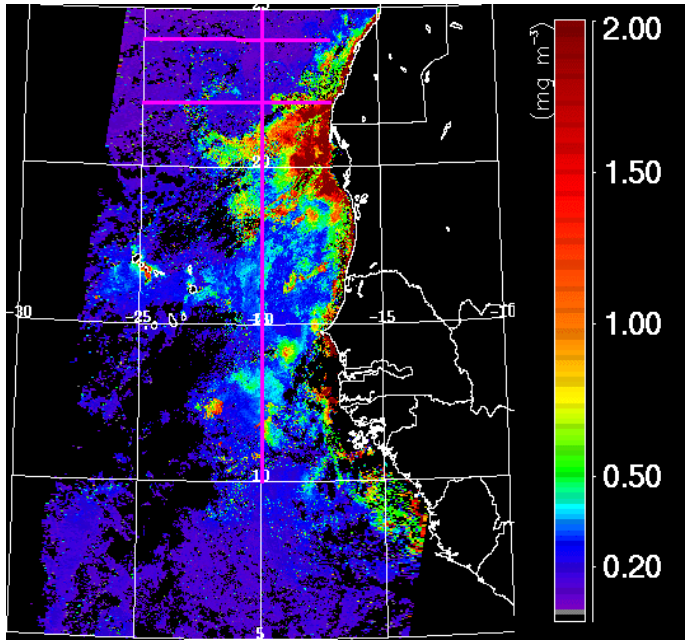
(mg m^{-3})
2.00
1.50
1.00
0.50
0.20

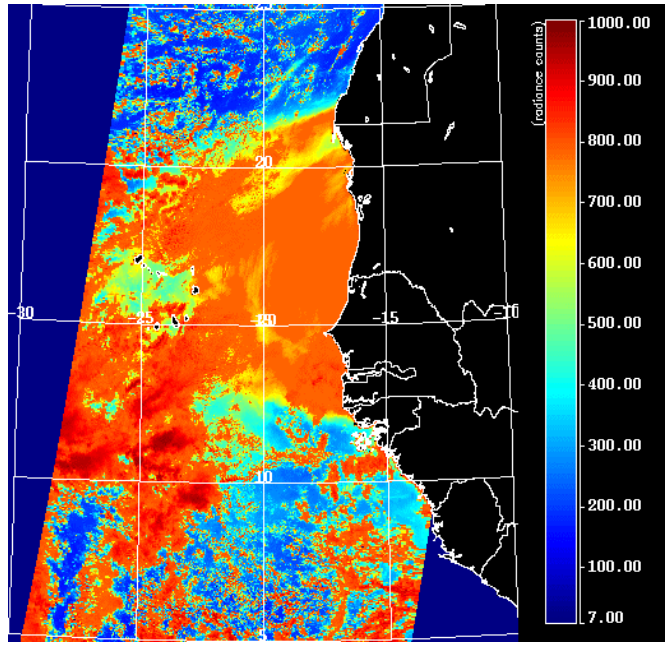
(radiance counts)
1000.00
900.00
800.00
700.00
600.00
500.00
400.00
300.00
200.00
100.00
7.00

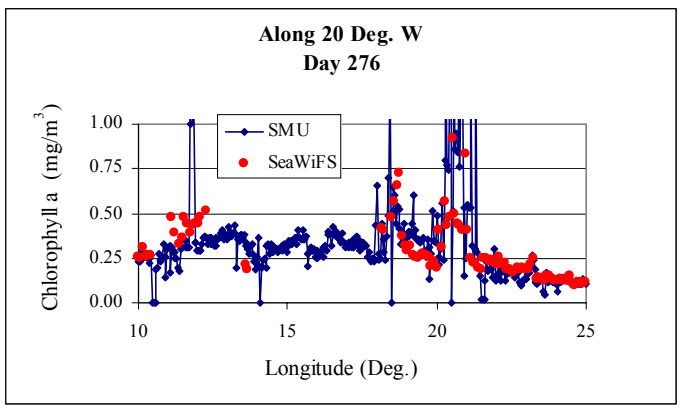
Along 20 Deg. W
Day 276
Chlorophyll a (mg/m^3)
SMU
SeaWiFS
1.00
0.75
0.50
0.25
0.00
10
15
20
25
Longitude (Deg.)

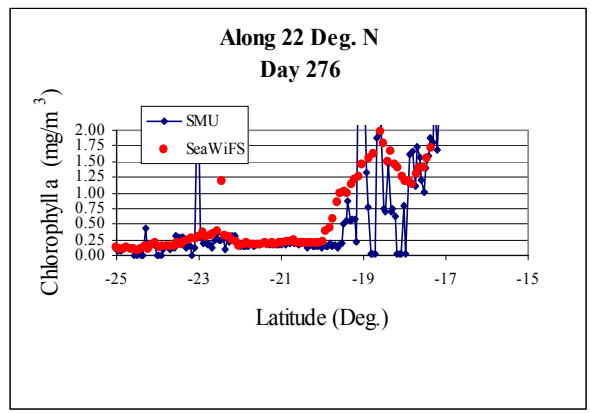
Along 22 Deg. N
Day 276
Chlorophyll a (mg/m^3)
SMU
SeaWiFS
2.00
1.75
1.50
1.25
1.00
0.75
0.50
0.25
0.00
-25
-23
-21
-19
-17
-15
Latitude (Deg.)

Conclusions

- There is good agreement between the spectral matching algorithm (SMA) and the SeaWiFS *Chl a* where SeaWiFS data exist.
- The SMA coverage is considerably increased in dusty areas.